



UNIVERSITY of STRATHCLYDE
**POWER NETWORKS
DEMONSTRATION CENTRE**

Testing of the Enhanced Frequency Control Capability (EFCC) Scheme: Part 3 - Impact of Communication Performance on the EFCC Scheme Operation



Document No.: PNDC/NGR-001/FR-03 V0.2

Classification: Confidential

13 November 2018



DOCUMENT INFORMATION

Title: Testing of the Enhanced Frequency Control Capability (EFCC) Scheme: Part 3
Impact of Communication Performance on the EFCC Scheme Operation

**Document
No.:**

Classification:

Client(s):

DOCUMENT AUTHORIZING, REVIEW AND APPROVAL

Version No.: V0.1

Prepared By: Dr Qiteng Hong

Reviewed By: Dr Ibrahim Abdulhadi

**Authorised
By**

Date of Issue 13 November 2018

PROJECT CONTRIBUTORS

The following people contributed to this project:

DOCUMENT DISTRIBUTION

National Grid

COPYRIGHT ©The University of Strathclyde 2018

This document and its contents are the property of the University of Strathclyde and are confidential and protected by copyright. Disclosure, use or copying of this document in whole or in part without the written permission of the University constitutes an infringement of the University's proprietary rights.

LIMITATION

This report has been prepared for the members of the Power Networks Demonstration Centre and is provided subject to the provisions of the Membership Agreement between the University of Strathclyde and the members of the Power Networks Demonstration Centre. The University of Strathclyde accepts no liability or responsibility whatsoever for or in respect of any use or reliance upon this report by any third party.

EXECUTIVE SUMMARY

This report presents the methods and results of the tests conducted at the Power Network Demonstration Centre (PNDC) at the University of Strathclyde (UoS) to evaluate the impact of communication performance on the operation of the Enhanced Frequency Control Capability (EFCC) scheme. This work is part of the EFCC project led by National Grid under Ofgem's Network Innovation Competition (NIC) funding framework. This report is Part 3 of a set of three reports, where the other two reports focus on the testing of the EFCC scheme's local and wide-area operational modes respectively.

The operation of the EFCC scheme requires two main types of communication networks, i.e. the wide-area communication between the Regional Aggregators (RAs) and Local Controllers (LCs), and regional communication between Phasor Measurement Units (PMUs) and RAs. In this work, both types of communication networks were emulated using a communication emulator and the impact of the communication performance of both networks have been evaluated for the following communication parameters: latency, latency with jitter, the rate of loss of packets and Bit Error Rate (BER). The tests firstly evaluated how these different emulated communication conditions would affect the EFCC controllers in receiving and processing the data (i.e. how the confidence levels in the EFCC controllers were affected under the various emulated conditions). Then the performance of the EFCC scheme during frequency and fault events was tested with the emulated communication conditions.

The EFCC controllers handle degraded communication conditions through buffering data over a certain time window (referred as "buffering window") and perform appropriate interpolation to deal with data losses. In the fixed latency tests, it was found that, for 100 ms buffering window, the maximum latency limits at the regional and wide-area networks are around 82 ms and 78 ms respectively. For LCs, even if one of communication links between the RAs and the LCs experience a communication latency larger than the maximum limit, it could lead to the EFCC controllers exhibiting different behaviours. If the LC misses data from two out of three RAs (i.e. the confidence level becomes smaller than the configurable threshold of 50%), this will lead to the LC losing wide area visibility and it will automatically switch to local mode.

For the jitter tests, generally the higher of the mean latency and jitter level will result in a higher probability that the packets will exceed the maximum latency limit, thus being discarded by the controllers. From the tests, it was found that, the statistical nature of jitter would lead to the LC's behaviour being inconsistent. A mathematical analysis has been conducted to evaluate the probability of the EFCC scheme can function as required at different latency and jitter levels. Specifically, to achieve 90% of confidence that the EFCC scheme can maintain wide-area visibility in order to make correct decisions for a period of 500 ms following an event, the jitter needs to be controlled within 10.2 ms for a mean latency of 60 ms and 13 ms for a mean latency of 50 ms. A comprehensive probability analysis across a wide range of mean latency values is included in the report.

Similar to the jitter tests, in random loss of packet tests, it was found that as the loss of packets rate increased, the EFCC scheme became more likely to experience compromised behaviours. To achieve 90% of confidence that the EFCC scheme will make correct decisions for a period of 500 ms following an event, the loss of packet rate needs to be smaller than 3.8%.

For BER tests, it was found that in the regional network, if the BER exceeds 10^{-2} , the data from the PMU will be discarded by the RAs. In the wide-area network, this value is 10^{-5} . It was also found that when a BER of 10^{-5} at the wide area network is the limit at which the EFCC can still exhibit a desirable behaviour during frequency and fault disturbances.



LIST OF ABBREVIATIONS

BER	Bit Error Rate
CS	Central Supervisor
EFCC	Enhanced Frequency Control Capability
GB	Great Britain
LC	Local Controller
NG	National Grid
NIC	Network Innovation Competition
PMU	Phasor Measurement Unit
PNDC	Power Networks Demonstration Centre
RA	Regional Aggregator
RoCoF	Rate of Change of Frequency
UoS	University of Strathclyde

Contents

Executive summary	3
List of abbreviations	4
1 Introduction	7
2 Objectives	7
2.1 Evaluation of the impact of wide-area networks' communication performance	7
2.2 Evaluation of the impact of regional networks' communication performance	7
2.3 Evaluation of the EFCC scheme's behaviour under degraded communication conditions	8
3 Data recording	8
4 Test limitations	8
5 Impact of communication performance on the confidence levels of the EFCC controllers	8
5.1 Overview of communication networks required to support the EFCC operation	8
5.2 Emulation of wide-area communication network: RAs to LCs	10
5.3 Emulation of the regional communication network: PMUs to RAs	24
6 Performance of the EFCC scheme during system disturbances with degraded communication conditions	25
6.1 Test 0: base case - EFCC's operation with ideal communication networks	26
6.2 Test 1: latency between RA1 and LC1 exceeding the latency limit	28
6.3 Test 2: latency between RA2 to LC1 exceeding latency limit	30
6.4 Test 3: latency between RA3 to LC1 exceeding latency limit	32
6.5 Test 4: latency between RA2 and RA3 to LC1 exceeding latency limit	35
6.6 Test 5: EFCC scheme performance under high latency and jitter	38
6.7 Test 6: EFCC scheme performance with loss of packets	44
6.8 Test 7: EFCC scheme performance with high BER (10^{-5})	48
6.9 Summary of the tests:	50
7 Key findings and conclusions	51
8 References	52
Appendix A: Physical network connections for the communication impact tests	53
Appendix B: Test results for the emulation of the wide-area communication network using a buffering window of 200 ms	54
B1. Impact of latency	54
B2. Impact of latency with jitter	54
Appendix C: Test results for the emulation of the regional communication network	57
C1. Impact of latency	57
B2. Impact of latency with jitter	58
B3. Impact of BER	59
B4. Impact of loss of packets	60
Appendix C: Resource availability information	62
Appendix D: Mathematical analysis of the impact of jitter and loss of packets	63



Appendix E: Raw data for the statistical analysis of impact of jitter and loss of packets..... 65

1 INTRODUCTION

The role of the UoS within the EFCC project is to provide a realistic testbed using the facilities at the PNDC to conduct comprehensive validation of the scheme against its design specifications. The tests presented in this report focus on the evaluation of the impact of communication performance on the operation of the EFCC scheme and this report is Part 3 of a set of total three reports, where the other two reports focus on the testing of EFCC's local and wide-area operational modes respectively.

The operation of the EFCC scheme requires two main types of communication networks: the wide-area communication between the RAs and LCs, and regional communication network between PMUs and RAs (the functionalities of the RAs and LCs are described in [1] and the operation of the EFCC scheme with these two types of communication networks are further discussed in Section 5). In this work, the impact of the communication performance of both of the networks have been evaluated under different values of the following communication parameters:

- Latency: the communication delay for sending data from one device to the receiving device.
- Latency with jitter: the communication delay is normally not a constant in a communication network, so the latency with jitter refers to the changes in communication delay.
- Rate of loss of packets: communication packets might be lost during the data transmitting process. Rate of loss of packets refers to the percentage of packets that were lost during the data transmission.
- BER: in digital communications, the transmitted data may experience bit errors (e.g. binary value of "1" changes to "0"). BER refers to the rate where the number of bits with errors over the total number of transmitted bits.

In this work, a communication emulator [2] was used to emulate a wider range of the above degraded communication conditions. The EFCC scheme's performance with degraded communication conditions during frequency and fault events is also tested and compared against the case with ideal communication. In the tests presented in this report, "ideal" communication networks or links are used to refer to the case where there is no intentionally introduced delay, loss of packets, etc.

This document is organised as follows: Section 2 defines the objectives of the tests presented in this report. Section 3 describes the data that was recorded in the tests; Section 4 discusses the assumptions of the tests conducted. In Section 5, test results for evaluating the impact of the various emulated communication conditions on the EFCC controllers' confidence levels are presented. In Section 6, the performance of the EFCC scheme during frequency and fault events with various emulated degraded communication conditions is evaluated. Section 7 provides conclusions and highlights the key findings from the tests.

2 OBJECTIVES

2.1 Evaluation of the impact of wide-area networks' communication performance

LCs can be distributed at different locations in the transmission and distribution systems, so the communication between the RAs and LCs is over a wide area and it is referred to as a wide-area communication network in this report. The impact of various communication parameters in the wide-area communication network on the operation of the LCs will be evaluated.

2.2 Evaluation of the impact of regional networks' communication performance

RAs receive real-time measurement data from a set of PMUs installed within their corresponding region. The communication networks between these PMUs and the RAs are referred as regional communication networks in this report. The quality of the data from PMUs will affect the regional aggregation that is performed within the RAs, and subsequently affect the system aggregation in the LCs, which is directly linked to the event detection and resource allocation functions. Therefore, one objective of these tests is to evaluate how the RAs and LCs will be affected when the regional network have degraded communication performance.

2.3 Evaluation of the EFCC scheme's behaviour under degraded communication conditions

The first two objectives focus mainly on evaluating how various emulated communication conditions affect the EFCC controllers in receiving and processing data, i.e. the impact on the controllers' confidence levels. However, the reduction in confidence levels does not necessarily mean it will affect the EFCC scheme's operation as the EFCC scheme has a built-in interpolation mechanism to handle data losses and bad data. Therefore, the EFCC scheme will also be tested during both frequency and fault events with a wide range of emulated conditions to evaluate the limits of the communication degradation level that the EFCC scheme can tolerate in order to provide desirable response.

3 DATA RECORDING

In the tests presented in this report, test results are all recorded in PhasorPoint [3]. The data captured from each type of EFCC controllers are listed below:

- **LCs:** system frequency, local frequency, system Rate of Change of Frequency (RoCoF), local RoCoF, positive power request command, negative power request command, system confidence level, event detection, fault detection flag and system RoCoF quality.
- **RAs:** aggregated regional angle and frequency, regional angle and frequency's confidence levels and fault detection flag.
- **PMUs:** frequency, RoCoF, voltage magnitude and angle.

4 TEST LIMITATIONS

As mentioned previously, there are two main types of communication networks involved in the EFCC operation, i.e. wide-area network connecting RAs and LCs and regional network connecting the PMUs and RAs. In reality, the performance of both communication networks will both affect the operation of the EFCC scheme. In the tests, as there is only one communication network emulator is available, regional and wide-area communication network cannot be emulated simultaneously and only one type of network is emulated at a time in the tests. Although this does not entirely reflect the actual communication condition, the purpose the tests is mainly to quantify the impact of the communication performance on the EFCC operation, so emulating the communication network individually will not affect the overall impact evaluation.

5 IMPACT OF COMMUNICATION PERFORMANCE ON THE CONFIDENCE LEVELS OF THE EFCC CONTROLLERS

5.1 Overview of communication networks required to support the EFCC operation

The design and functionalities of the EFCC scheme are fully documented in [1]. The scheme, as shown in Figure 1, mainly relies on fast-real-time communication (as indicated in yellow lines with high report rates, e.g. 50 frames/s) for real-time measurement and monitoring purposes (from PMUs to RAs and from RAs to LCs) and near-real-time communication for sharing resource and system operating condition information (in the order of seconds). In this report, the focus of the tests will be placed on the testing of fast-real-time communication paths, because these communication links are time-critical and could be directly affected by the changes in communication performance, and as such can have a bearing on the control scheme performance. The near-real-time communication between CS and LCs is not tested, as it is less sensitive to communication delays (further details are available in [1]).

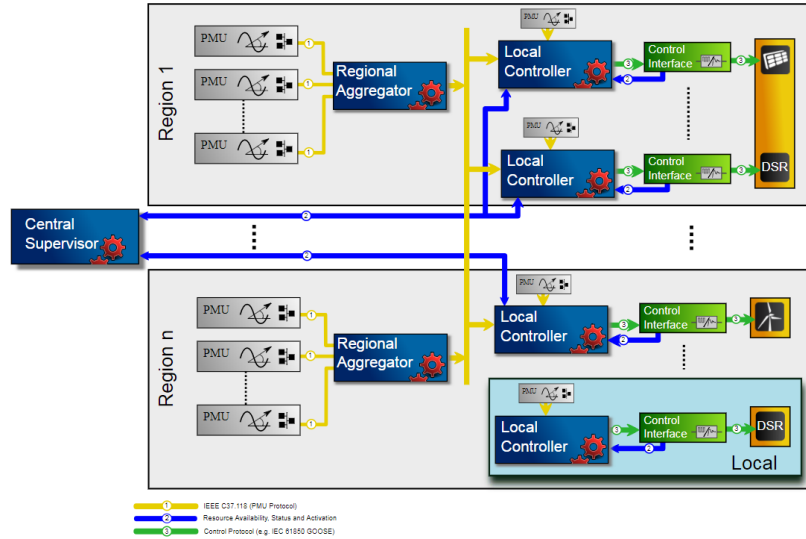


Figure 1. Schematic of the EFCC scheme

Figure 2 presents the schematic of the tested EFCC scheme, where only real-time communication links are shown. PMUs are installed across the network for real-time measurement of phase, frequency and RoCoF. The measured data is aggregated and processed at regional levels by the RAs and fed to all LCs for decision making [4]. According to the EFCC scheme user manual [1], confidence levels are defined, for both RAs and LCs, to evaluate the quality of the received data. For RAs, the confidence levels are used to evaluate the percentage of good quality data from PMUs for each sample. Similarly, for LCs, the confidence levels are used to evaluate the percentage of good quality data from RAs. The definition of good or bad quality of the data is defined as part of the IEEE C37.118.2 standard [5].

In the RAs, a weighting factor (W_{PMU}^i) is assigned to each PMU's measurement to reflect that PMUs observability of the surrounding inertia in the region. The confidence level of the region is defined to assess the quality and the availability of PMU data in the RA and it can be calculated based on the following equation [1]:

$$C_{RA} = \frac{\sum W_{PMU}^i \times Q_{PMU}^i}{\sum W_{PMU}^i}$$

where C_{RA} is the confidence level of the RA; W_{PMU}^i and Q_{PMU}^i are the weighting and data quality of the i^{th} PMU in a region respectively.

In the LC, the confidence level is defined in a similar method:

$$C_{LC} = \frac{\sum W_{RA}^i \times Q_{RA}^i}{\sum W_{RA}^i}$$

where C_{LC} is the confidence level of the LC; W_{RA}^i and Q_{RA}^i are the weighting and data quality of the i^{th} RA in the system respectively.

In this report, the focus is on testing the impact of communication performance, so the weightings of all PMUs and RAs are set as equal. For example, if an LC expects data packets from three RAs at each time instance, and one of the RAs' packets is lost or is with poor quality such that it cannot be used, then the confidence level at that time instance will drop by one third to 66.67%.

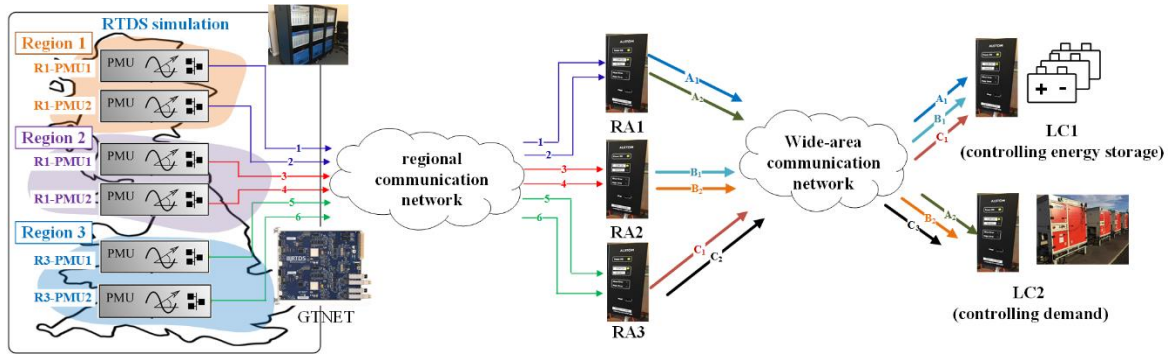


Figure 2. EFCC scheme operation with regional and wide-area communication networks

As shown in Figure 2, the real time communication involves a regional communication network between PMUs and RAs, and the wide-area communication network between RAs and LCs. In this section, emulation of both wide-area and regional communication networks will be conducted with different communication performance conditions to evaluate their impact on the RAs' and LCs' confidence levels.

It should be noted that, reduction in confidence levels does not necessarily mean it will affect the normal operation of the EFCC scheme as it has a built-in interpolation mechanism, as shown in Figure 3, to handle poor communication conditions. The communication condition limits for the correct operation of the EFCC scheme during frequency disturbances are evaluated in Section 6 (except for the fixed latency limit, as the interpolation mechanism will not work in the case where the latency permanently exceeds the maximum limit, which is evaluated in Section 5.2.2).

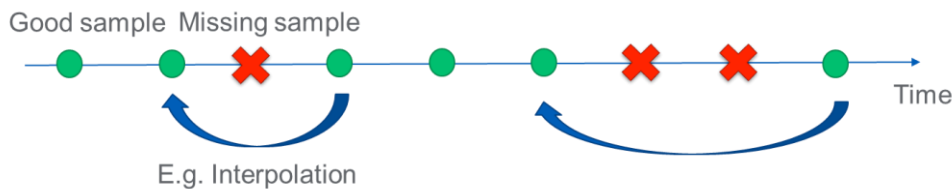


Figure 3. Interpolation of missing data in EFCC

5.2 Emulation of wide-area communication network: RAs to LCs

5.2.1 Wide-area network test configuration

The experimental setup for emulating wide-area network communication performance to evaluate its impact on the EFCC scheme is shown in Figure 4. The Great Britain (GB) transmission network, modelled in RTDS, is divided into three regions. Each region equipped with an RA receiving real-time measurements from two PMUs modelled in RTDS for aggregating PMU measurements through regional communication networks.

The aggregated signals from the RAs are forwarded to the LCs, installed at resource sites providing EFCC-type frequency response, through a wide-area communication network. In this setup, there are two LCs being tested. An off the shelf communication emulator [2] is used to emulate a wide range of communication conditions in the wide-area communication network. In this set of tests, the emulator is used to emulate the wide-area network between the RAs and LCs. No degraded communication conditions were emulated in the regional network between PMUs and RAs. The physical connections of the various controllers and communication devices is provided in Appendix A.

The built-in interpolation mechanism is based on buffering data over a certain time window, which is configurable in the RAs and LCs [1]. In the tests presented in this report the size of the buffering window is set as 100 ms, which is chosen based on the recommendations from GE considering the feasibility of actual communication network implementation and response speed requirements for the EFCC scheme during disturbances. A buffering window of 200 ms were also tested and the results were presented in Appendix B.

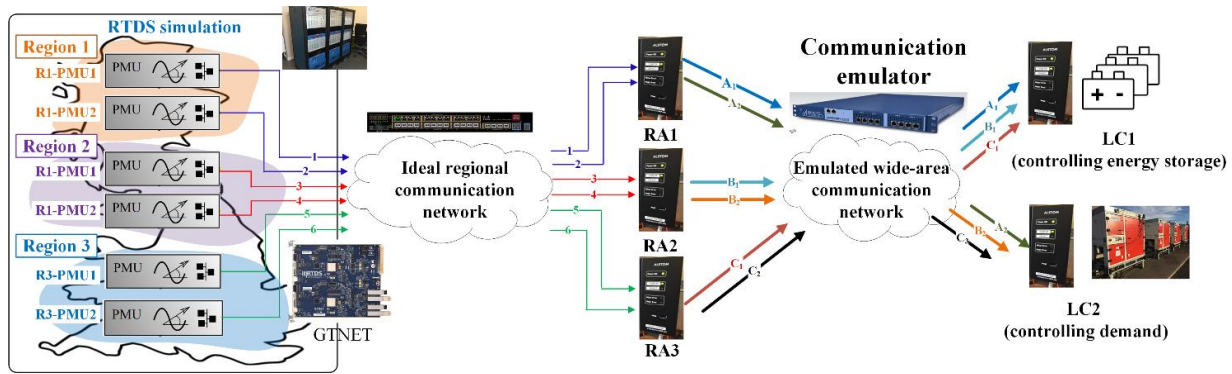


Figure 4. Test setup for emulating wide-area network communication impact on the EFCC scheme

5.2.2 Impact of latency

In this test, fixed latencies were introduced in the communication links between the RAs and LC1. The communication links between the RAs to LC2 remain ideal for comparison. The test results are shown in Figure 5. The communication network emulation parameters and the key observations are presented in Table 1. The numbers in circles Figure 5 correspond to the numbered time show in Table 1.

The first plot in Figure 5 shows the confidence levels measured in the two LCs. The second plot shows the RoCoF quality of the LCs, which is an indicator whether the LCs have wide-area visibility for evaluating system aggregated RoCoF. The last plot shows the system RoCoF measured by the LCs. It should be noted that the changes in RoCoF are caused by small disturbances that were intentionally introduced during the tests to more clearly show how the degraded communication conditions can affect RoCoF measurements.

From the test results, it can be seen that, when the latency between RA1 and LC1 increased to 78 ms, the confidence level dropped by 1/3 at T_2 , i.e. the data from RA1 is no longer considered as good quality. Similar results are also observed for the link between RA2 and LC1. When the data from RA1 and RA2 both cannot be used by LC1, the RoCoF quality signal dropped to zero and the measured RoCoF also became zero.

From this test, it can be found that, for a buffering window size of 100 ms, the maximum latency limit between the RAs and the LCs that cannot be violated is 78 ms. According to GE’s feedbacks from various steering group meetings, the difference between the 78 ms latency limit and the 100 ms buffering window could be due to the fact that the packets are sent every 20 ms from RAs.

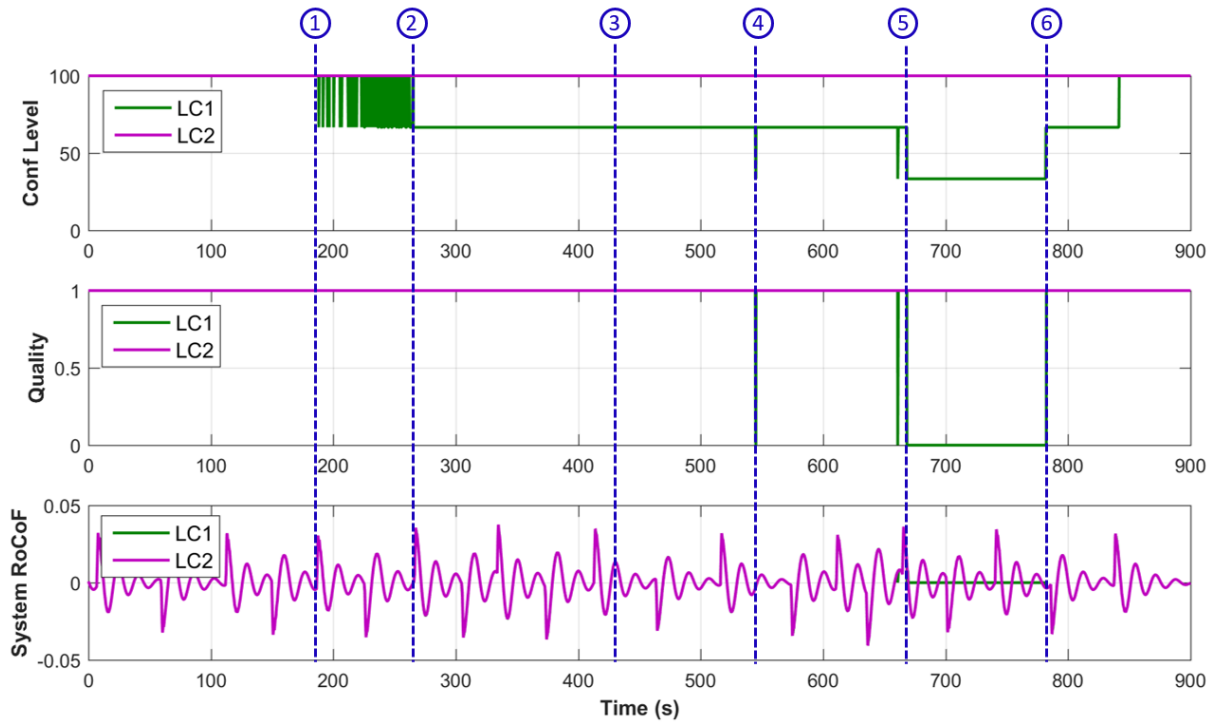


Figure 5. Impact of fixed latency in the wide-area network

Table 1. Key observations of fixed latency test in the wide-area network

Time	Observations
T ₁ (180 s)	<ul style="list-style-type: none"> • Latency between RA1 and LC1 increased from 0 ms to 77 ms. • LC1 confidence level started dropping to 66.67% frequently.
T ₂ (260 s)	<ul style="list-style-type: none"> • Latency between RA1 and LC1 increased to 78 ms. • LC1 confidence level dropped to 66.67%.
T ₃ (420 s)	Latency between RA2 and LC1 increased from 0 ms to 76 ms.
T ₄ (540 s)	<ul style="list-style-type: none"> • Latency between RA2 and LC1 increased to 77 ms. • LC1 confidence level started dropped to 33.33% occasionally.
T ₅ (660 s)	<ul style="list-style-type: none"> • Latency between RA2 and LC1 increased to 78 ms. • LC1 confidence level dropped to 33.33%. • LC1 RoCoF quality and the measured RoCoF became 0.
T ₆ (780 s)	Emulated latency started to be reduced to zero from this point.

5.2.3 Impact of latency with jitter

In this test, a range of latencies with jitter was introduced in the communication links between the RAs and LC1. Figure 6 illustrates how communication jitter can affect the data transmission. Assuming a packet is generated by and sent from an RA at T_0 , the LC has a buffering window within which it waits for the packet to arrive (i.e. the LC will wait until T_0 for the packet to arrive). If the packet arrives within the buffering window (as shown in the green circle case), the packet will be used for calculation. However, if the packet arrives beyond the buffering window (i.e. when it arrives, the data is too old to be used for any monitoring and control purposes as shown in the red circle case), the packet will be discarded, which is equivalent to the case where the packet is lost. Jitter is the change in latency, therefore if the jitter leads to the latency varying beyond the buffering window, then the packet risks being discarded.

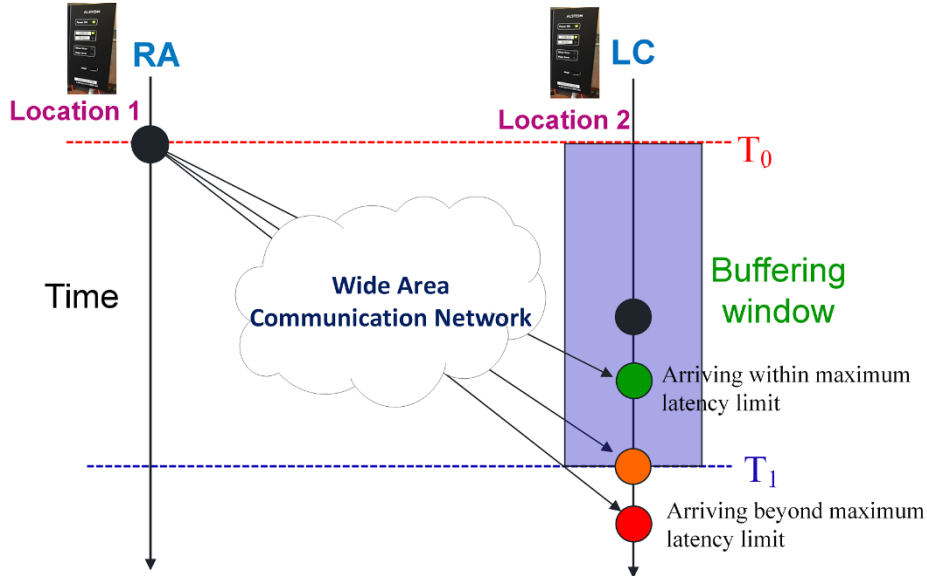


Figure 6. Impact of packets with communication jitter

In the tests, the emulated jitter follows a normal distribution as described in the following formula [6]:

$$f(x | \mu, \sigma^2) = \frac{1}{\sqrt{2\pi} \sigma} e^{-\frac{(x-\mu)^2}{2\sigma^2}} \quad (1)$$

where x is the latency; $f(x | \mu, \sigma^2)$ is the probability of the latency with a value of x ; μ is the mean latency in ms and σ is the standard deviation in ms. Figure 7 shows an example probability distribution of the latency with a mean latency $\mu = 60 \text{ ms}$ and a jitter level represented with different standard deviation values. For simplicity, in the rest of the report, a jitter level of 8 ms will mean the jitter follows a standard deviation of 8 ms.

It should be noted that the use of normal probability distribution for PMU data jitter is based on the work reported in [7]. However, other types of probability distributions can also be used. The key objective is to evaluate the probability at which the data will exceed the latency limit that could cause performance issues for the EFCC scheme and this has been achieved in Section 6.

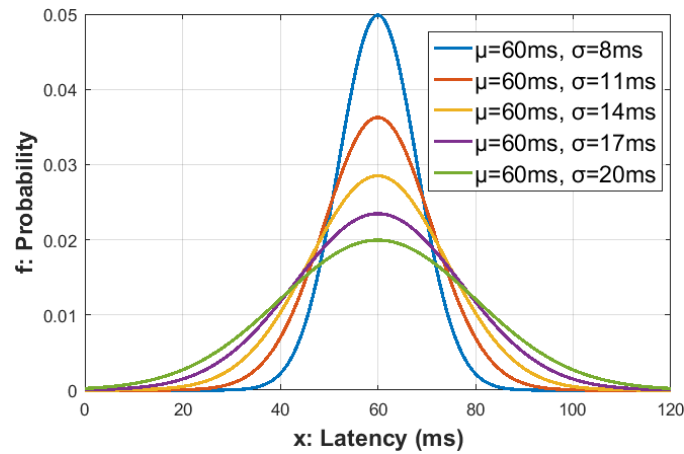


Figure 7. Probability distribution of latency with mean latency of 60 ms and different jitter levels

From Section 5.2.2, it was known that the absolute latency limit between the RAs and the LCs is around 78 ms. Therefore, in this test, a relatively low mean latency (40 ms) and a relatively high mean latency with various levels of jitter are emulated to evaluate how such changes will affect the confidence levels. These values have been chosen only to evaluate how the confidence levels will be affected by the changes in mean latency and jitter levels. The limits of these levels where the EFCC can operate correctly are evaluated in Section 6.

Firstly, a mean latency of 40 ms with jitter increasing from 0 ms to 13 ms were emulated in the communication links between the RAs and LCs. A jitter of 13 ms is the maximum jitter level that can be introduced by the communication emulator for a mean latency of 40 ms¹. The details of the test sequence and emulation parameters are listed in Table 2. The test results are shown in Figure 8.

Then, a mean latency of 70 ms with jitter increasing from 0 ms to 23 ms (the largest configurable jitter at this mean latency level in the communication emulator) were emulated in the communication links between the RAs and LCs. The details of the test sequence and emulation parameters are listed in Table 3. The test results are shown in Figure 9.

¹ This is because if the jitter level (i.e. the standard deviation value σ as presented in Equation (1)) is larger than the maximum configurable value at this mean latency level, it will result in the possibility of latency being a negative value, which does not have physical meanings.

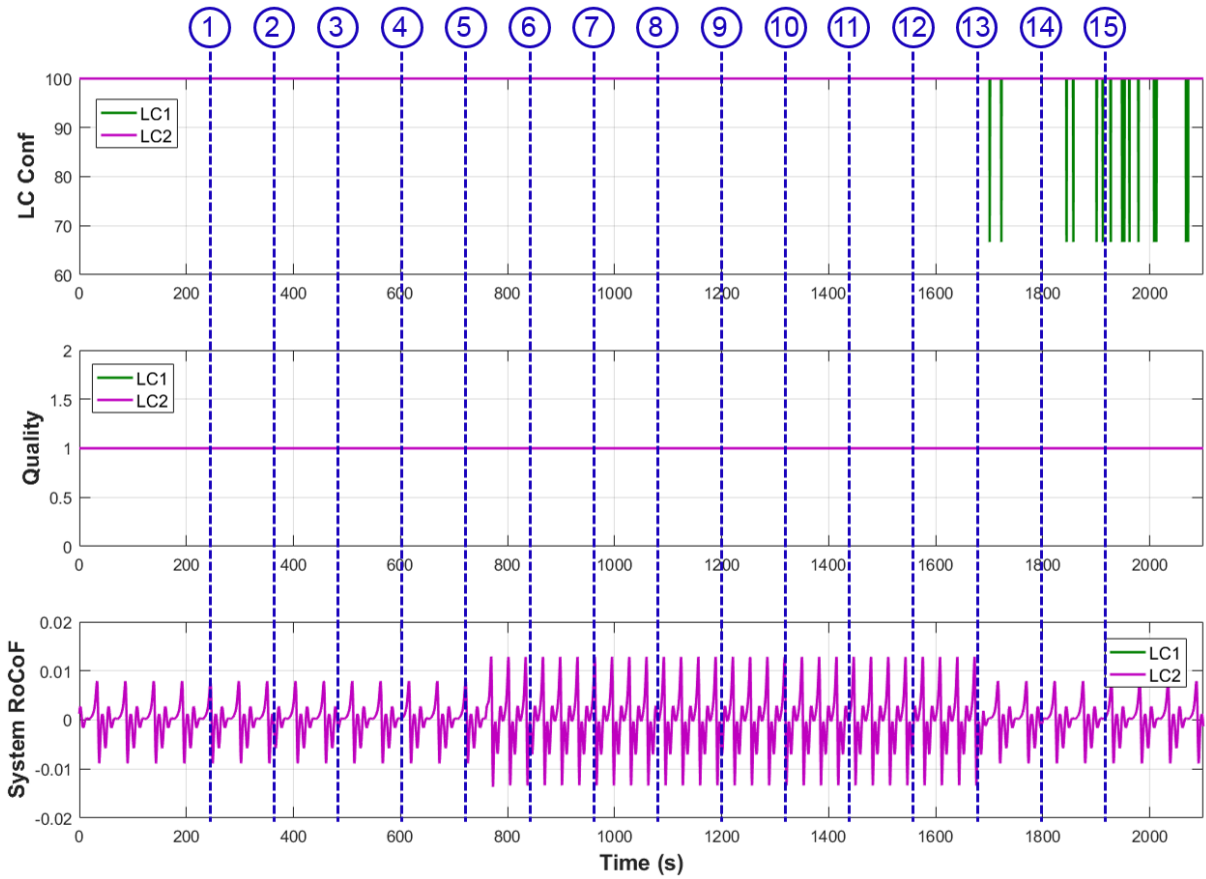


Figure 8. Test results of jitter emulation in the wide-area communication network with a mean latency of 40 ms

Table 2. Jitter emulation in the wide-area communication network with a mean latency of 40 ms

Time	Communication link	Jitter (Standard Deviation σ)
0 s	RA1 to LC1 RA2 to LC1 RA3 to LC1	0 ms
T ₁ (240 s)	RA1 to LC1	5 ms
T ₂ (360 s)	RA2 to LC1	5 ms
T ₃ (480 s)	RA3 to LC1	5 ms
T ₄ (600 s)	RA1 to LC1	7 ms
T ₅ (720 s)	RA2 to LC1	7 ms
T ₆ (840 s)	RA3 to LC1	7 ms
T ₇ (960 s)	RA1 to LC1	9 ms
T ₈ (1080 s)	RA2 to LC1	9 ms
T ₉ (1200 s)	RA3 to LC1	9 ms

T ₁₀ (1320 s)	RA1 to LC1	11 ms
T ₁₁ (1440 s)	RA2 to LC1	11 ms
T ₁₂ (1560 s)	RA3 to LC1	11 ms
T ₁₃ (1680 s)	RA1 to LC1	13 ms
T ₁₄ (1800 s)	RA2 to LC1	13 ms
T ₁₅ (1920 s)	RA3 to LC1	13 ms

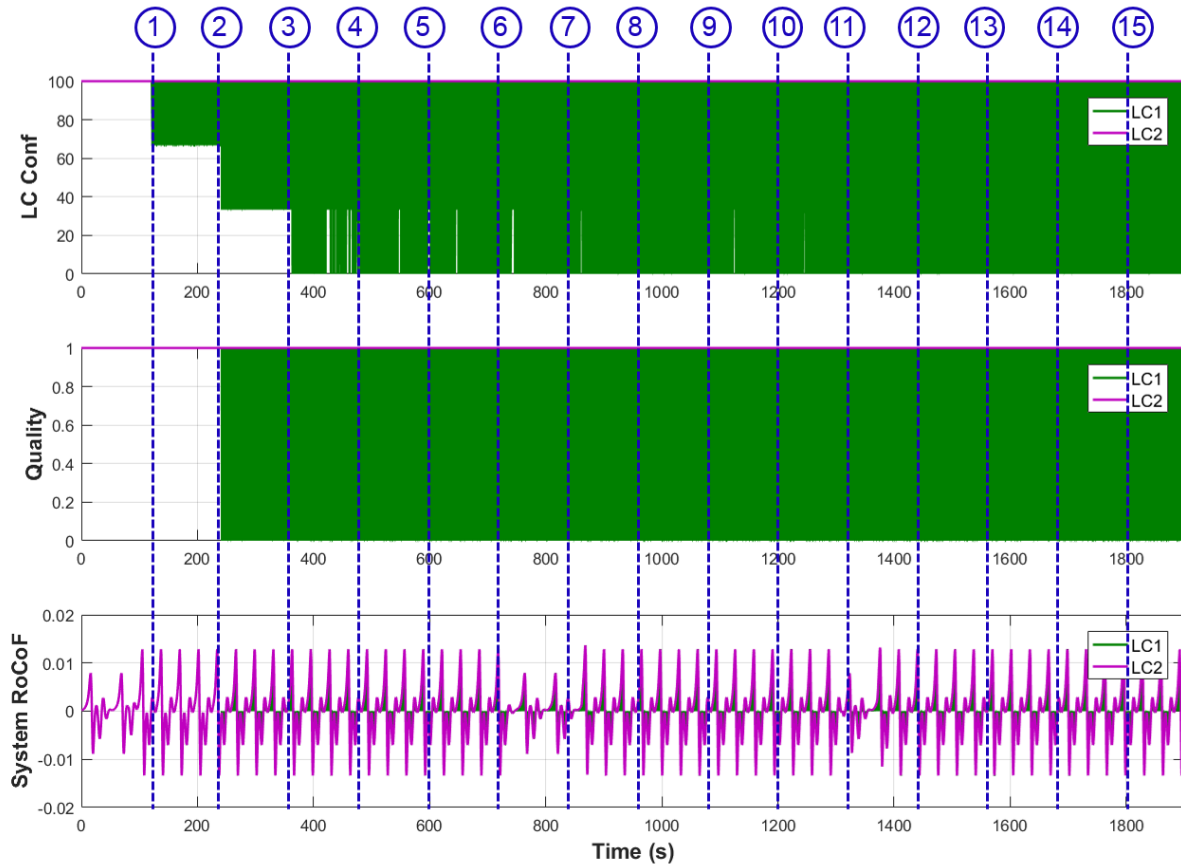


Figure 9. Test results of jitter emulation in the wide-area communication network with a mean latency of 70 ms

Table 3. Jitter emulation in the wide-area communication network with a mean latency of 70 ms

Time	Communication link	Jitter (Standard Deviation)
0 s	RA1 to LC1 RA2 to LC1 RA3 to LC1	0 ms
T ₁ (120 s)	RA1 to LC1	11 ms



T ₂ (240 s)	RA2 to LC1	11 ms
T ₃ (360 s)	RA3 to LC1	11 ms
T ₄ (480 s)	RA1 to LC1	14 ms
T ₅ (600 s)	RA2 to LC1	14 ms
T ₆ (720 s)	RA3 to LC1	14 ms
T ₇ (840 s)	RA1 to LC1	17 ms
T ₈ (960 s)	RA2 to LC1	17 ms
T ₉ (1080 s)	RA3 to LC1	17 ms
T ₁₀ (1200 s)	RA1 to LC1	20 ms
T ₁₁ (1320 s)	RA2 to LC1	20 ms
T ₁₂ (1440 s)	RA3 to LC1	20 ms
T ₁₃ (1560 s)	RA1 to LC1	23 ms
T ₁₄ (1680 s)	RA2 to LC1	23 ms
T ₁₅ (1800 s)	RA3 to LC1	23 ms

It can be seen that from Figure 8, with the increasing levels of jitter between the three RAs and LC1, the confidence level are more likely to reduce, i.e. the data packet is more likely to be discarded by the LC. Comparing the results from Figure 8 and Figure 9, it can be concluded that, the higher the the mean latency, the less tolerant the System RoCoF measurement is to jitter. A zoomed-in view of the test results presented in Figure 9 is shown in Figure 10. It can be seen that, with the increasing mean latency and jitter in the communication links, the probability of LC1 discarding data from two or more RAs will also increase, thus increasing the risk of losing wide-area visibility (the system quality and system RoCoF measurements are more likely to be zero).

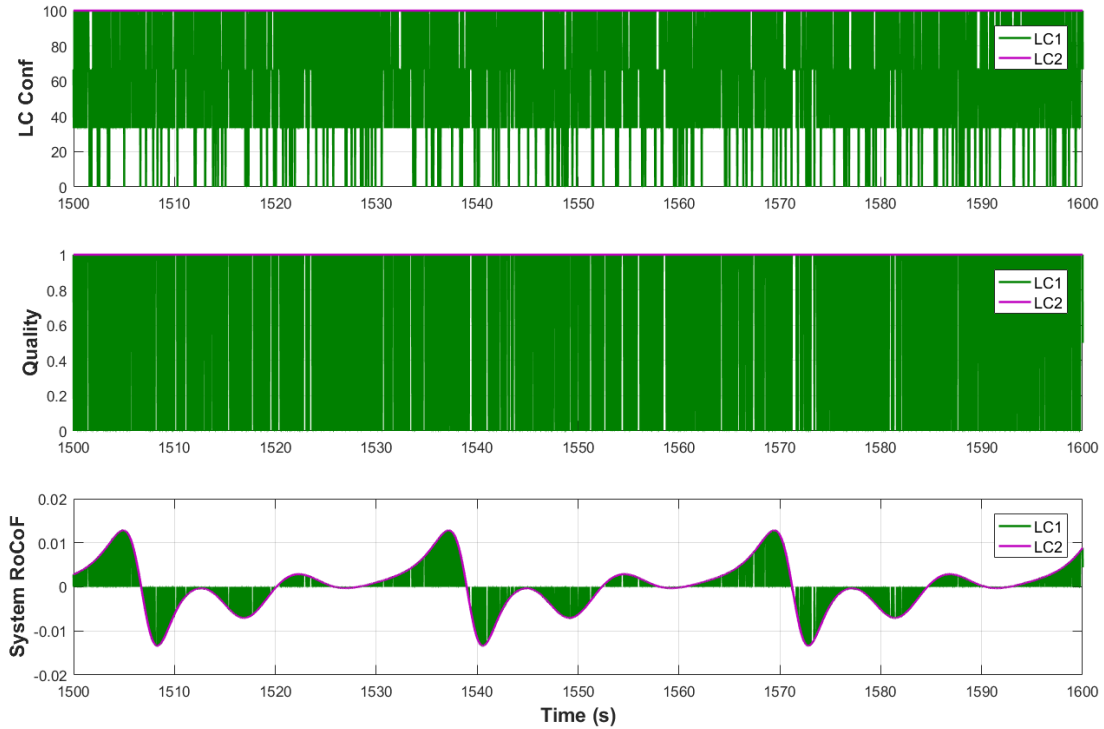


Figure 10. A zoomed-in view of test results of jitter emulation in the wide-area communication network with a mean latency of 70 ms

These findings can be explained by the probability distribution curves for mean latencies of 40 ms and 70 ms as shown in Figure 11 (a) and (b). The absolute max latency as found in Section 5.2.2 is around 78 ms, so whenever the jitter results in a latency larger than 78 ms, the packet will be discarded (because it is considered to be too old to be used with a 100 ms buffering window size setting). From Figure 11, it can be seen that, for the same mean latency, a higher level of jitter will increase the probability of the latency being larger than the maximum limit. Comparing Figure 8 and Figure 9, for same level of jitter, e.g. 11 ms, a larger mean latency will also lead to the latency being more likely to be exceed the tolerable limit.

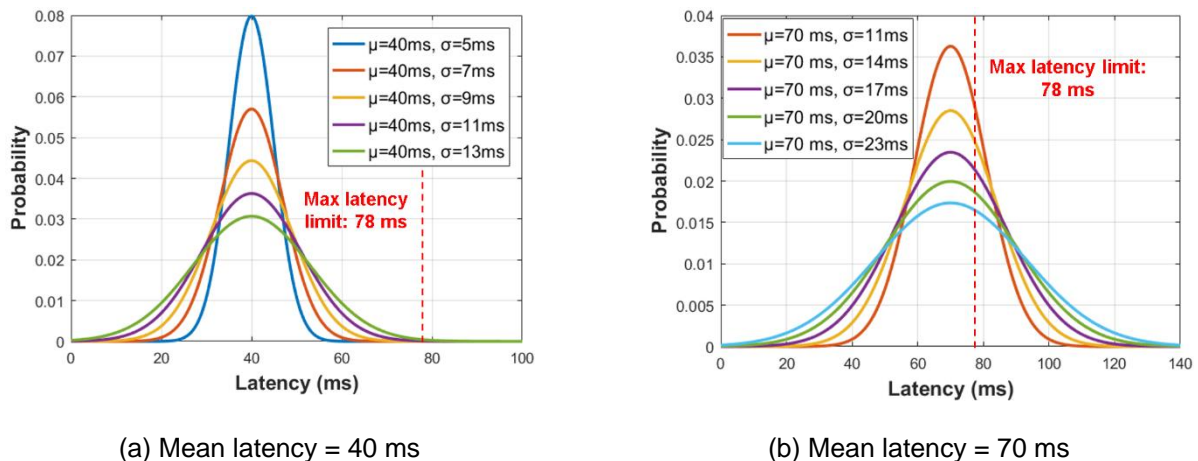


Figure 11. Probability distribution of latency with jitter with maximum LC latency limit shown

5.2.4 Impact of BER

In this test, bit errors were introduced in the communication links between the RAs and LC2. The values of the BERs in the links between the RAs and LC2 were gradually increased from 0 to 10^{-4} , at which point all the packets were discarded by the LCs. The detailed steps of the BER levels introduced

in the various communication links are provided in Table 4 and the test results are shown in Figure 12.

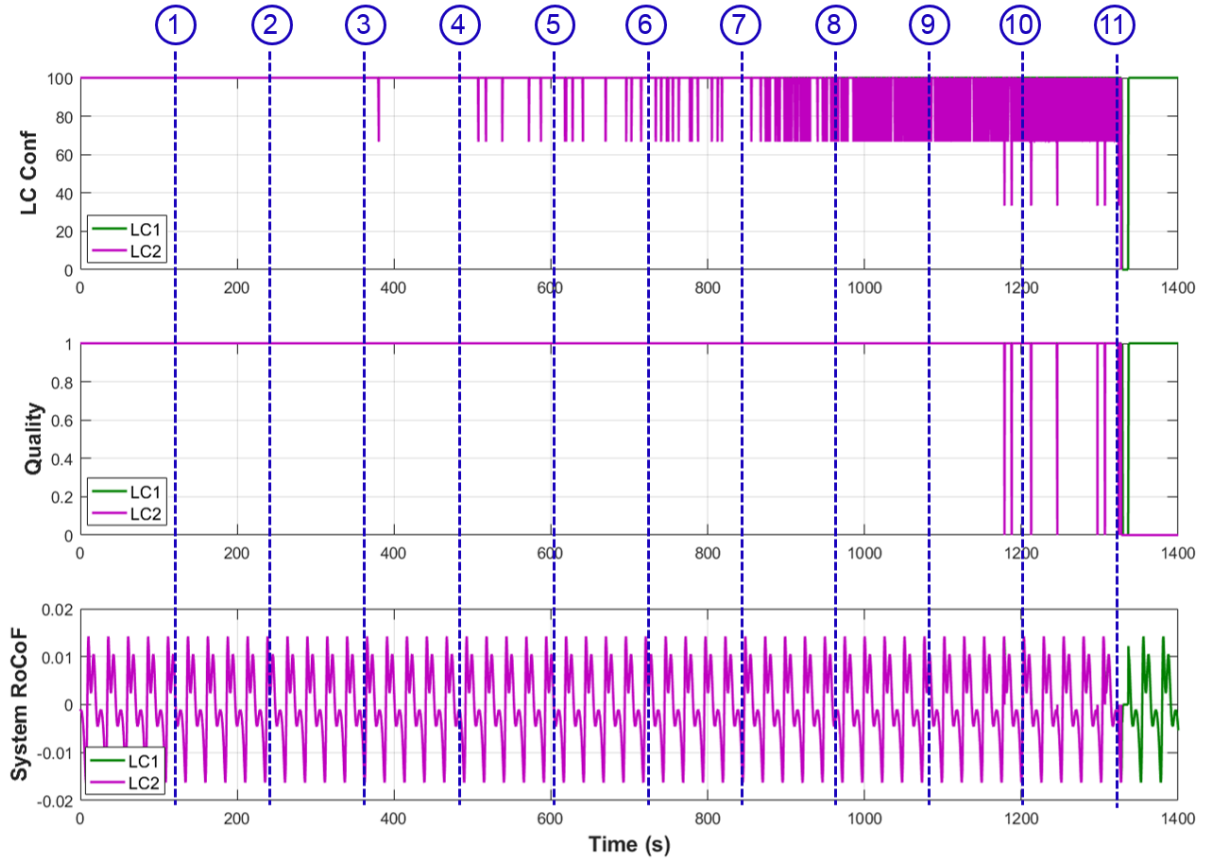


Figure 12. Test results of BER emulation in the wide-area communication network

Table 4. BER emulation in the wide-area communication network

Time	Communication link	BER
0 s	RA1 to LC2 RA2 to LC2 RA3 to LC2	0
T ₁ (120 s)	RA1 to LC2	1 × 10 ⁻⁷
T ₂ (240 s)	RA2 to LC2	1 × 10 ⁻⁷
T ₃ (360 s)	RA3 to LC2	1 × 10 ⁻⁷
T ₄ (480 s)	RA1 to LC2	1 × 10 ⁻⁶
T ₅ (600 s)	RA2 to LC2	1 × 10 ⁻⁶
T ₆ (720 s)	RA3 to LC2	1 × 10 ⁻⁶
T ₇ (840 s)	RA1 to LC2	1 × 10 ⁻⁵
T ₈ (960 s)	RA2 to LC2	1 × 10 ⁻⁵

T_9 (1080 s)	RA3 to LC2	1×10^{-5}
T_{10} (1200 s)	RA1 to LC2	1×10^{-4}
T_{11} (1320 s)	RA2 to LC2	1×10^{-4}

It can be seen that as the BER is increased, the confidence level dropped more frequently and when the two of the links' BER changed from 10^{-5} to 10^{-4} at T_{10} and T_{11} respectively, LC2 completely lost the wide-area visibility - its RoCoF quality became 0 and there was no RoCoF measurement after T_{11} . This shows that the maximum limit of tolerable BER is between 10^{-5} and 10^{-4} . Therefore, further tests were conducted to include BER from 10^{-5} to 10^{-4} with a step of 10^{-5} . The test results are shown in Figure 13: before T_1 , all the links are with BER of 10^{-5} ; at T_1 , the BER at the link between RA1 and LC2 changed to 2×10^{-5} ; and at T_2 , the BER at the link between RA2 and LC2 also changed to 2×10^{-5} . It can be seen that when the BER goes above 10^{-5} at T_2 , the wide-area visibility is lost (with RoCoF quality and measured RoCoF value both dropped to 0).

Therefore, it can be concluded that in order for the LCs to make use of the packets, the BER rate should not exceed 10^{-5} . According to the technical specification for communication services for tele-protection, the required BER should be smaller than 10^{-8} [8]. Therefore, the value of 10^{-5} is a high BER value that the LC can tolerate is a high BER value for power system applications. However, this is only a limit where the LCs can still interpret the packets. The actual limit where the EFCC scheme can still provide the correct functionality is evaluated in Section 6.

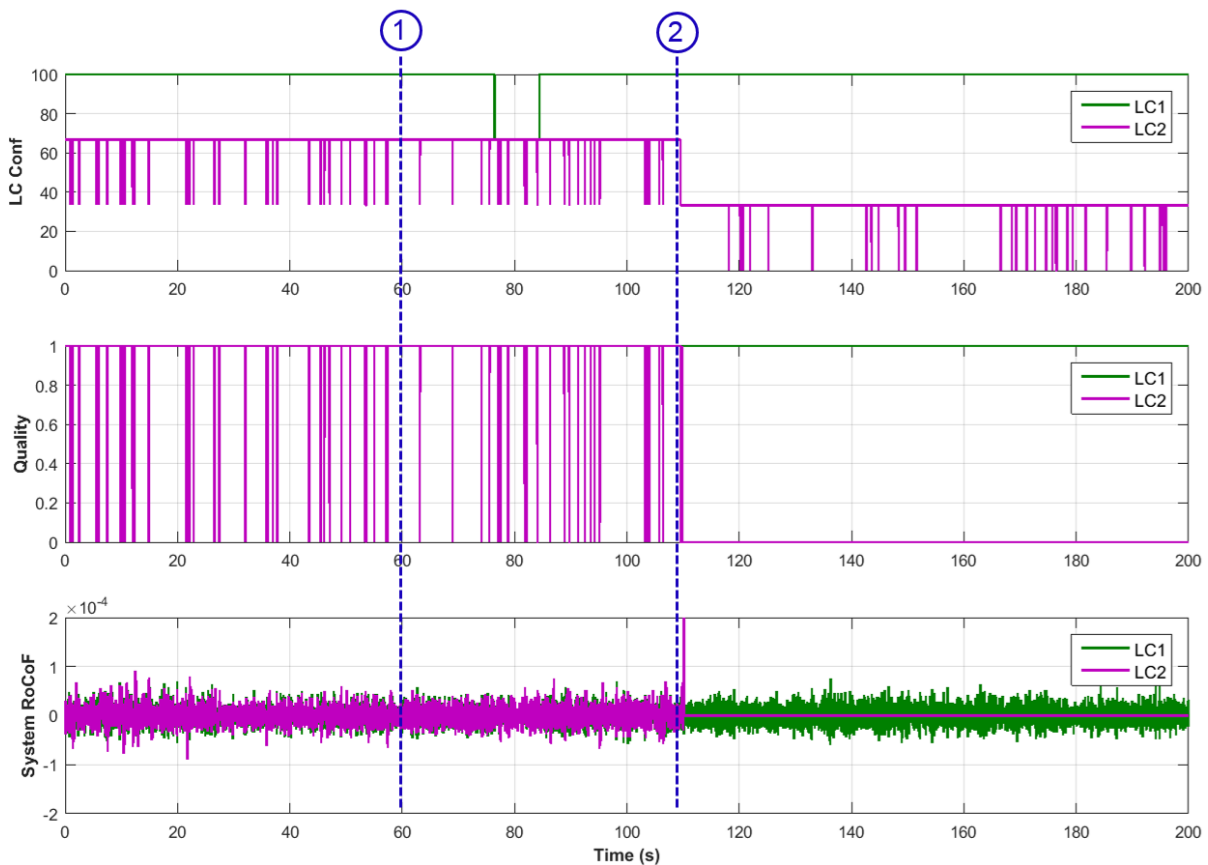


Figure 13. Test results of BER emulation in the wide-area communication network - BER between 10^{-5} and 10^{-4}

5.2.5 Impact of loss of packets

In this test, random loss of packets was introduced in the communication links between the RAs and LC1. The detailed steps of introducing the loss of packets rate at the various communication links are provided in Table 5 and the test results are shown in Figure 14.

It can be seen that as the loss of packets rate increased, the confidence level dropped more frequently and the higher the loss of packets rate is, the probability of data loss from more than one RA was also increased. Figure 15 shows a zoomed-in view of the results presented in Figure 14, where it can be seen that in some instances, the data loss at more than one RA to LC1 link could result in the wide-area visibility being lost.

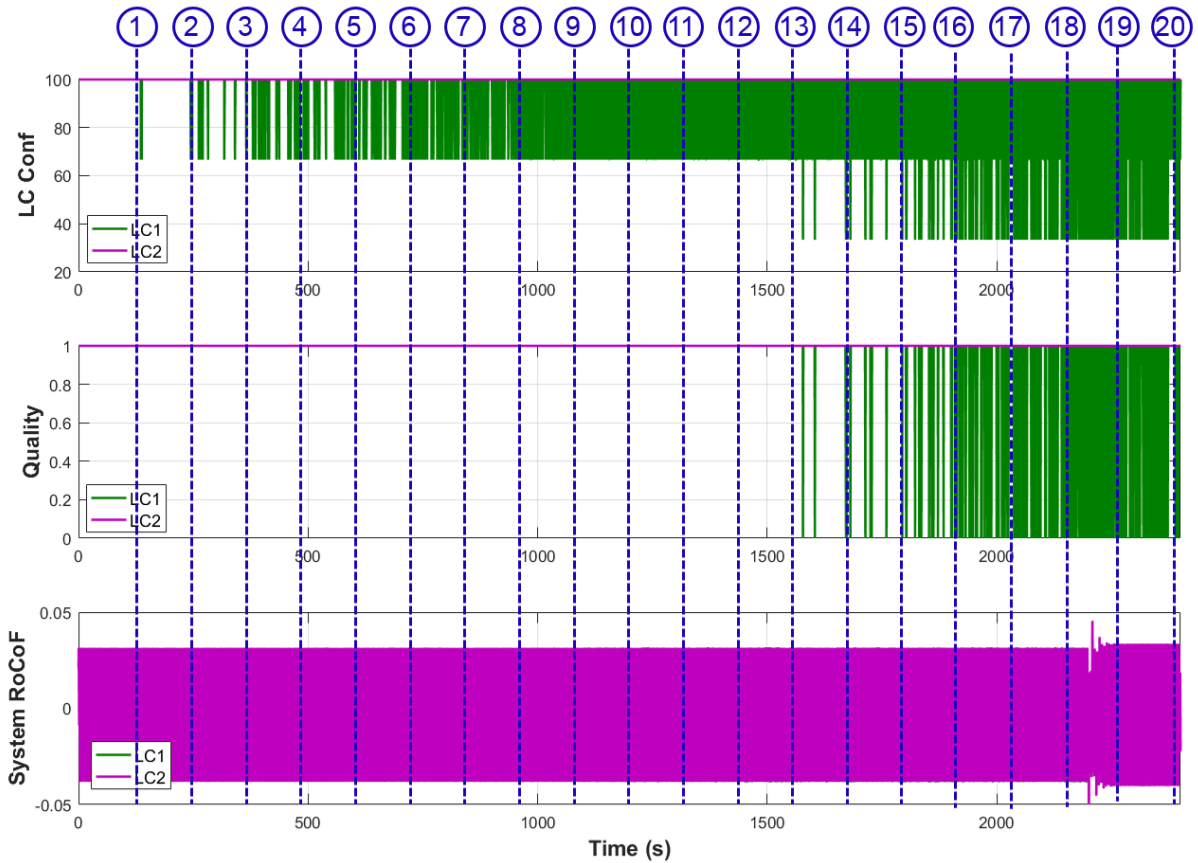


Figure 14. Test results of loss of packets emulation in the wide-area communication network

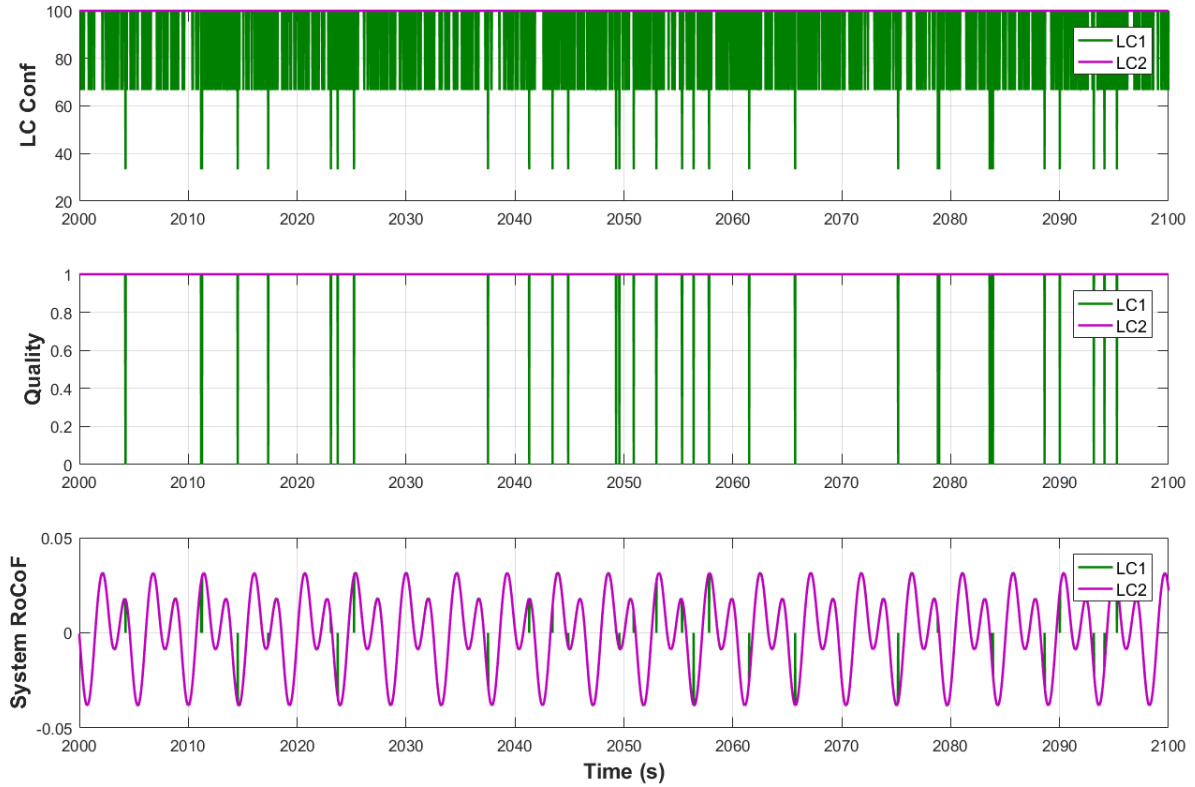


Figure 15. Zoom-in view of the test results of loss of packets emulation in the wide-area communication network

Table 5. Loss of packets emulation in the wide-area communication network

Time	Communication link	Loss of Packets Rate
0 s	RA1 to LC1 RA2 to LC1 RA3 to LC1	0
T ₁ (120 s)	RA1 to LC1	0.1%
T ₂ (240 s)	RA1 to LC1	0.2%
T ₃ (360 s)	RA1 to LC1	0.3%
T ₄ (480 s)	RA1 to LC1	0.4%
T ₅ (600 s)	RA1 to LC1	0.6%
T ₆ (720 s)	RA1 to LC1	0.8%
T ₇ (840 s)	RA1 to LC1	1%
T ₈ (960 s)	RA1 to LC1	2%
T ₉ (1080 s)	RA1 to LC1	4%
T ₁₀ (1200 s)	RA1 to LC1	6%

T ₁₁ (1320 s)	RA1 to LC1	8%
T ₁₂ (1440 s)	RA1 to LC1	10%
T ₁₃ (1560 s)	RA2 to LC1	1%
T ₁₄ (1680 s)	RA2 to LC1	2%
T ₁₅ (1800 s)	RA2 to LC1	4%
T ₁₁ (1920 s)	RA2 to LC1	6%
T ₁₂ (2040 s)	RA2 to LC1	8%
T ₁₃ (2160 s)	RA2 to LC1	10%
T ₁₄ (2280 s)	RA3 to LC1	1%
T ₁₅ (2400 s)	RA3 to LC1	2%

5.2.6 Summary of the tests

In this set of tests, the impact of latency, jitter, BER and loss of packets rate in the wide-area network between the RAs and the LCs on the confidence level (and thus the wide-area visibility represented by RoCoF quality and system RoCoF measurement) have been evaluated.

It was found that, for a 100 ms of buffering window, the absolute maximum latency limit in the communication links is 78 ms.

For the jitter tests, the impact on the confidence levels of the LCs is associated with the probability of the jitter resulting in a latency being larger than the maximum tolerable latency limit. Generally, a higher mean latency has a smaller tolerance of jitter and for the same amount of mean latency, the higher the jitter, the higher the probability that the latency will be beyond the tolerable maximum limit.

For the BER tests, it was found that a higher BER rate will also lead to the reduction of confidence level more frequently and when the BER level increased above 10^{-5} for the three links between the RAs to the LC, the packets can no longer be interpreted by the LC, leading to the wide-area visibility being lost.

For the loss of packets tests, it was found that a higher rate of packet loss will lead to the reduction of confidence level more frequently. It also increased the risk of packets from more than one RA being lost, which will also lead to the loss of wide-area visibility.

The above tests have also been tested with a buffering window of 200 ms and the test results are presented in Appendix B. It should be noted that the change of buffering window size is only relevant to the latency and latency with jitter tests, as the other communication parameters (i.e. loss of packets and BER) are not relating to communication delays. It was found that, when the buffering window is increased to 200 ms, the maximum latency limit increased to 178 ms. Detailed discussion of the impact of jitter levels at this buffering window size is provided in Appendix B.

5.3 Emulation of the regional communication network: PMUs to RAs

5.3.1 Regional network test configuration

The regional communication network refers to the communication network between the PMUs within the regions and the corresponding RAs. The experimental setup for emulating the regional communication network's performance impact on the EFCC scheme is shown in Figure 16. Each region contains two PMUs, e.g. R1-PMU1 and R1-PMU2 are the two PMUs installed in Region 1 and supply real-time measurements to RA1. In this set of tests, the communication emulator was connected between the RTDS and the RAs, so the various communication conditions can be emulated at the communication links between the PMUs and the RAs. The physical connection of the various controllers and communication devices is provided in Appendix A.

The buffering window of RAs in the tests was set to 100 ms and the weighting of all PMUs were set equally. A higher weighting of a PMU means the data quality change of the PMU will affect a larger percentage of the confidence level in the RA. More details about the PMU weighting are available in the user manual [1].

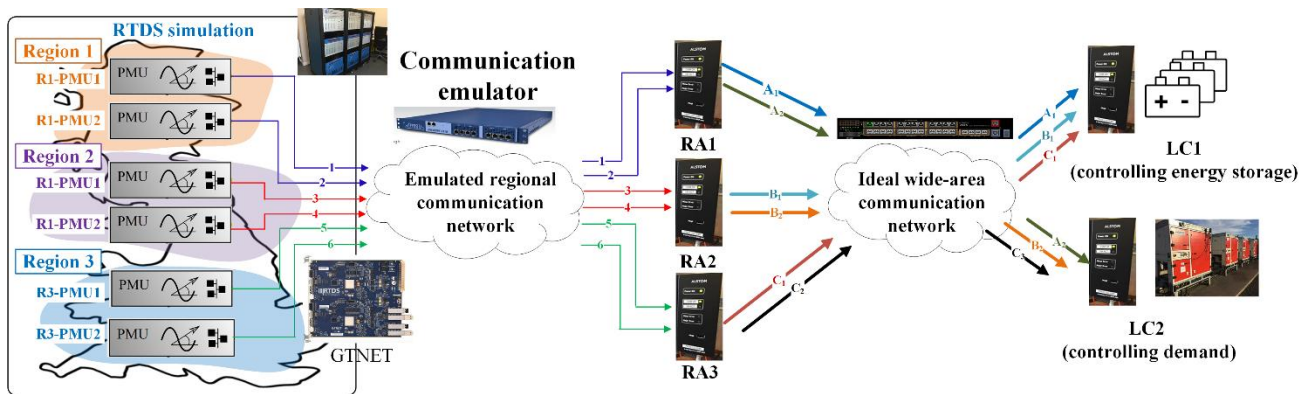


Figure 16. Test setup for emulating the regional network communication parameters and evaluating their impact on the EFCC scheme

5.3.2 Test results of regional communication network emulation

The observations related to changes in different levels of latency, jitter, BER and loss of packets rate are largely similar to the observations from the emulation of the wide-area network, so the test results are provided in Appendix C and summarised below.

5.3.3 Summary of the tests

As mentioned, the impact of the various emulated communication conditions in the regional network on the confidence levels of RAs are largely similar to those in the wide-area network on the confidence levels of LCs. The main differences and additional findings are summarised as follows:

- The maximum tolerable latency limit between the PMUs and the RAs is 82 ms. This is slightly higher than the limit between the RAs and LCs, which is 78 ms. This could be due to the differences between how PMUs and the RAs process and send the data packets.
- The change in the confidence levels at the RAs could also change the confidence levels at LCs. If the confidence level dropped to or under 50% at an RA, the confidence level at all of the LCs will drop by 1/3, i.e. it is considered that the data from this particular RA is no longer valid. From discussion with GE, the threshold of 50% is configurable via settings.
- The maximum BER value allowed between the PMUs and RAs is 10^{-3} . It should be noted that, this value only stands for a limit where the link between PMUs and RAs are not completely lost and it does not mean the EFCC scheme can still function at this level. The levels of BER and other parameters at which the EFCC can still perform its functions are evaluated in Section 6.

6 PERFORMANCE OF THE EFCC SCHEME DURING SYSTEM DISTURBANCES WITH DEGRADED COMMUNICATION CONDITIONS

In this set of tests, the EFCC scheme's behaviour during various system events were evaluated under a range of different communication performance conditions. Both frequency disturbances (i.e. loss of generation events) and fault events were triggered to evaluate the dependability and security of the EFCC scheme under degraded communication network conditions.

The EFCC scheme's event detection and resource allocation functions are performed in the LCs, and the LCs use data from the RAs for decision making. Therefore, the communication emulation is performed in the wide-area communication network, which connects the RAs and LCs. The test setup is the same as in tests presented in Section 5 and is shown in Figure 4.

In the following tests, Test 0 is used as the base case, where no degraded communication conditions are emulated. Tests 1-4 focus on the evaluation of the EFCC's behaviour during disturbances when the latency exceeds the maximum limit as established in Section 5.2.2 (i.e. 78 ms for 100 ms buffering window at the wide-area network). These tests will apply latencies larger than the limit at different communication links connecting the RAs with the LC and evaluate how losing data from different RAs will affect the LCs' operation. Test 5 and Test 6 aim to evaluate the probability of the EFCC scheme can function as required with different level of jitters and loss of packets rates. Test 7 focuses on determining the maximum BER limit.

The under-frequency events used in all of the following tests are a 1 GW loss of infeed in Region 1 as shown in Figure 17. The resource availability information for LC1 and LC2 in all of the frequency disturbance tests is provided in Appendix C.

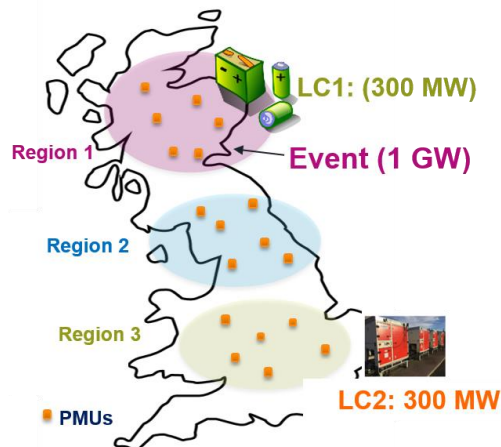


Figure 17. Resource and event location for frequency tests

In order to evaluate the security of the EFCC scheme during faults and under degraded communication network performance, a Phase-Earth (Ph-E) fault is applied at the location shown in Figure 18. The duration of the fault is 80 ms with a fault resistance of 3 Ω . The duration and the resistance of the faults were chosen to be comparable with the faults applied in the dependability tests as presented in Part 2 of the report for evaluating the performance of the EFCC scheme in its wide-area mode.

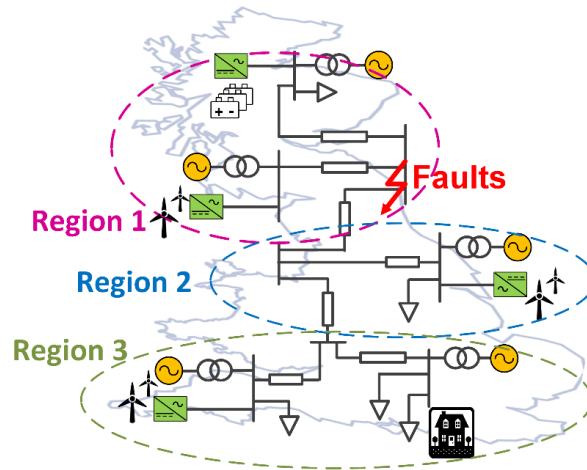


Figure 18. Location of faults for evaluating the EFCC scheme’s performance with degraded communication conditions

6.1 Test 0: base case - EFCC’s operation with ideal communication networks

In this test, the EFCC scheme’s performance with ideal communication conditions (i.e. no intentional latency, jitter, data loss, etc.) was evaluated. The test is used as the base case to evaluate the EFCC scheme’s performance against in the other tests where different degraded communication conditions were emulated.

6.1.1 EFCC scheme’s performance in an under-frequency event

Figure 19 shows the performance of the EFCC scheme during the under-frequency disturbance. It can be seen that both LCs successfully detected the event and instruct power to respond to the event. LC1 is located in the region where the event occurred (region 1), while LC2 is region 3. LC1 responded faster and with a higher amount of active power deployed. By comparing the frequency profile with and without the EFCC response, it can be seen that the frequency nadir has been maintained above 49.50 Hz with the EFCC response, whereas the case without the EFCC response, the frequency nadir dropped to around 49.30 Hz.

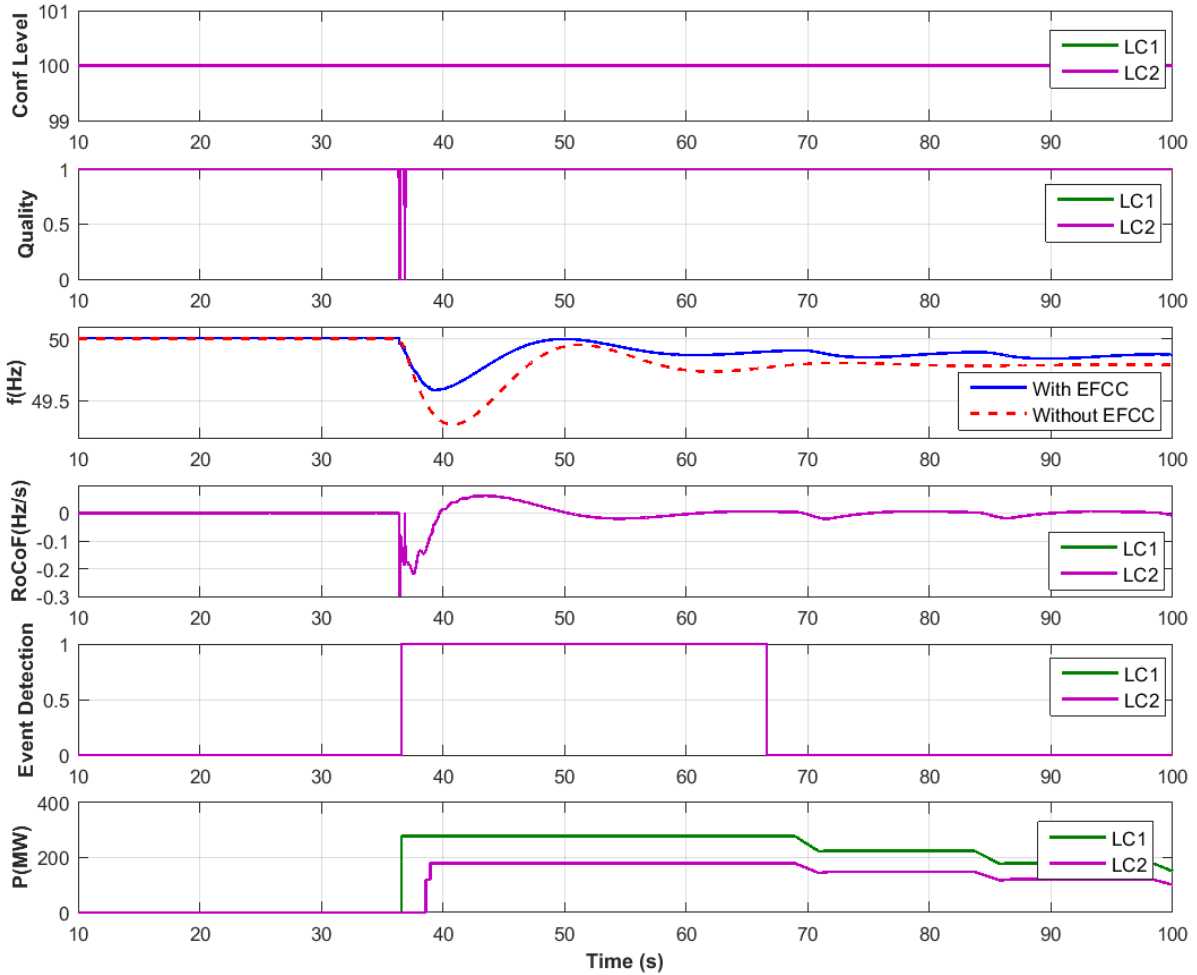


Figure 19. EFCC scheme’s performance during an under-frequency event with ideal communication conditions

6.1.2 EFCC scheme’s performance in a fault event

Figure 20 shows the performance of the EFCC scheme during a fault with ideal communication network conditions. It can be seen that all of the RAs have successfully detected the fault and no response was deployed undesirably. The event detection was also successfully blocked by the fault detection signal, which is desirable based on the design specifications.

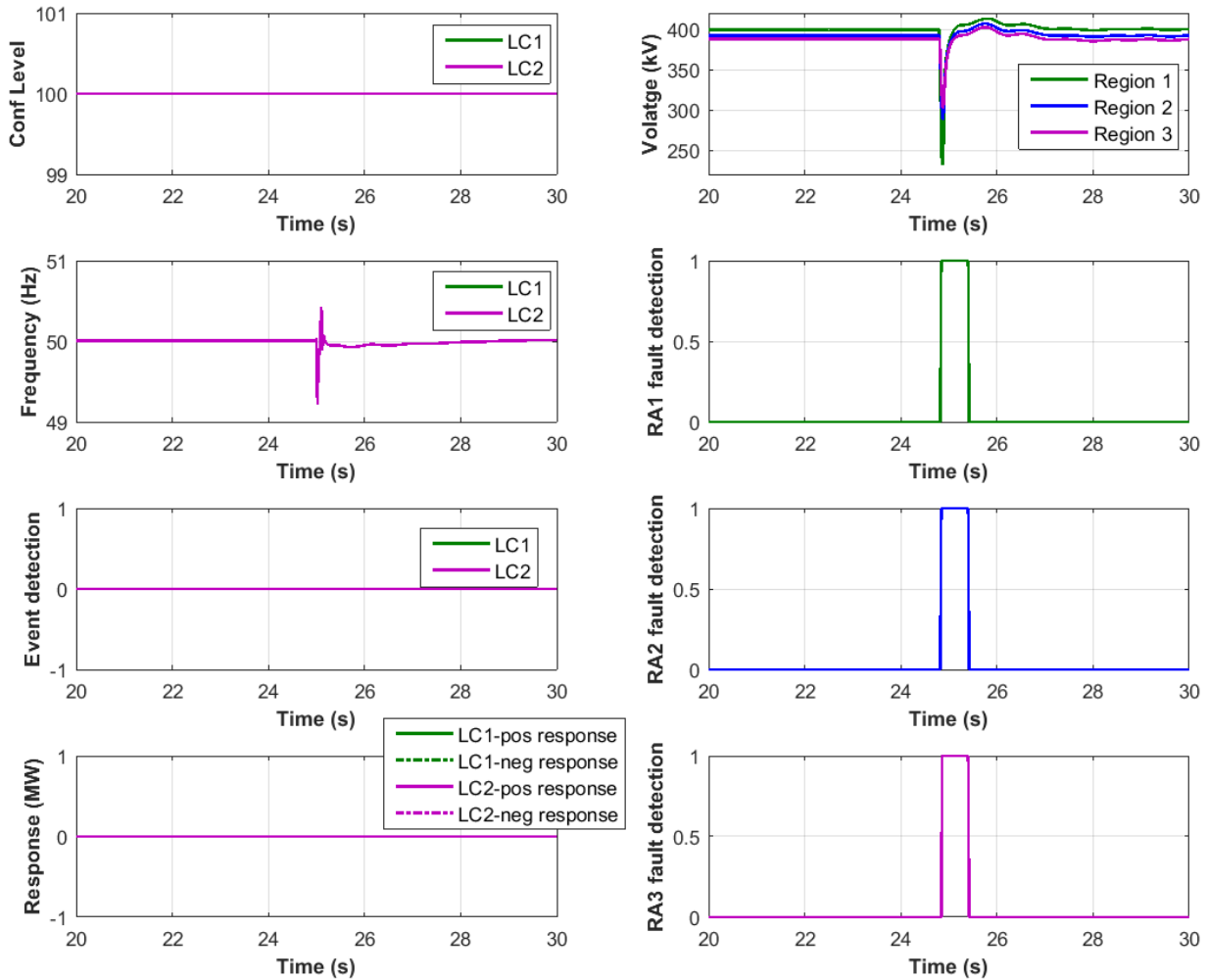


Figure 20. EFCC scheme's performance during a fault event with ideal communication conditions

6.2 Test 1: latency between RA1 and LC1 exceeding the latency limit

In this test, a latency of 100 ms, which exceeded the maximum latency limit of 78 ms, was introduced to the communication link between RA1 and LC1 to evaluate how this affects the EFCC scheme operation during frequency and fault events. For comparison, no degraded communication condition was emulated in the links between the RAs to LC2.

Figure 21 shows the performance of the EFCC scheme during the emulated communication conditions. The first and second plot show the confidence levels and RoCoF quality from the LCs respectively. From the third to the last plot, the frequency profile, EFCC scheme's event detection signal and the resource deployment commands when the EFCC is operating with ideal and emulated degraded communication conditions are presented and compared.

Due to the latency between RA1 and LC1 is beyond the acceptable limit, the confidence level of LC1 dropped to 66.67%. The under-frequency event occurred at around 12.12 s.

In the case with ideal communications, the event was detected at 12.34 s. In the test where latency was introduced between RA1 and LC1 (with LC2's communication links remain unchanged), LC2 still detected the event at 12.34 s while LC1 detects the event 40 ms earlier at 12.30 s. The response deployment commands were also different compared to the base case – the response from LC1 was slower and with a smaller amount. As a result, the frequency nadir was lower than the base case with ideal communication conditions.

According to the EFCC user manual [1], the event detection and resource allocation functions in the LCs are based on the analysis of the data from RAs. In this test, when the latency at one of the RAs exceeded the maximum limit, the data from that particular RA will be excluded from the calculation, therefore, it will affect both event detection and the resource allocation functions. This is evident by the test results. The tests presented in the following sections will illustrate the impact on the EFCC's behaviour when the latency at the communication links with different RAs exceed the maximum limit.

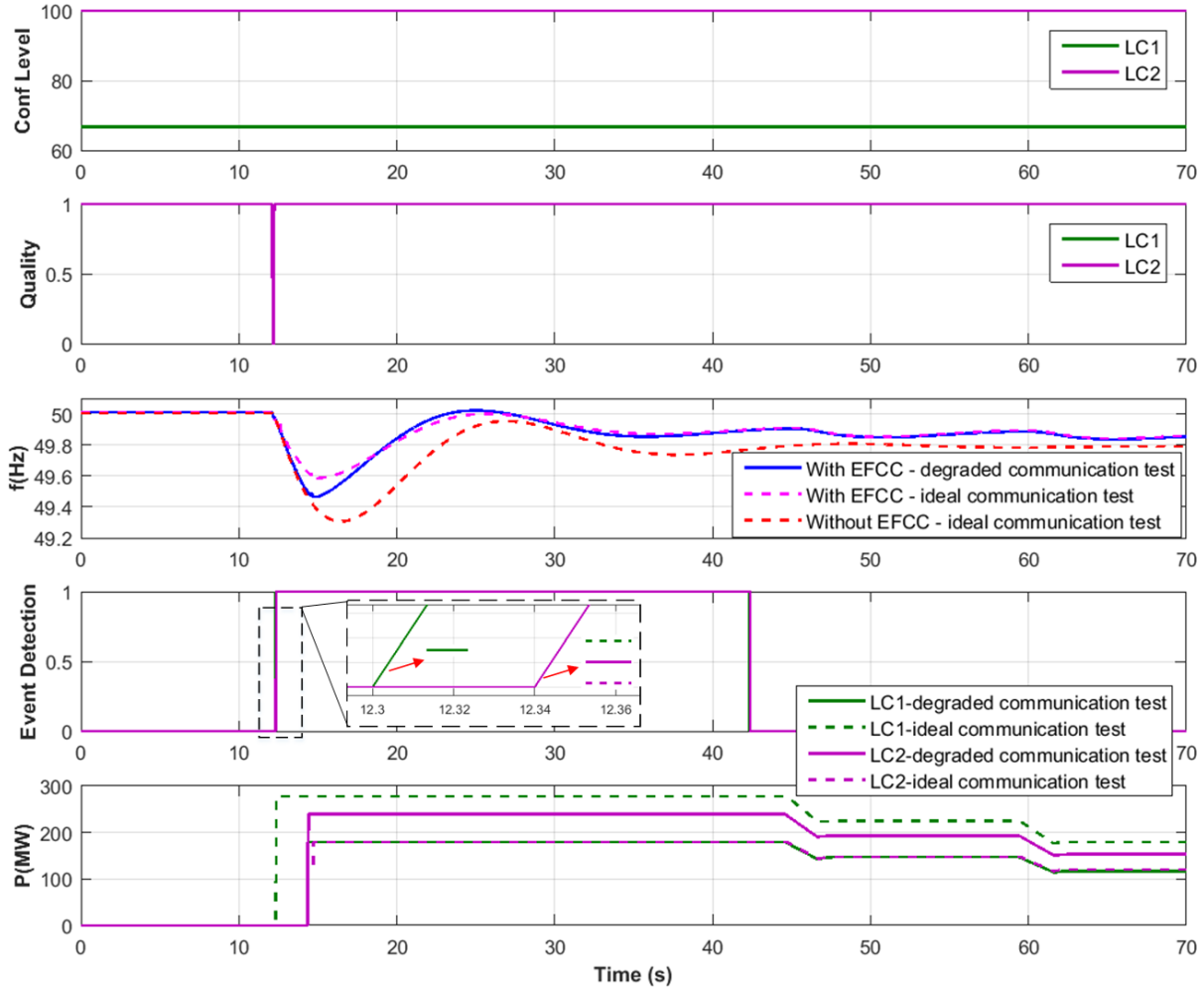


Figure 21. EFCC performance during a frequency event with the latency between RA1 and LC1 exceeding the maximum tolerable limit

Figure 22 shows the performance of the EFCC scheme during a grid fault event with the emulated communication conditions. It can be seen that the performance of the EFCC scheme remained similar to the case with ideal communication conditions. i.e. the faults were all successfully detected by all RAs and the LCs do not deploy any resources during the fault.

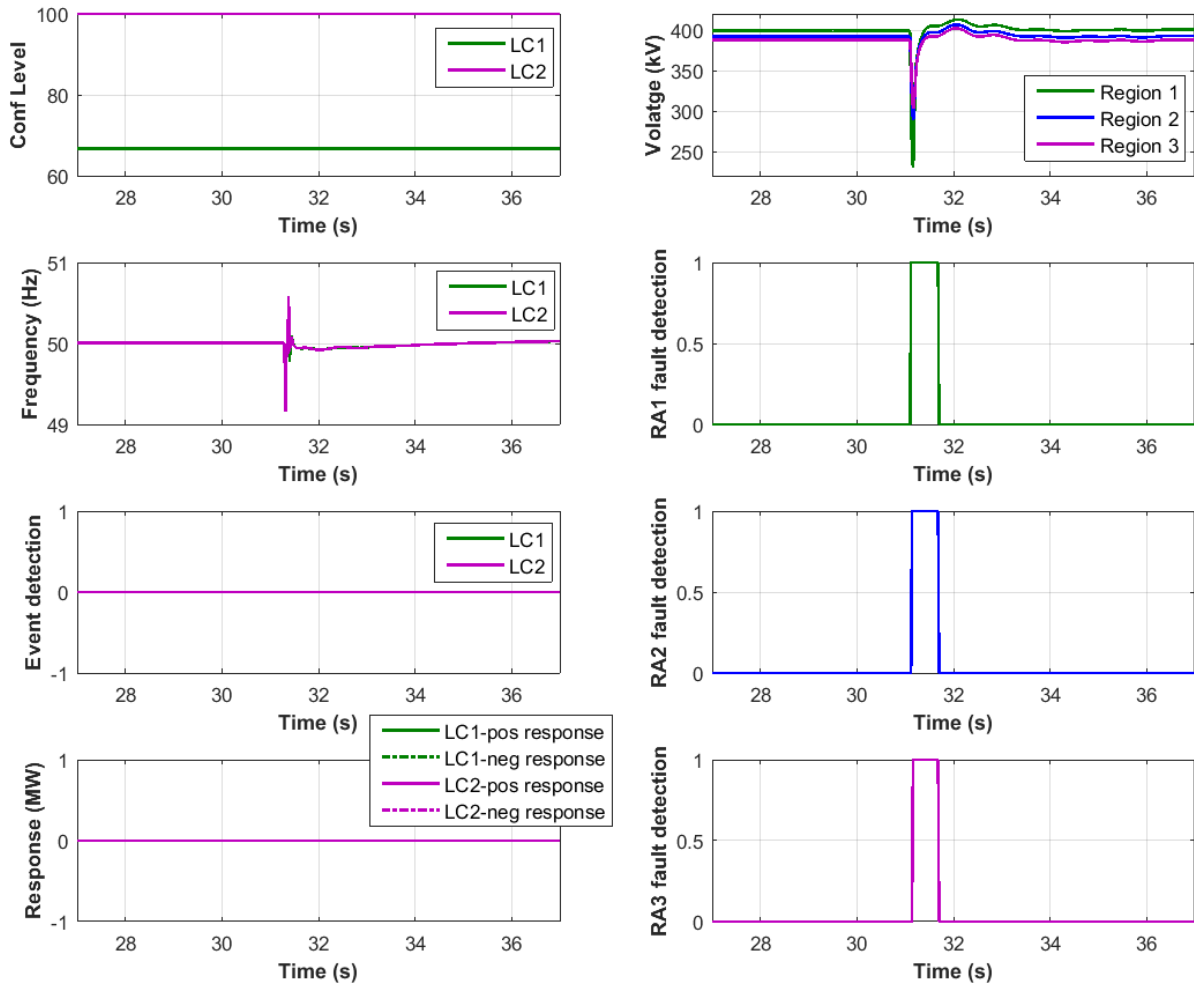


Figure 22. EFCC performance during a fault with the latency between RA1 and LC1 exceeding the maximum tolerable limit

6.3 Test 2: latency between RA2 to LC1 exceeding latency limit

In this test, a latency of 100 ms, exceeding the maximum latency limit of 78 ms, was introduced to the communication link between RA2 and LC1 to evaluate how this affects the EFCC scheme’s operation during frequency and fault events. Figure 23 shows the performance of the EFCC scheme during the emulated communication conditions.

The under-frequency event occurred at around 12.20 s. Similar to the test results shown in Test 1, the loss of the data at the link between RA2 and LC1, due to the latency violating the maximum limit, led to a slower response from LC1 and a smaller amount of resource being dispatched compared to the based case with ideal communication conditions. As a result, the frequency nadir was lower than the base case. For event detection, the LC1 detected the event 20 ms slower than the LC with ideal communication links.

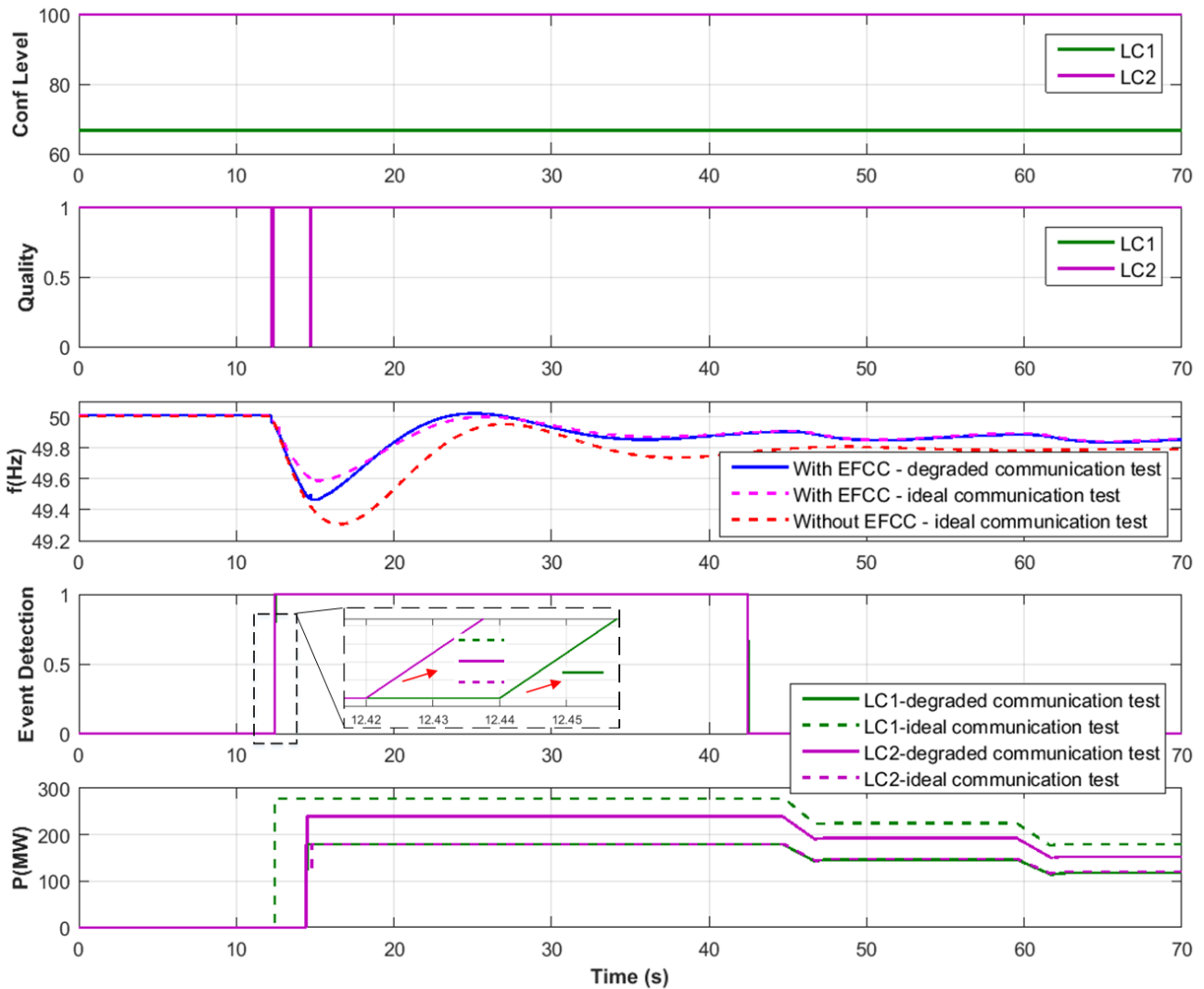


Figure 23. EFCC performance during a frequency event with the latency between RA2 and LC1 exceeding the maximum tolerable limit

Figure 24 shows the performance of the EFCC scheme during a grid fault event with the emulated communication conditions. It can be seen that the performance of LC1 remained similar to the case with ideal communication conditions, i.e. the faults were all successfully detected by all RAs and no resource was dispatched during the fault.

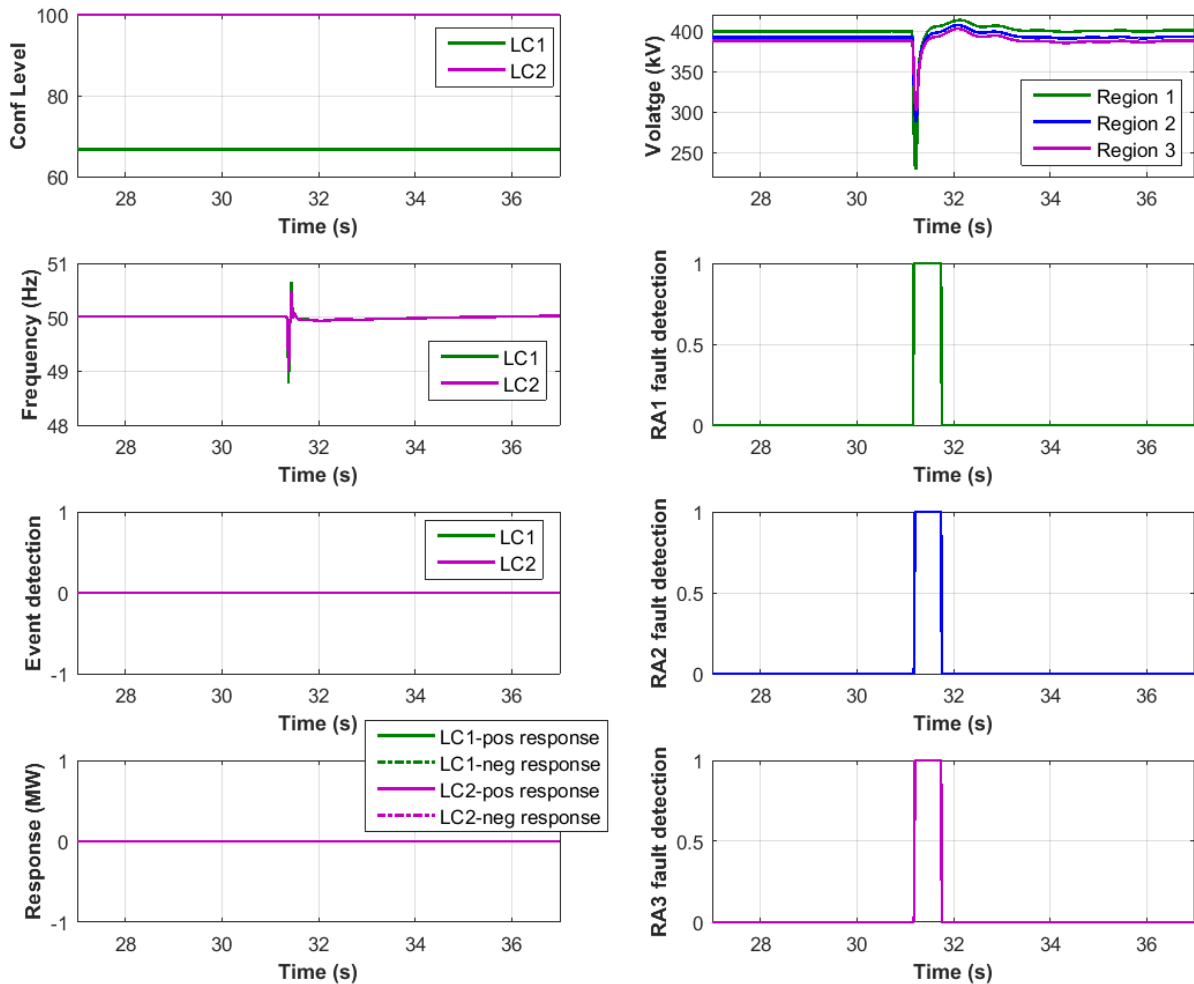


Figure 24. EFCC performance during a fault with the latency between RA2 and LC1 exceeding the maximum tolerable limit

6.4 Test 3: latency between RA3 to LC1 exceeding latency limit

In this test, a latency of 100 ms, exceeding the maximum tolerable level of 78 ms, was introduced to the communication link between RA3 and LC1 to evaluate how this affects the EFCC scheme’s operation during frequency and fault events.

Figure 25 shows the performance of the EFCC scheme during the emulated communication conditions. The latency between RA3 and LC1 resulted in the confidence level of LC1 reducing to 66.67%. The under-frequency event occurred at around 14.46 s.

In this test, the event detection in LC1 is not measurably affected by the degraded communication condition. However, for the frequency response command, similar to previous tests, the response from LC1 was slower and the amount of resource being dispatched was smaller compared to the base case with ideal communication conditions.

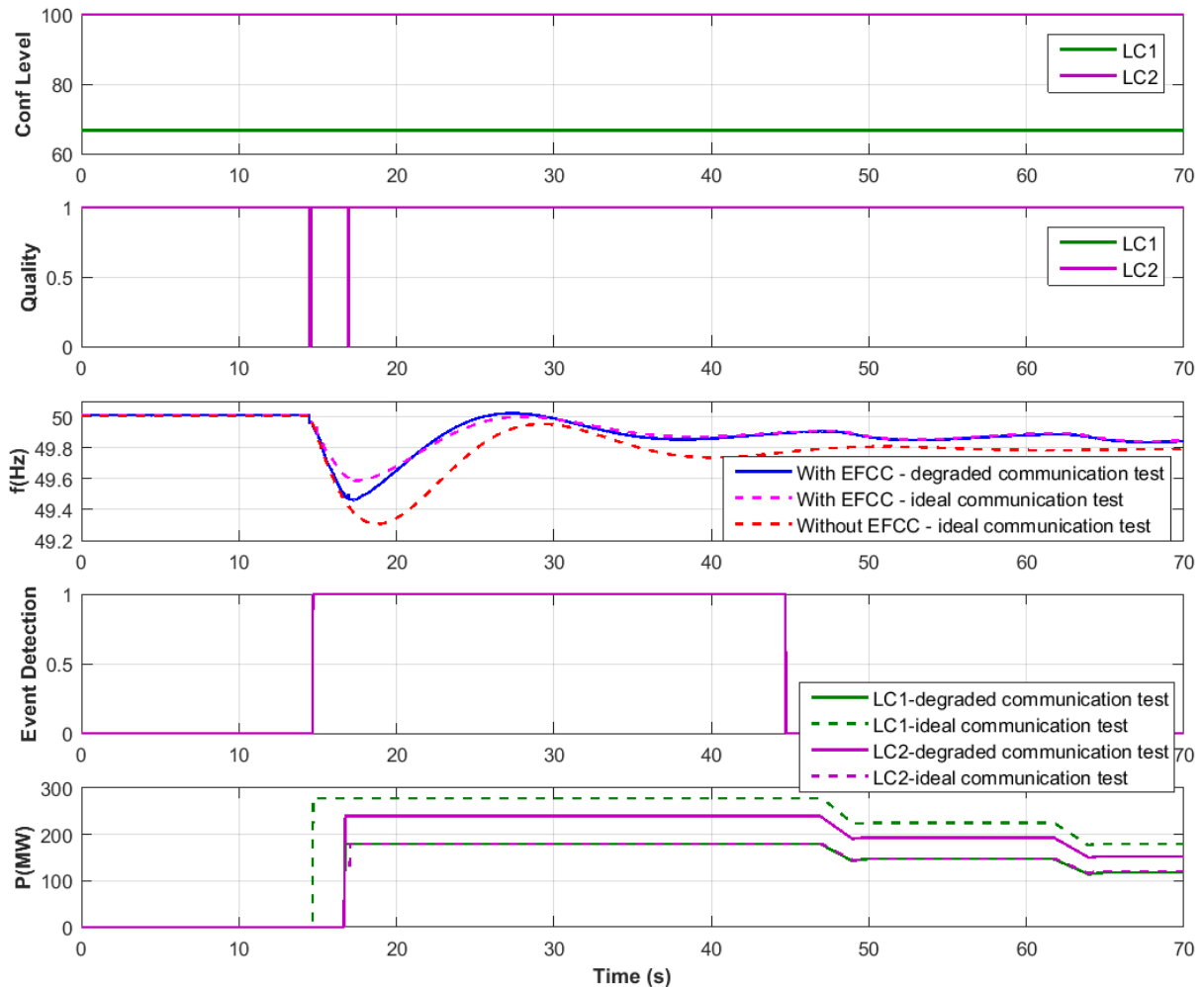


Figure 25. EFCC performance during a frequency event with the latency between RA3 and LC1 exceeding the maximum tolerable limit

Figure 26 shows the performance of the EFCC scheme during a grid fault event with the emulated communication conditions. It can be seen that LC1 unexpectedly detected the fault as an frequency event and dispatched response, which is not required by design.

In this case, the latency between RA3 and LC1 was beyond the acceptable limit and RA3 was located in Region 3, which was least affected by the fault. Therefore, when LC1 aggregated the system frequency and RoCoF without data from RA3, it led to a higher system frequency and RoCoF. This is evident by the test results as shown in Figure 27. It can be seen that the fault was initially detected by all RAs, which also successfully blocked the RoCoF measurements in both LCs. However, after the blocking period, LC1 has higher RoCoF than LC2 due to the loss of RA3 data, so it detected the fault as an event. This shows that, losing the data from one RA could lead to LC's unexpected behaviour during faults and the impact of such loss of data largely depends on the relative location of the fault and the associated RA. It should be noted that the timings for the three plots in Figure 27 are not directly comparable as LC1 and LC2 will lag the output from RAs by approximately 100 ms due to the buffering window they used to handle communication delays.

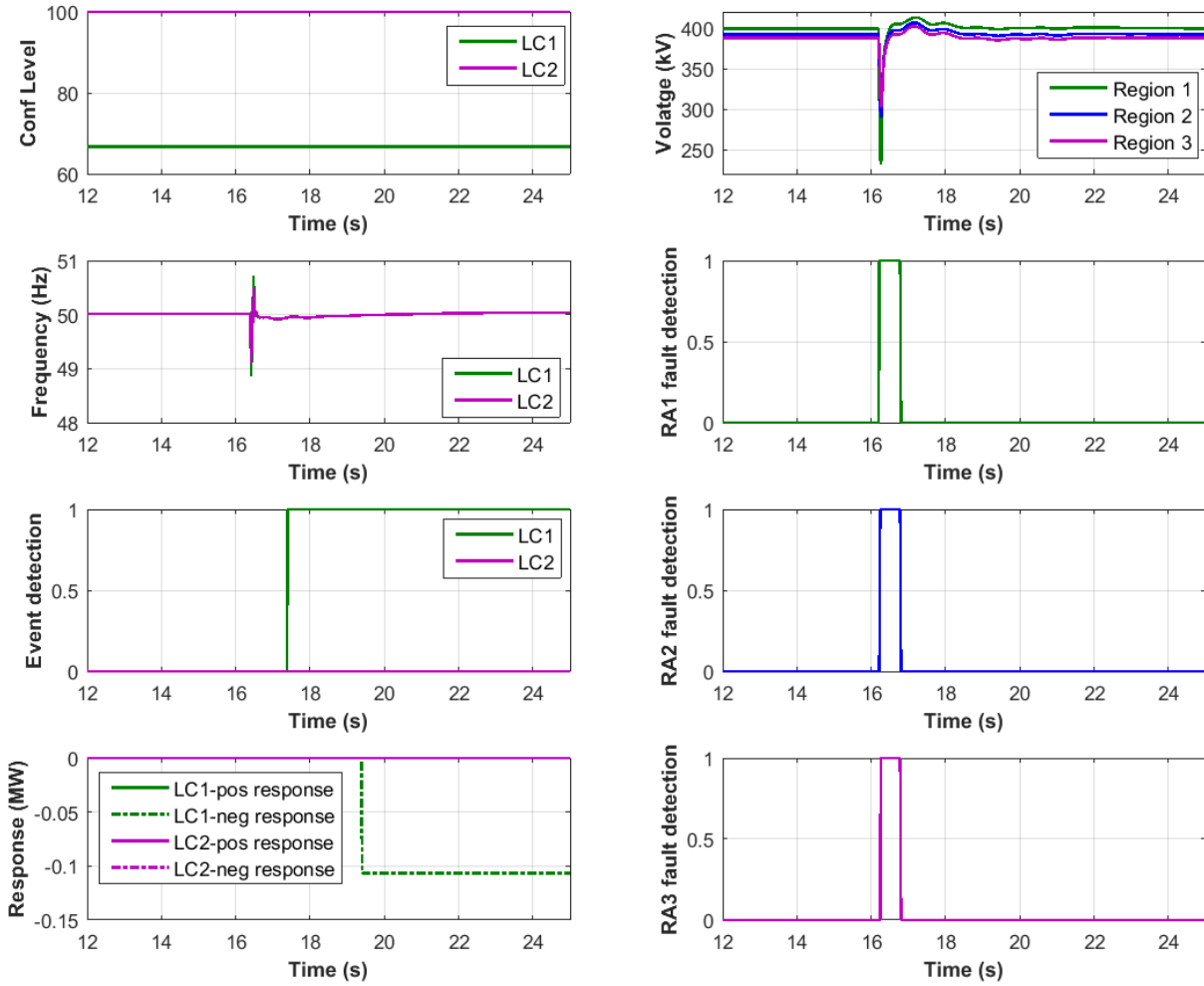


Figure 26. EFCC performance during a frequency event with the latency between RA3 and LC1 exceeding the maximum tolerable limit

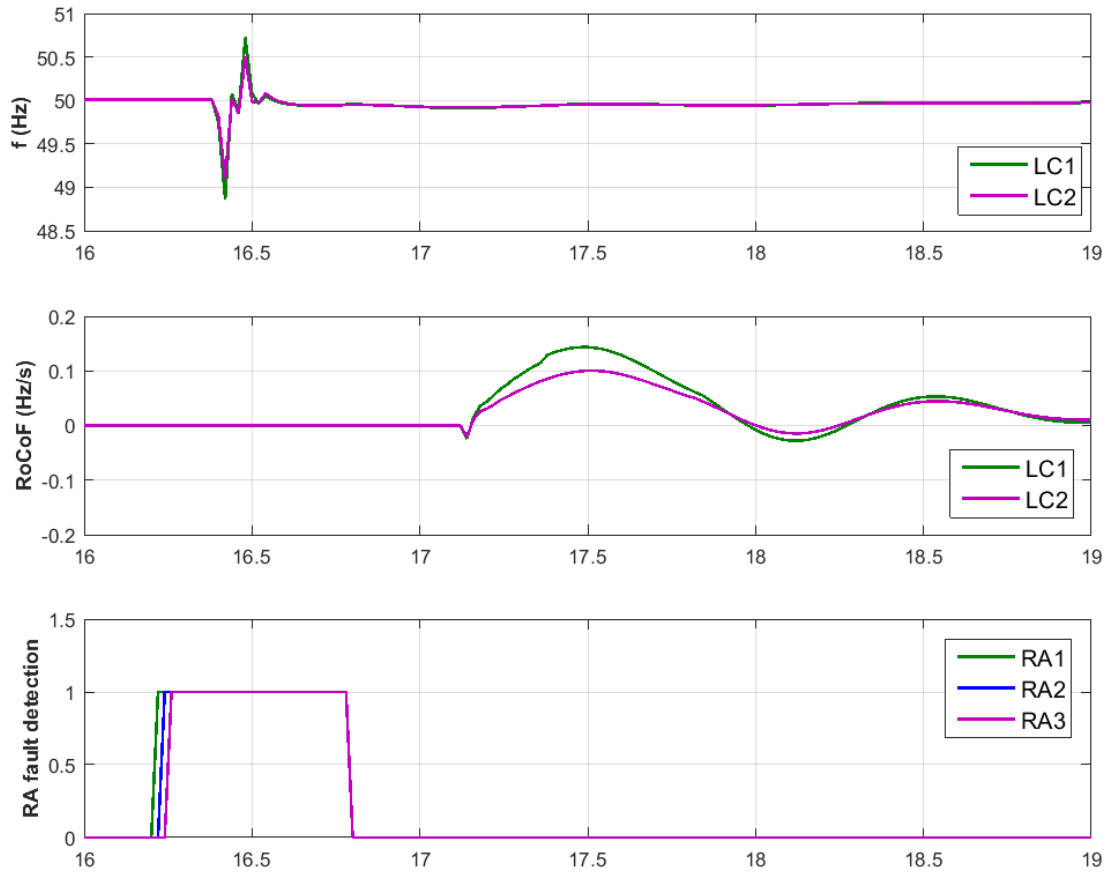


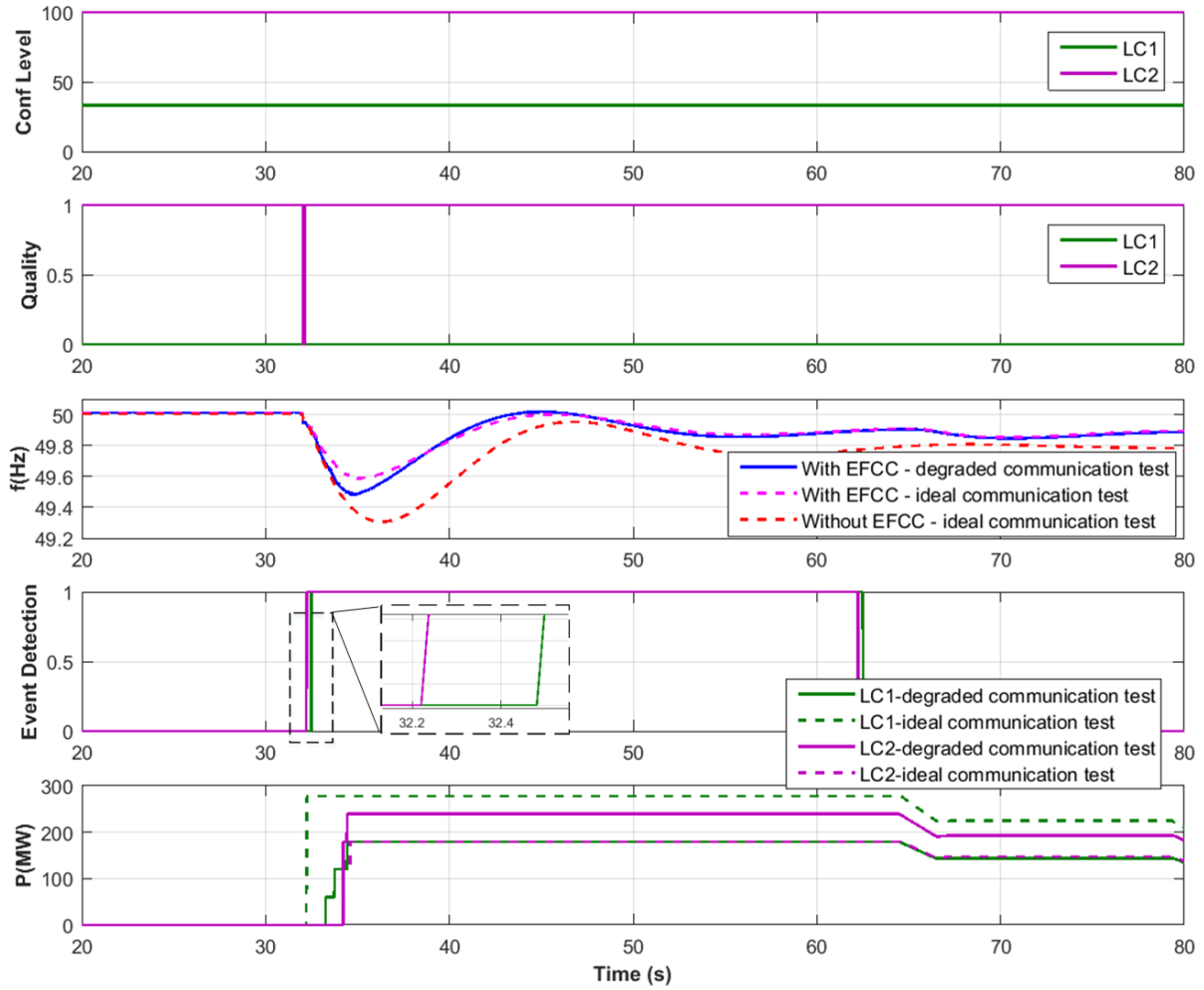
Figure 27. Comparison of system frequency and RoCoF measurement of both LCs in Test 3

6.5 Test 4: latency between RA2 and RA3 to LC1 exceeding latency limit

In this test, a latency of 100 ms, exceeding the maximum tolerable level of 78 ms, was introduced at the communication links between RA2 and RA3 and LC1 to evaluate how this affects the EFCC's operation during frequency and fault events. Figure 28 shows the performance of the EFCC scheme during the emulated communication conditions.

Due to the latency between the two RAs (RA2 and RA3) and LC1 exceeding the maximum tolerable limit, the confidence level of LC1 dropped to 33.33%. The under-frequency event occurred at around 32.00 s.

From the third plot, it can be seen that the event detection in LC1 became slower by 0.26 s compared to the base case. The last plot shows that the response from LC1 is also slower and was triggered in steps with each step of 60 MW (20% of the total available power). This is an indication that LC1 operated in the local mode in this test (as the power command triggering times aligned with the corresponding local mode frequency thresholds and the deployed power also aligned with the local mode operation). Therefore, losing data from two out of three RAs will lead to the LC1 losing wide area visibility and it will automatically switch to local mode. Consequently, the frequency nadir became 49.48 Hz compared to 49.59 Hz as in the base case.



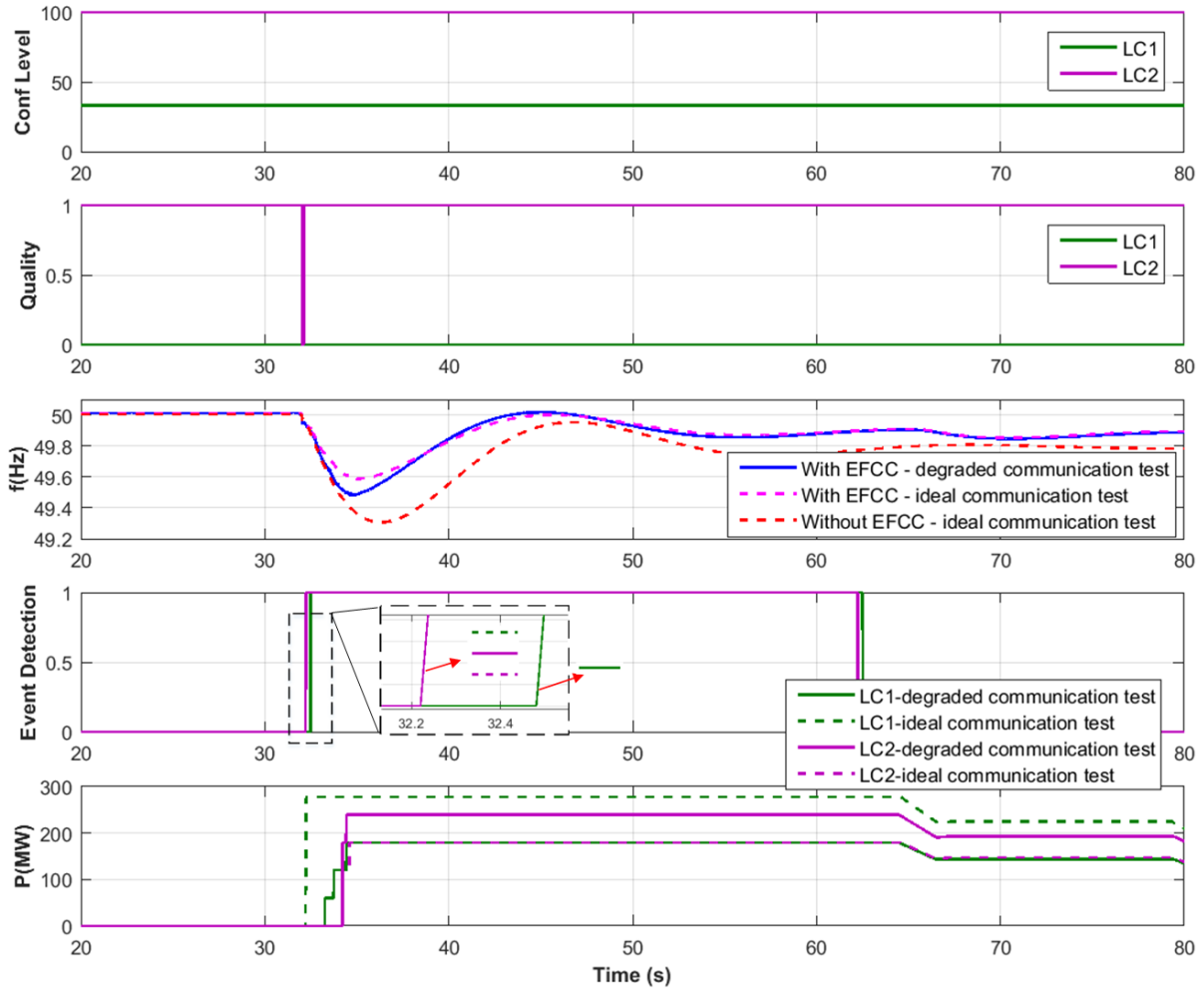


Figure 28. EFCC performance during a frequency event with the latency between two RAs and LC1 exceeding the maximum tolerable limit

Figure 29 shows the performance of the EFCC scheme during a grid fault event with the emulated communication conditions. From the frequency event test, it was known that LC1 operated in the local mode when data from two RAs was lost, therefore, in this test the fault detection flags within LCs are also plotted in Figure 29. In wide-area mode, fault response blocking is achieved by the fault detection flag in the RAs, while in the local mode, it is achieved by the fault flags in the LCs [1].

From the test results, it can be seen that all of the RAs and LCs detected the fault. LC1 operated in the local mode so it would have used its internal fault flag to block the event detection and resource deployment - it can be seen that both event detection and resource allocation was successfully blocked. Since there was no intentional latency in LC2 communication links, and from the frequency test results, it was known that it still operated in wide-area mode. Therefore, it would have used the RAs fault detection flag for blocking event detection and resource allocation. From the results, it can be seen that the event was successfully blocked by the fault block signal and no resource was deployed.

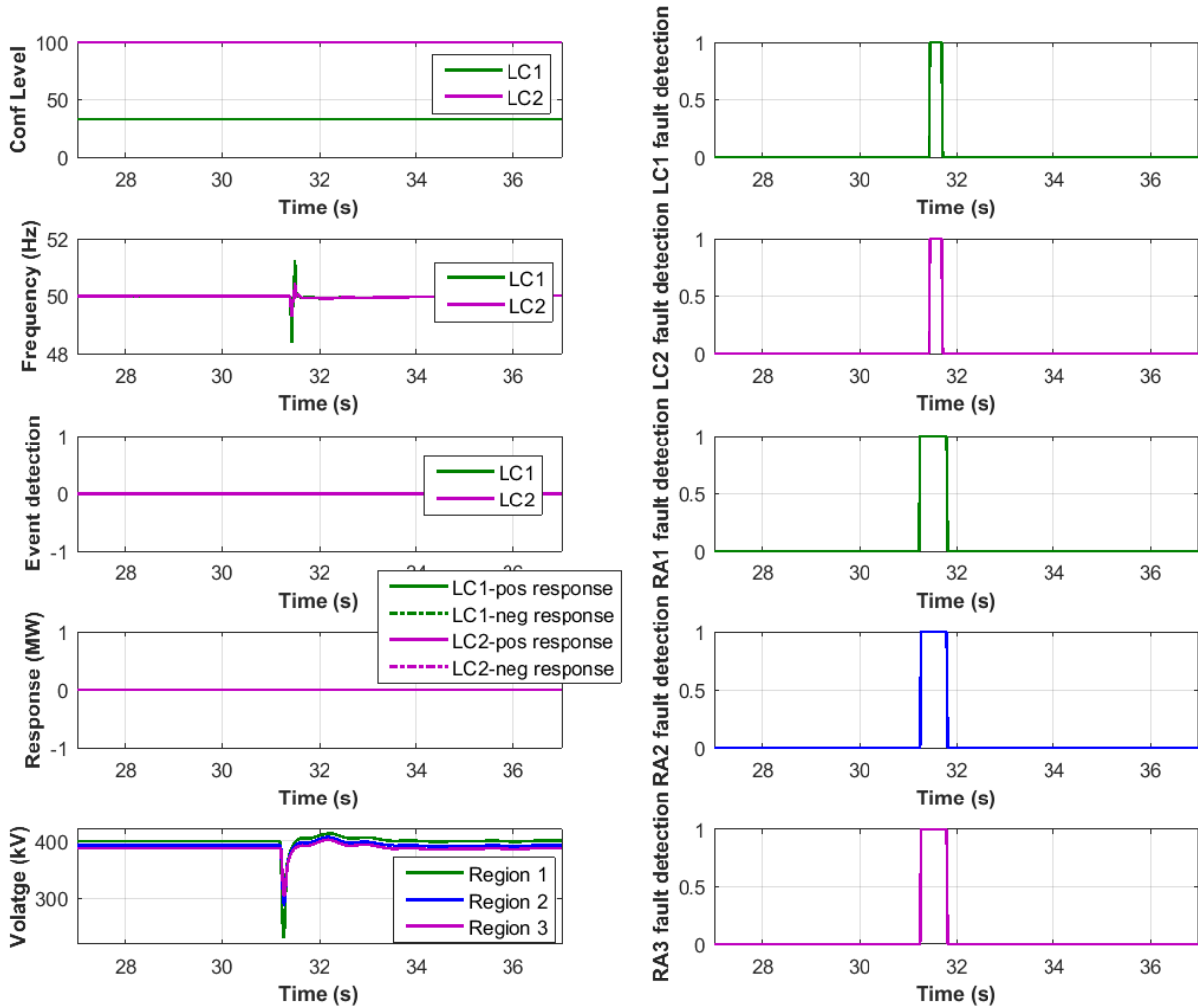


Figure 29. EFCC performance during a fault with the latency between two RAs and LC1 exceeding the maximum tolerable limit

6.6 Test 5: EFCC scheme performance under high latency and jitter

In this test, a range of latencies with jitter was introduced to the communication links between the RAs and LC1. During the tests, it was observed that the statistical nature of jitter could lead to inconsistencies in the EFCC scheme's performance (i.e. the control actions from the LCs and the time it takes the LCs to make decisions are not always the same). The frequency of the inconsistent performance tended to increase with the increase of jitter.

From the test presented in Section 5.2.2, it was known that the maximum latency limit is 78 ms for a 100 ms buffering window. Therefore, in this work, the tests started from an extreme case where a mean latency of 78 ms with a jitter level of 26 ms was emulated to test the EFCC scheme's performance. This is the maximum latency limit with the maximum jitter level that can be introduced using the communication emulator, so it represents the most severe jitter condition that can be tested with the communication emulator at the 78 ms latency limit. Using Equation (1) presented in Section 5.2.3, it can be calculated that this latency and jitter level results in 50% of the data packets not arriving at the LCs on time and consequently being discarded, which is equivalent to packet loss.

Figure 30 shows the performance of the EFCC scheme during the emulated latency and jitter. Expected behaviour was observed with a mean latency of 78 ms and a jitter level of 26 ms. It can be seen that, at this level of latency and jitter, LC1 missed packets from two RAs for the majority of the test period (confidence level dropped to 33.33%). In some cases, LC1 missed data from all of the three RAs (confidence level dropped to 0%). As a result, LC1 lost wide-area visibility most of the time during the test - this is evident in the second plot where the RoCoF quality dropped frequently to 0 and in the third plot where the system frequency measurement at LC1 also dropped frequently to 0. However, when the frequency event occurred, the test results show that the EFCC controllers can still detect the event promptly and respond correctly to the event - very similar behaviour with the base case where the communication links were operating under ideal conditions, which is also shown in Figure 30.

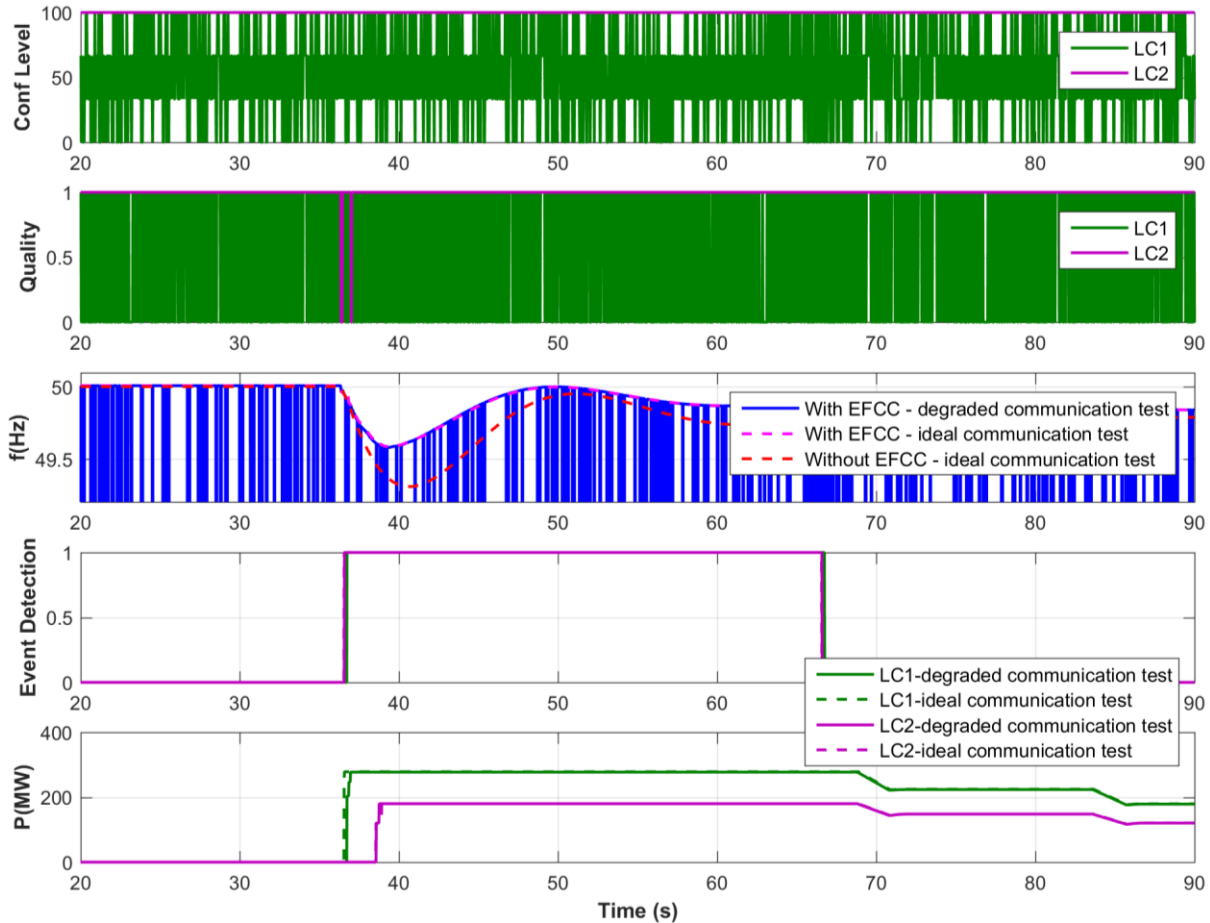


Figure 30. Desirable EFCC performance during a frequency event at a latency of 78 ms and a jitter of 26 ms applied to the communication links between RAs and LC1

However, when repeating the same event under the same arrangement, a compromised response of EFCC was also observed. As shown in Figure 31, a slower action from LC1 with a smaller deployed power was observed. A zoomed-in view of the test results is shown in Figure 32. It can be seen that after the event occurred, the wide-area visibility was lost in a number of instances, which led to the delay in event detection and compromised power deployment actions. These subsequently resulted in the frequency control being less effective.

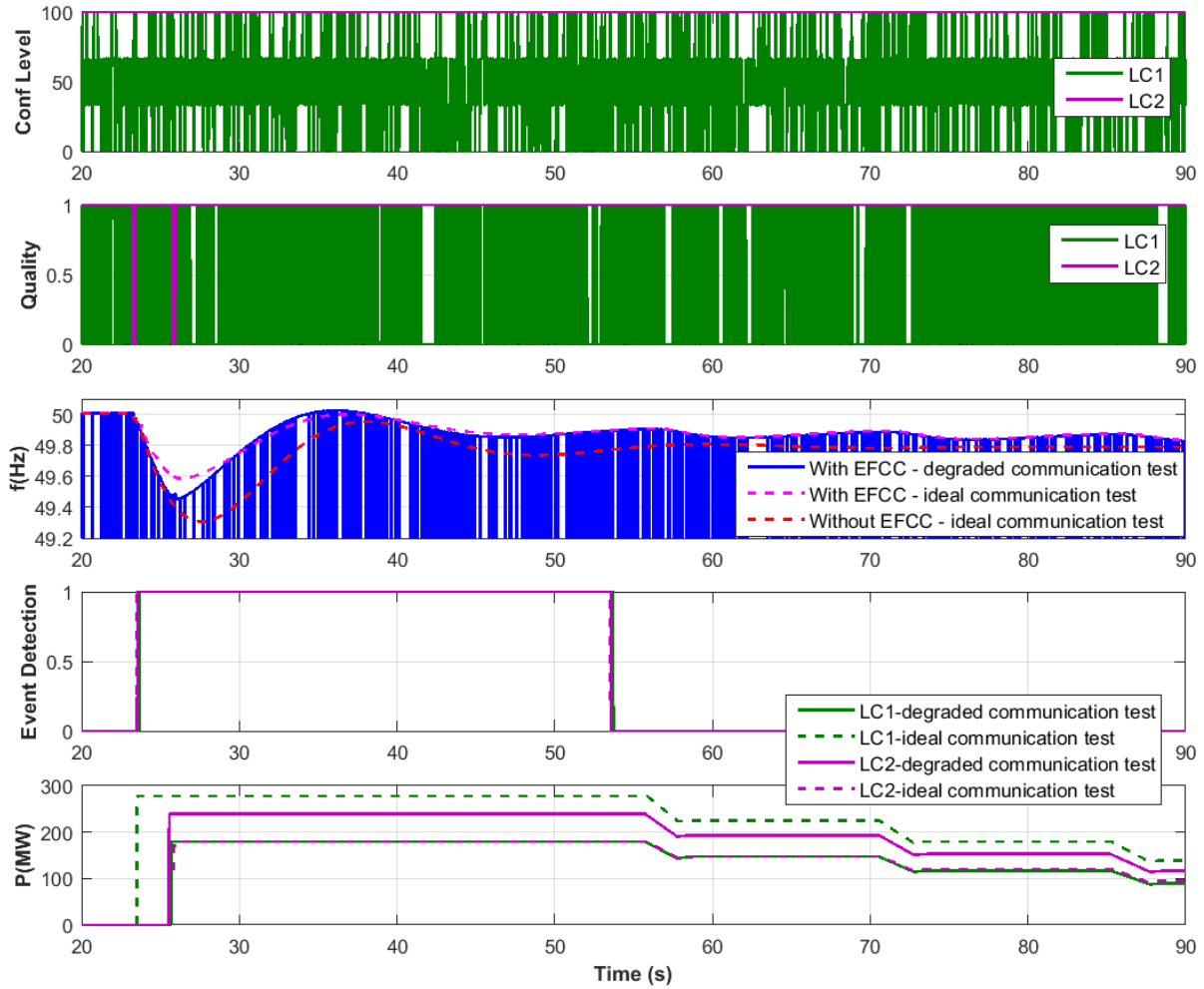


Figure 31. Compromised EFCC performance during a frequency event at a latency of 78 ms and a jitter of 26 ms applied to the communication links between RAs and LC1

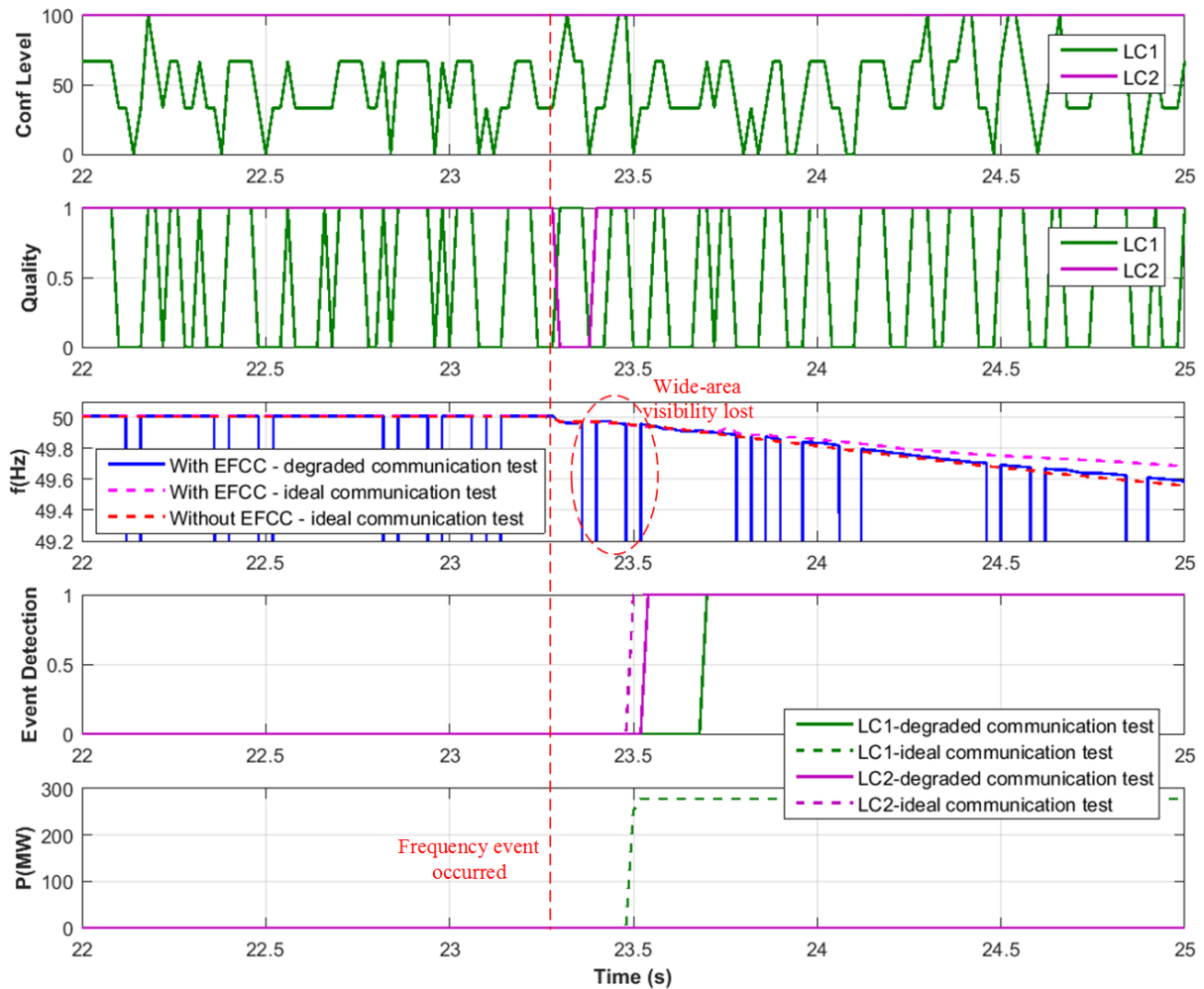


Figure 32. Detailed view of compromised EFCC performance in a frequency event at a latency of 78 ms and a jitter of 26 ms applied to the communication links between RAs and LC1

From the test results, it can be seen that, in order to ensure the EFCC scheme operates as required, it is essential that the wide-area visibility is maintained when an event occurs until the event is correctly detected and the power is correctly deployed.

In Appendix D, a mathematical analysis of the probability of the EFCC scheme maintaining wide-area visibility is provided. For the particular setup and settings in this test, the EFCC scheme will require data from at least two out of three RAs in order to maintain wide-area visibility. Since the targeted time for the EFCC to make event detection and resource deployment decisions is within 500 ms, the relationship between the probability of a packet is discarded (due to the longer latency and high jitter levels) and the probability of the EFCC scheme’s ability to maintain wide-area visibility is shown in Figure 33.

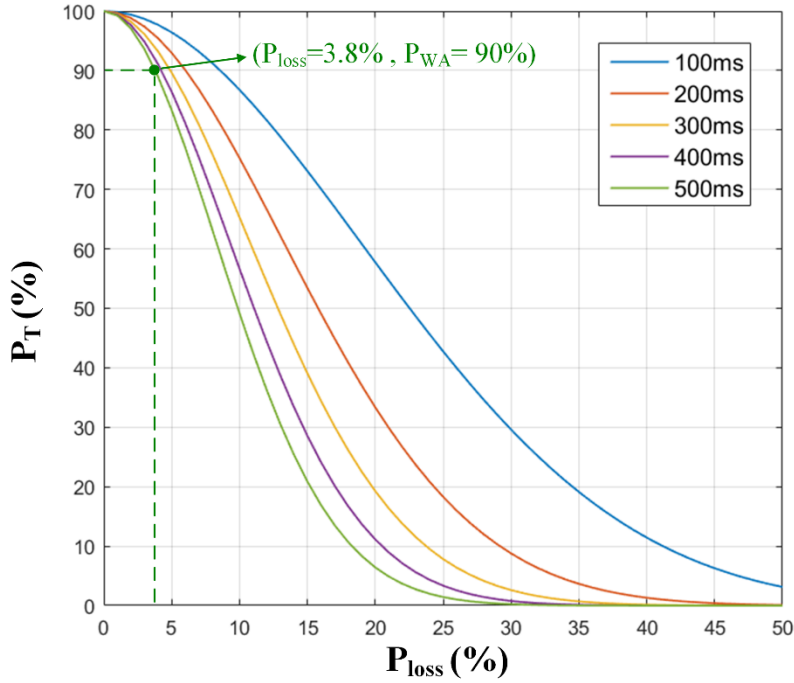


Figure 33. Probability of maintaining wide-area visibility

P_{loss} is the probability of data being discarded due to latency being larger than the maximum limit at each of the links between the RAs and LCs. P_T is the probability of the EFCC scheme maintaining wide-area visibility for a period of time ranging from 100 ms to 500 ms. For example, the green curve shows for any 500 ms period, the probability of wide-area visibility can be maintained in relation to P_{loss} , while the blue curve evaluates the value of P_T over a 100 ms time period.

It can be seen that with the increase of P_{loss} , P_T will decrease in all cases. For a certain value of P_{loss} , the value of P_T will become smaller with a longer time period. The time period of 500 ms is the most conservative case, as it requires the wide-area visibility to be maintained for the longest period of time. In reality, the EFCC scheme could make decisions in less than 500 ms. However, since the time taken for the EFCC scheme to make decisions after an event occurs varies, the use of the 500 ms period for the probability evaluation provides the highest confidence for the correct operation of the scheme.

The value of P_{loss} is associated with the mean latency and the jitter level. For example, for a latency probability distribution with a mean latency of 60 ms and jitter of 15 ms as shown in Figure 34, if the latency is greater than the maximum limit (L_{max}), then the packet will be discarded. The relationship between P_{loss} and the latency (μ) and jitter (σ) can be expressed as (2) [6]:

$$P_{loss} = 1 - \int_0^{L_{max}} \frac{1}{\sqrt{2\pi} \sigma^2} e^{-\frac{(x-\mu)^2}{2\sigma^2}} dt \quad (2)$$

For $L_{max} = 78$ ms, the relationship between the jitter level at various mean latency levels with P_{loss} is shown in Figure 35². The raw data for the curve presented in Figure 33 and Figure 35 are provided in Appendix E.

² It should be noted that the maximum jitter level is 1/3 of the mean latency, otherwise it will lead to negative latencies, which do not have a physical meaning.

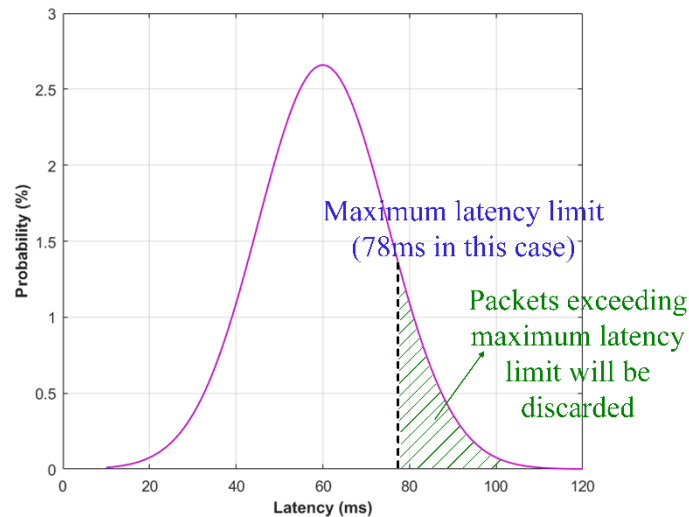


Figure 34. Example latency probability distribution

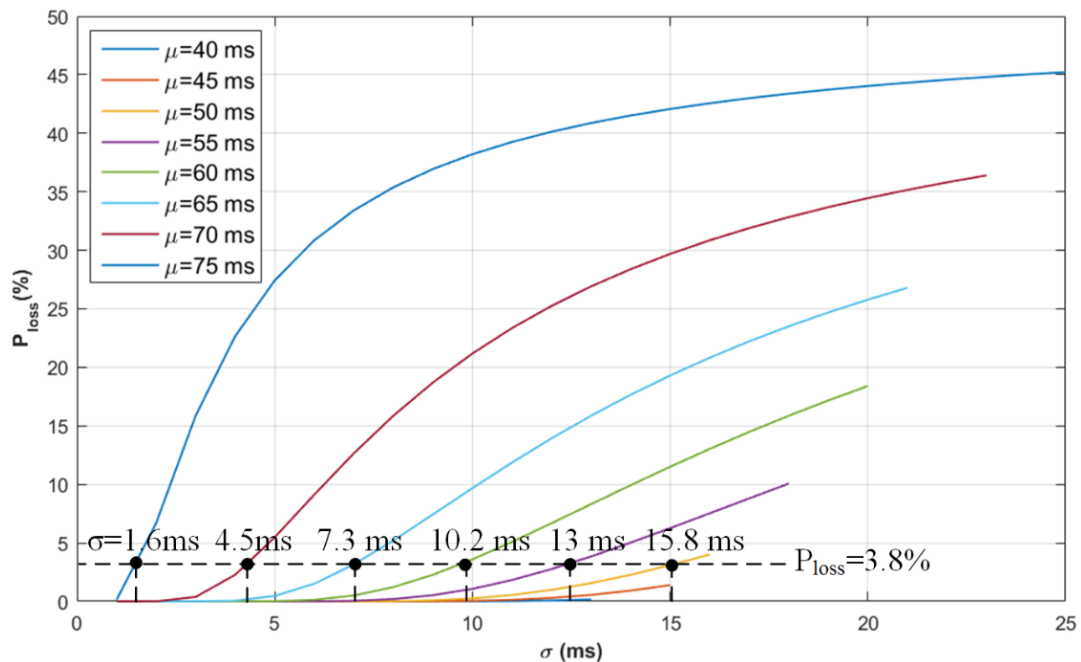


Figure 35. Relationship between jitter level and the probability of packets violating the maximum latency limit

The results can be used to specify the requirements for communication network performance. For example, if it is required that for any 500 ms period, the probability of maintaining wide-area visibility need to be at least 90%, then from Figure 33, it can be seen that the probability of the packet being discarded due to large latency and jitter (i.e. P_{loss}) should be maintained to be less than 3.8%. This means, referring to Figure 35, for a mean latency of 75 ms, the jitter needs to be smaller than 1.6 ms; for a mean latency of 70 ms, the jitter needs to be smaller than 4.5 ms; for a mean latency of 65 ms, the jitter needs to be smaller than 7.3 ms; for a mean latency of 60 ms, the jitter needs to be smaller than 10.2 ms; for a mean latency of 55 ms, the jitter needs to be smaller than 13 ms; and for a mean latency of 50 ms, the jitter needs to be smaller than 15.8 ms. For mean latencies of 45 ms and below, no matter what the jitter level is, P_{loss} will always be smaller than 3.8%, i.e. the probability of maintaining wide area visibility for any 500 ms period will always be greater than 90%.

It should be noted that during the tests, fault events were also applied to verify the EFCC scheme's performance with communication jitter. Figure 36 shows the EFCC performance during a grid fault event with a mean latency of 78 ms and a jitter of 26 ms applied at the communication links between RAs and LC1. It was found that the EFCC scheme exhibited a similar performance to that in the base case - the RAs detected all faults and the LCs did not deploy any power to respond to the fault in all of the tested cases. The tests were repeated and it was found that even when the EFCC scheme has inconsistent performance for frequency events due to jitter, the fault performance is consistent and always similar to the base case. Therefore, the above statistical analysis, ensuring the confidence of the EFCC scheme to operate correctly in frequency events will also ensure it operates correctly during fault conditions.

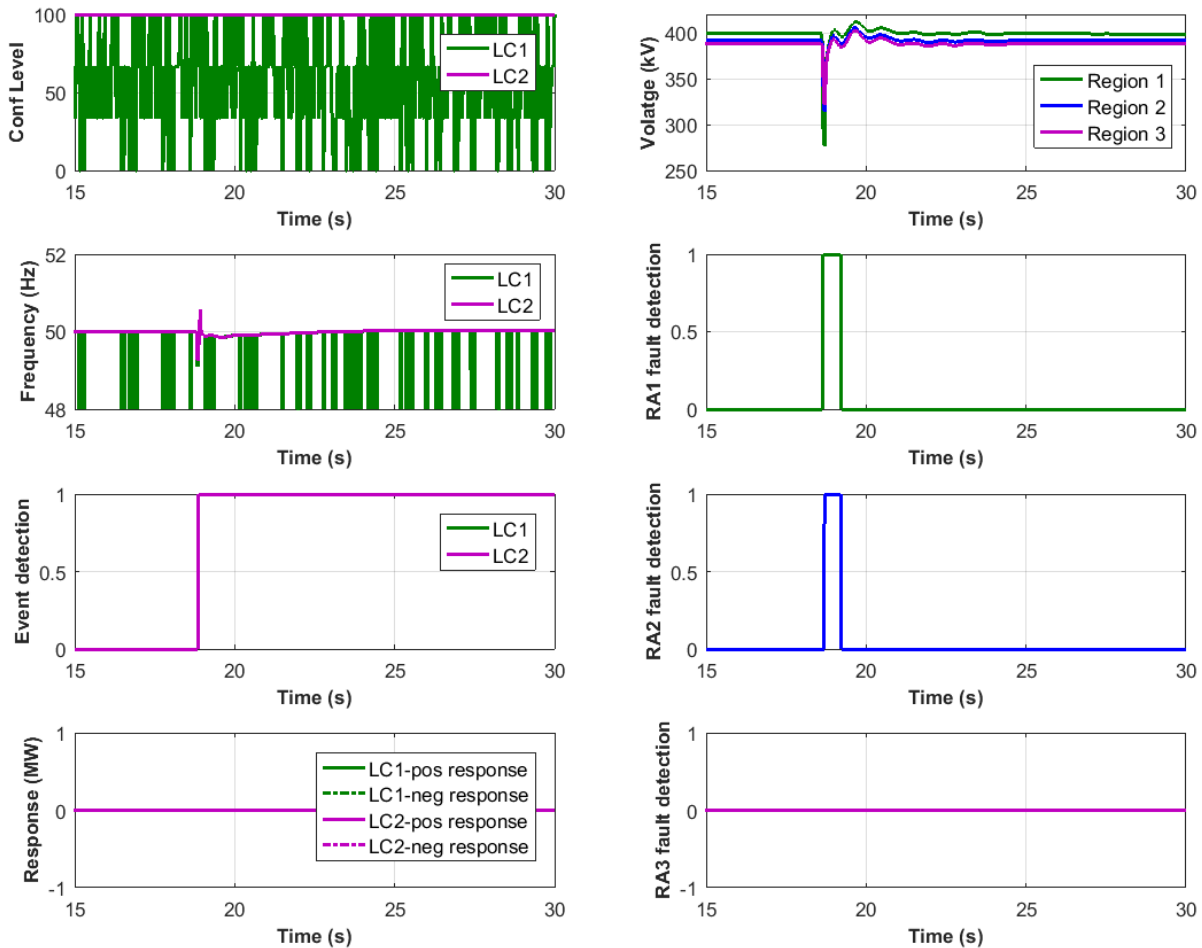


Figure 36. EFCC performance during a fault with the latency and jitter applied to the communication links between RAs and LC1

6.7 Test 6: EFCC scheme performance with loss of packets

In this test, random loss of packets was emulated in the communication links between the RAs and LC1. Similar to the findings in the jitter level tests as reported in Section 6.6, it was observed that the EFCC scheme's performance became inconsistent as the rate of loss of packets increased.

Figure 37 shows a case where desirable performance of the EFCC scheme was observed with a loss of packet rate of 60% applied to the communication links between the RAs and LC1. It can be seen that the confidence level dropped frequently to 33.33%. However, during the frequency disturbance, the EFCC scheme exhibited similar performance as in the case with ideal communication links.

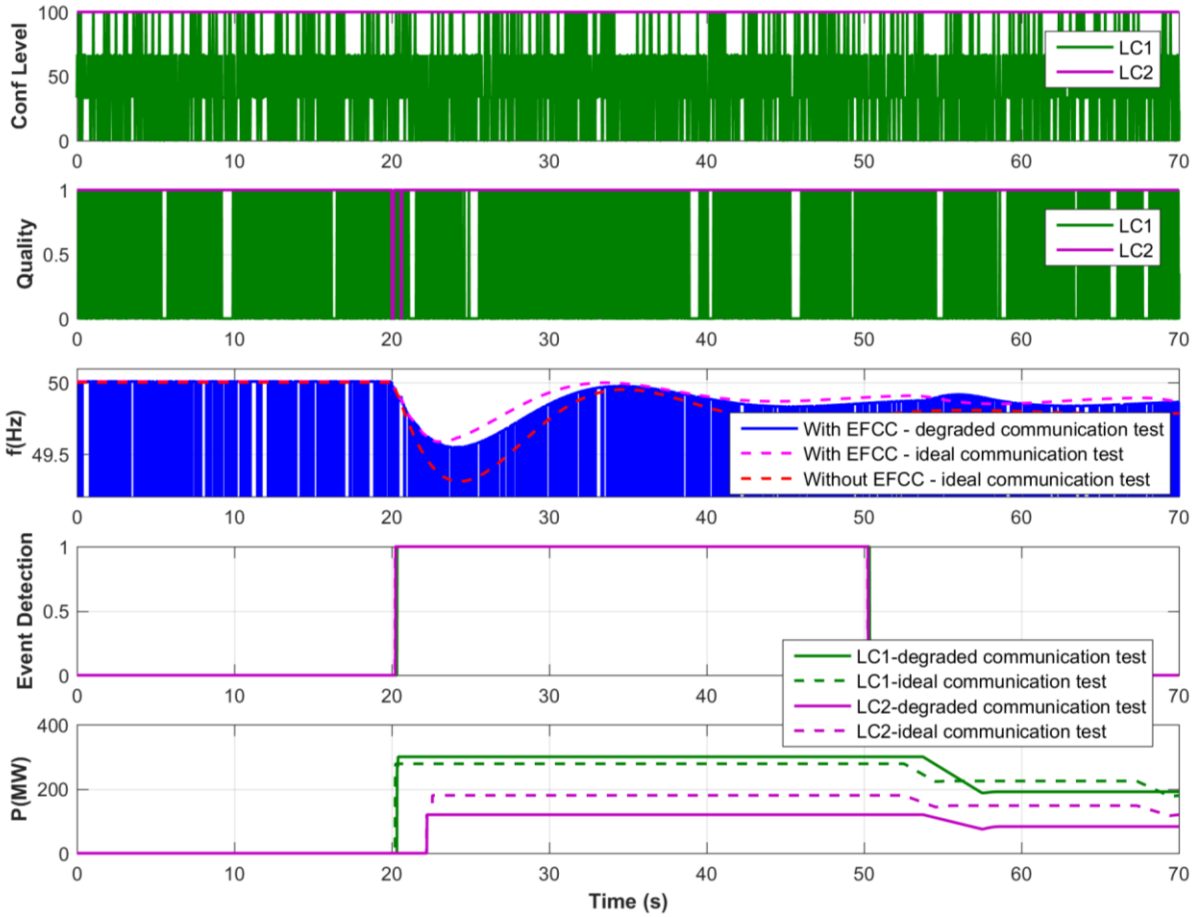


Figure 37. Desirable EFCC performance during a frequency event with 60% loss of packets rate in the communication links between the RAs and LC1

However, when repeating the same event under the exactly same arrangement, degraded EFCC scheme performance was also observed as shown in Figure 38, where a slower response from LC1 with a smaller deployed power were observed. A zoomed-in view of the test results are shown in Figure 39. It can be seen that after the event occurred, the wide-area visibility was lost in a number of instances, which led to the delay in event detection and degraded power deployment control response. These subsequently resulted in the frequency containment being less effective.

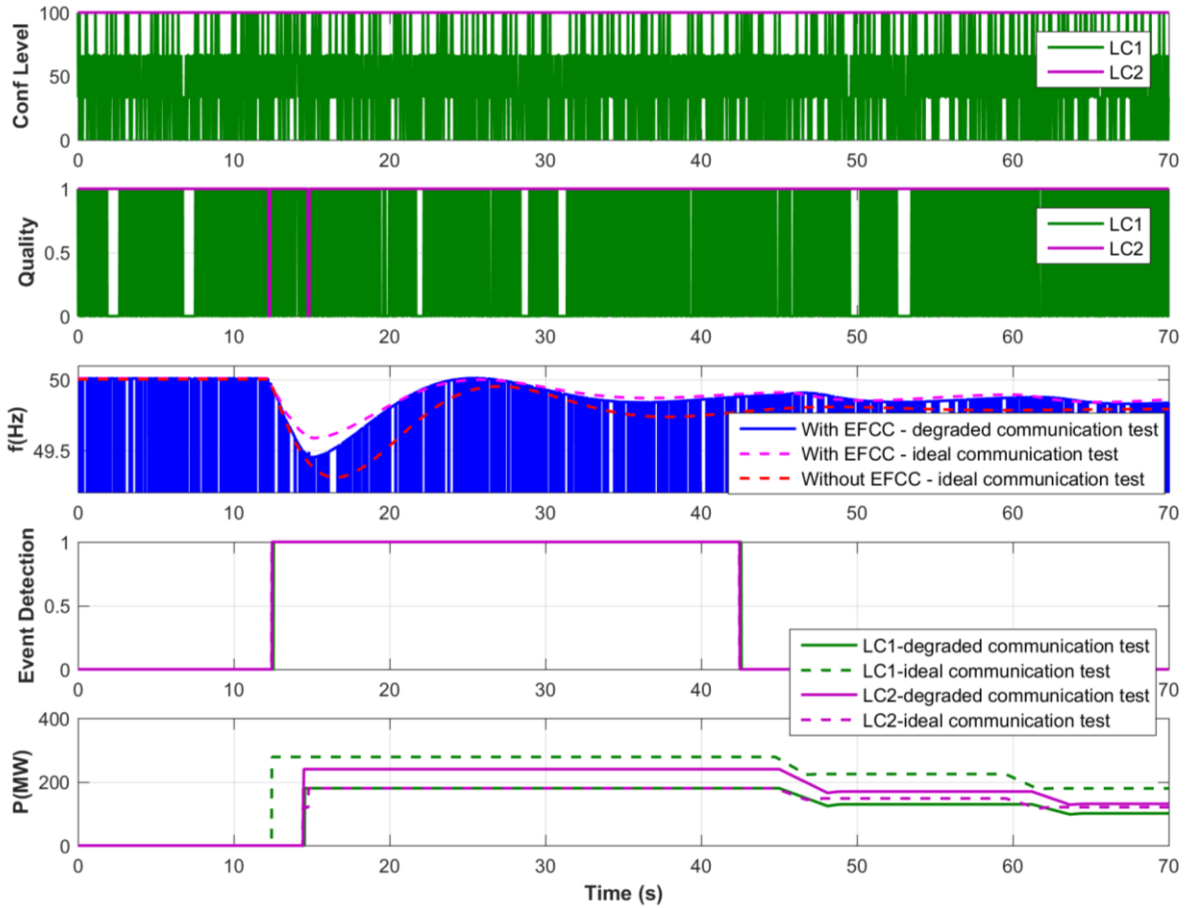


Figure 38. Compromised EFCC performance during a frequency event with 60% loss of packets rate in the communication links between the RAs and LC1

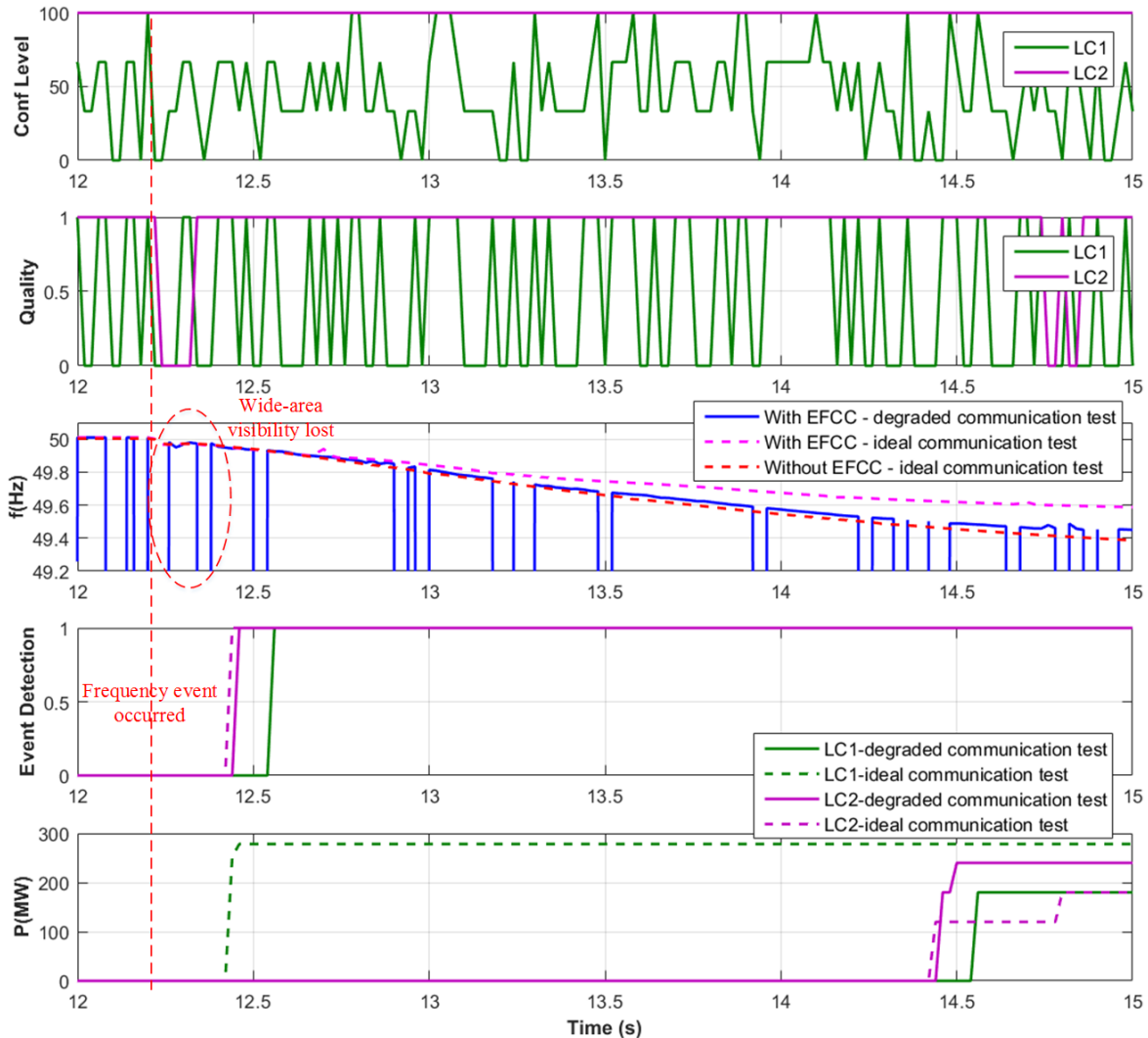


Figure 39. Detailed view of the compromised EFCC performance during a frequency event with 60% loss of packets rate in the communication links between the RAs and LC1

Similar to the jitter tests observations, from these test results, it can be seen that, in order to ensure the EFCC scheme performs as required, it is critical that the wide-area visibility should be maintained when an event occurs until the event is correctly detected and the power is correctly deployed.

The loss of packets are equivalent to the case where the packets being discarded due to large latency and jitter as presented in Section 6.6. Therefore, the relationship between the loss of packet rates (P_{loss}) and the probability that the EFCC scheme being able to maintain wide-area visibility is the same as shown in Figure 33. In Appendix D, a mathematical analysis of the probability of the EFCC scheme maintaining wide-area visibility in relation to the loss of packet rate is provided.

Similar to the jitter tests presented in Section 6.6, fault events were also applied to check the EFCC's behaviour with packet losses. Figure 40 shows the EFCC performance during a grid fault event with a loss of packet rate of 60% applied to the communication links between RAs and LC1. It was found that the EFCC scheme exhibited a similar response to that in the base case - the RAs detected all faults and the LCs did not deploy any power to respond to the fault in all of the tested cases. The tests were repeatedly conducted and the EFCC scheme's performance during faults was observed to be consistent and always similar to the base case. Therefore, the statistical results and analysis presented in Figure 33 and Appendix D, ensuring the confidence of the EFCC scheme to respond correctly in frequency events, will also ensure it responds correctly during faults.

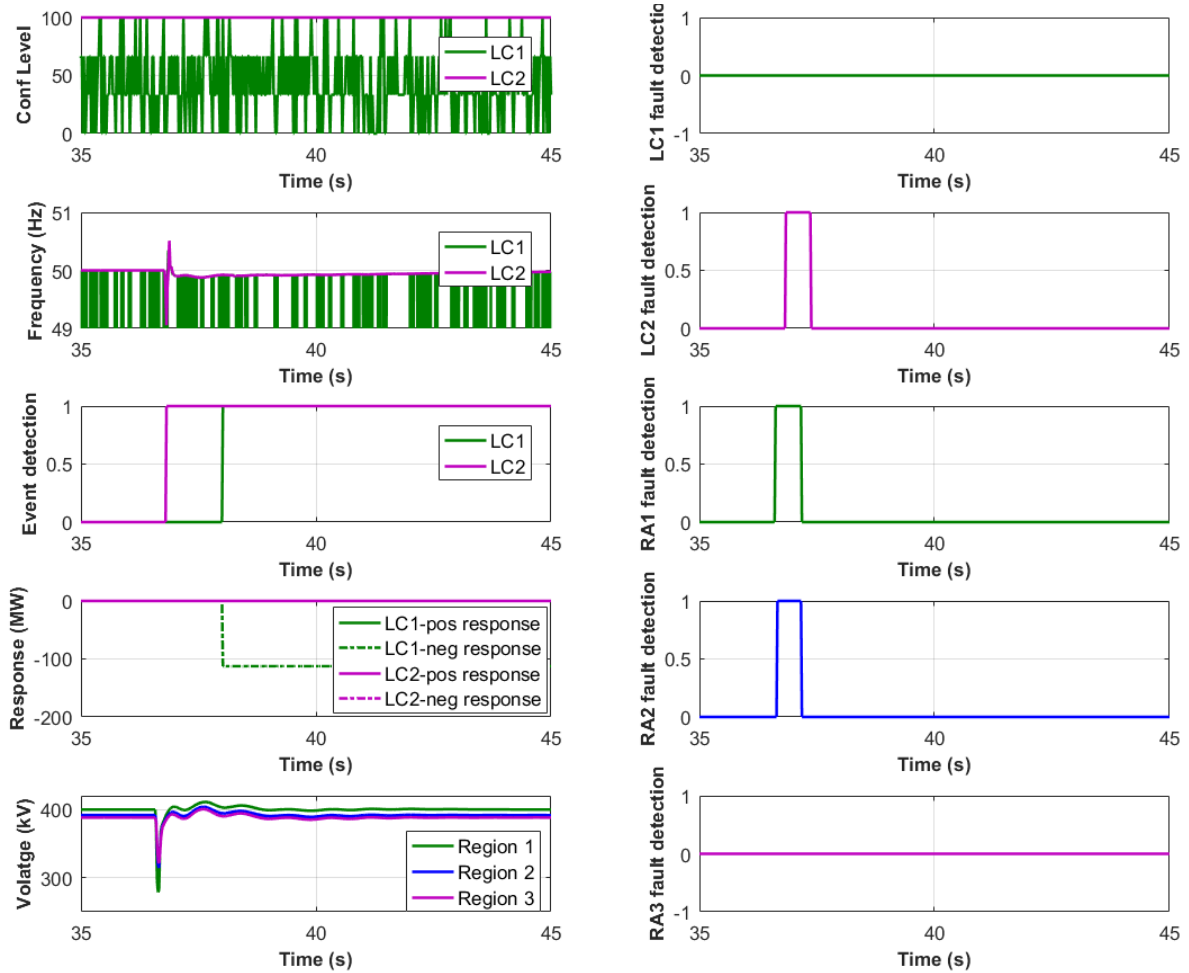


Figure 40. EFCC performance during a fault event with 60% loss of packets rate in the communication links between RAs and LC1

6.8 Test 7: EFCC scheme performance with high BER (10^{-5})

In this test, bit errors were introduced to the communication links between the RAs and LC1. From the test presented in Section 5.2.4, it was known that the maximum BER for the LCs to interpret the packets is 10^{-5} . Therefore, in this test, the performance of the EFCC scheme was evaluated under this extreme case.

Figure 41 shows the performance of the EFCC scheme during the emulated bit errors in the communication links between RAs and LC1. It can be seen that, the bit error led to some packets being discarded by LC1 – the confidence level dropped frequently to 66.67%. However, during the frequency disturbance, it can be seen that the EFCC scheme exhibited similar performance as in the case with ideal communication links. This means the LCs can tolerate a BER level up to 10^{-5} . During the tests, the same event have been repeatedly tested and the EFCC scheme appeared to have same desirable response at the BER rate of 10^{-5} . According to the technical specification for communication services for tele-protection, the required BER should be smaller than 10^{-8} [8]. Therefore, the value of 10^{-5} is a high BER value that the LC can tolerate is a high BER value for power system applications.

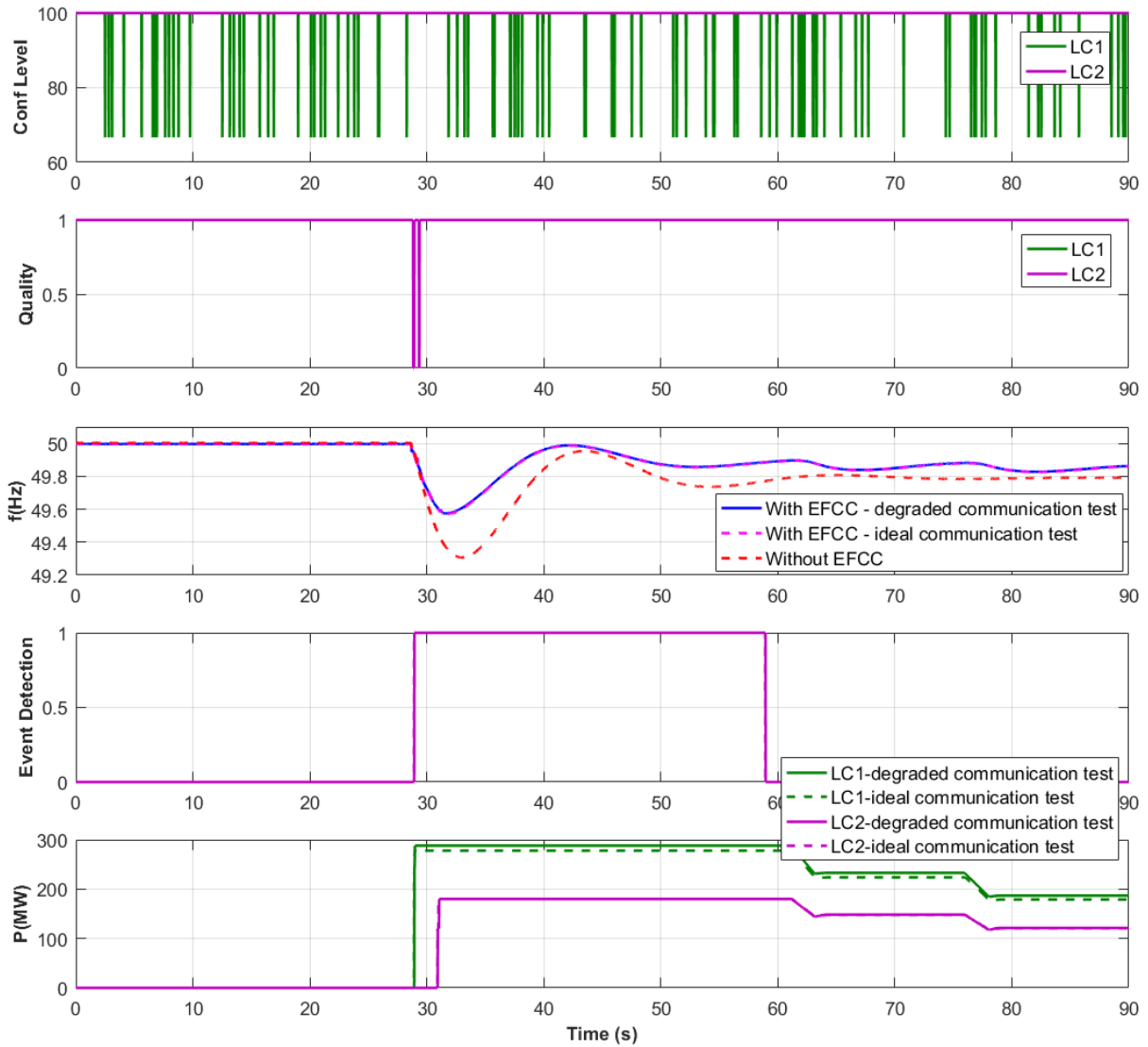


Figure 41. EFCC performance during a frequency event with high BER introduced to the communication links between the RAs and LC1

Figure 42 shows the EFCC performance during a grid fault event with BER of 10^{-5} introduced to the communication links between the RAs and LC1. It can be seen that the EFCC scheme exhibited a similar behaviour as in the base case - the RAs detected all faults and the LCs did not deploy any power to respond to the fault.

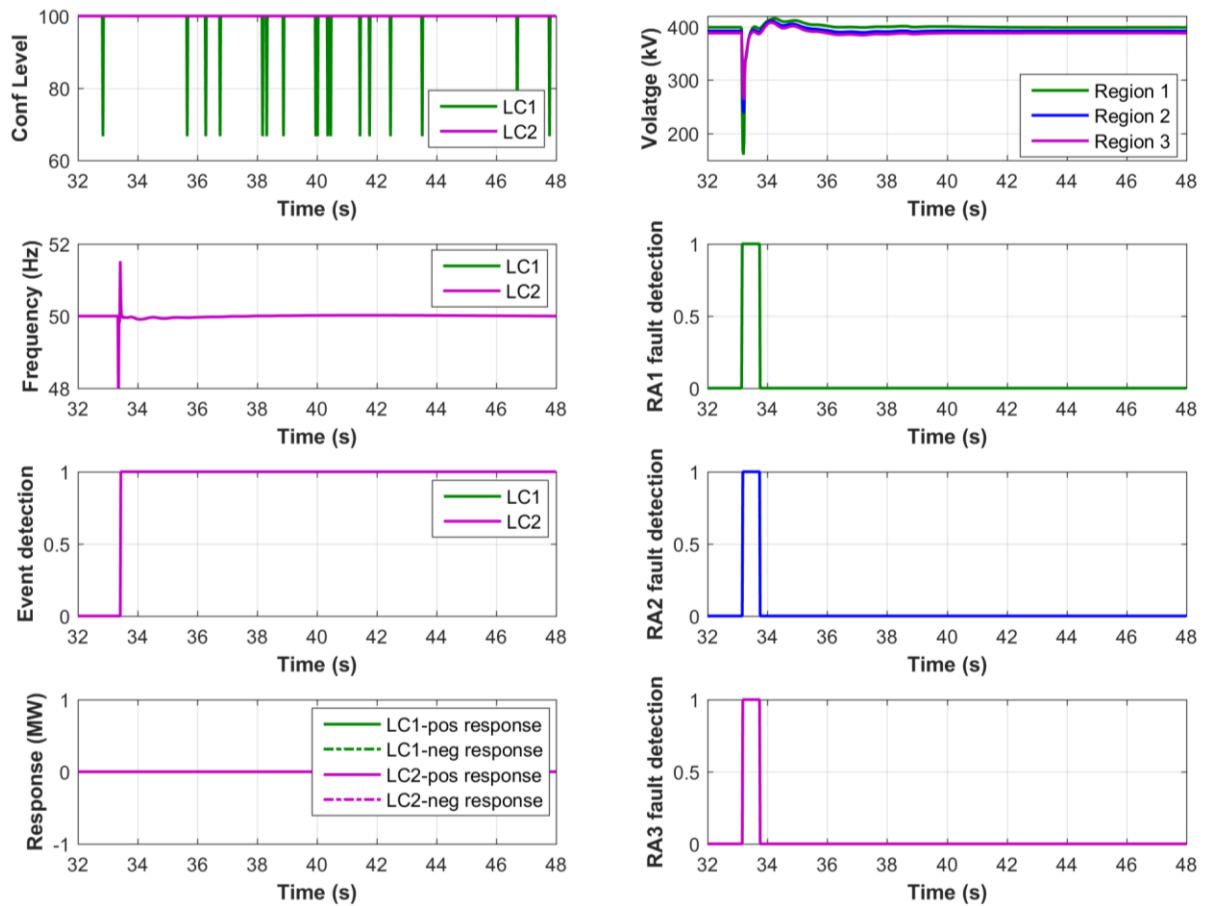


Figure 42. EFCC performance during a fault with high BER at the communication links between RAs and LC1

6.9 Summary of the tests

In this section, the EFCC scheme's performance during frequency and fault events were evaluated for a range of communication conditions.

In the fixed latency tests (Test 1 to Test 4), it was found that increasing the maximum latency limit in one link is sufficient to alter the behaviour of the LCs. If the LC misses data from two out of three RAs, the LC loses wide-area visibility and it will automatically switch to local mode.

In the jitter tests, it was found that with the increase of the mean latency and jitter level, the EFCC will be more likely to exhibit compromised behaviours. A mathematical analysis has been presented to quantify the probability of the EFCC being able to maintain wide-area visibility (thus operate correctly) in relation to the latency and jitter levels. Specifically, to achieve 90% of confidence that the EFCC scheme will maintain wide-area visibility for a period of 500 ms following an event, the jitter needs to be controlled within 10.2 ms for a mean latency of 60 ms and 13 ms for a mean latency of 50 ms.

Similarly, in the random loss of packet tests, it was found that as the loss of packets rate increases, the EFCC scheme is more likely to experience compromised behaviours. To achieve 90% of confidence that the EFCC scheme will maintain wide-area visibility in order to make correct decisions for a period of 500 ms following an event, the loss of packet rate needs to be smaller than 3.8%.

In the BER test, it was found that 10^{-5} was the maximum rate that EFCC can tolerate. When this BER is applied to the communication link, the EFCC scheme can still function as required. However, if the BER exceeds this value, the LC will not be able to use the data and will completely lose wide-area visibility.

7 KEY FINDINGS AND CONCLUSIONS

In this report, the test methods and results for evaluating the impact of the communication performance on the EFCC scheme have presented and analysed. Various degraded communication conditions were introduced in both of the regional communication network (connection between PMUs and RAs) and the wide-area network (connection between RAs and LCs).

The tests firstly evaluated how different emulated communication conditions (i.e. fixed latency, latency with jitter, BER and loss of packets) affect the EFCC controllers in receiving and processing the data (i.e. how the confidence levels in the controllers are affected under the various emulated communication conditions). Then the performance of the EFCC scheme during frequency and fault events with the various degraded communication conditions was then tested, where the associated communication performance limits for the EFCC scheme to provide a desirable behaviour have been analysed.

In the fixed latency tests, it was found that, for a buffering window of 100 ms, the maximum latency limit 78 ms and 82 ms at the wide-area and regional network respectively. For LCs, even if one of communication links between the RAs and the LCs experience a communication latency larger than the maximum limit, it could lead to the EFCC controllers exhibiting different behaviours. If the LC misses data from two out of three RAs, this will lead to the LC losing wide area visibility and it will automatically switch to local mode. According to the EFCC user manual [1], "*as long as the confidence level of the system aggregated values is high enough, the algorithm should continue to function while the confidence level is above a certain threshold which is a configurable value*". From the discussion with GE, it was told that the default value for confidence level threshold to switch from wide-area to local mode is 50%, which aligns with the test observations, where losing two out of three RAs caused the confidence level to reduce to below 50%, thus resulting in the local model operation.

In the jitter tests, it was found that with the increasing mean latency and jitter level, the EFCC will be more likely to exhibit compromised behaviours. A mathematical analysis has been presented to quantify the probability of the EFCC being able to maintain wide-area visibility (thus operate correctly) in relation to the latency and jitter levels. Specifically, to achieve 90% of confidence that the EFCC scheme will maintain wide-area visibility in order to make correct decisions for a period of 500 ms following an event, the jitter needs to be controlled within 10.2 ms for a mean latency of 60 ms and 13 ms for a mean latency of 50 ms. The probability of EFCC to function correctly is also evaluated at a wide range of other mean latency and jitter levels.

Similarly, in the random loss of packet tests, it was found that as the loss of packets rate increases, the EFCC scheme is more likely to experience compromised behaviours. To achieve 90% of confidence that the EFCC scheme will maintain wide-area visibility in order to make correct decisions for a period of 500 ms following an event, the loss of packet rate need to be smaller than 3.8%.

In the BER test, it was found that 10^{-5} was the maximum rate that EFCC can tolerate. When this BER is applied to the communication link, the EFCC scheme can still function as required. However, if the BER exceeds this value, the LC will not be able to use the data and will completely lose wide-area visibility.

8 REFERENCES

- [1] GE Grid Solutions, "SMART Frequency Control Application Function Blocks User Manual (Verion 1.0)," 2016.
- [2] Apposite® Technologies LLC. (04/06/2018). *Netropy® Network Emulator User's Guide*. Available: <http://apposite-tech.com/pdfs/netropy-usersguide.pdf>
- [3] Alstom Grid, "PhasorPoint User's Guide," 2015.
- [4] Q. Hong, M. Nedd, S. Norris, I. Abdulhadi, M. Karimi, V. Terzija, *et al.*, "Fast frequency response for effective frequency control in power systems with low inertia," 2018, pp. 1-8.
- [5] IEEE, "IEEE Std C37.118.2-2011 - IEEE Standard for Synchrophasor Data Transfer for Power Systems," ed, 2011.
- [6] Jun Shao, *Mathematical Statistics: Exercises and Solutions*: Springer, 2005.
- [7] K. Zhu, M. Chenine, L. Nordström, S. Holmström, and G. Ericsson, "An Empirical Study of Synchrophasor Communication Delay in a Utility TCP/IP Network," in *International Journal of Emerging Electric Power Systems* vol. 14, ed, 2013, p. 341.
- [8] Energy Network Association, "Technical Specification 48-6-7: Communication Service for Teleprotection systems," 2013.

APPENDIX A: PHYSICAL NETWORK CONNECTIONS FOR THE COMMUNICATION IMPACT TESTS

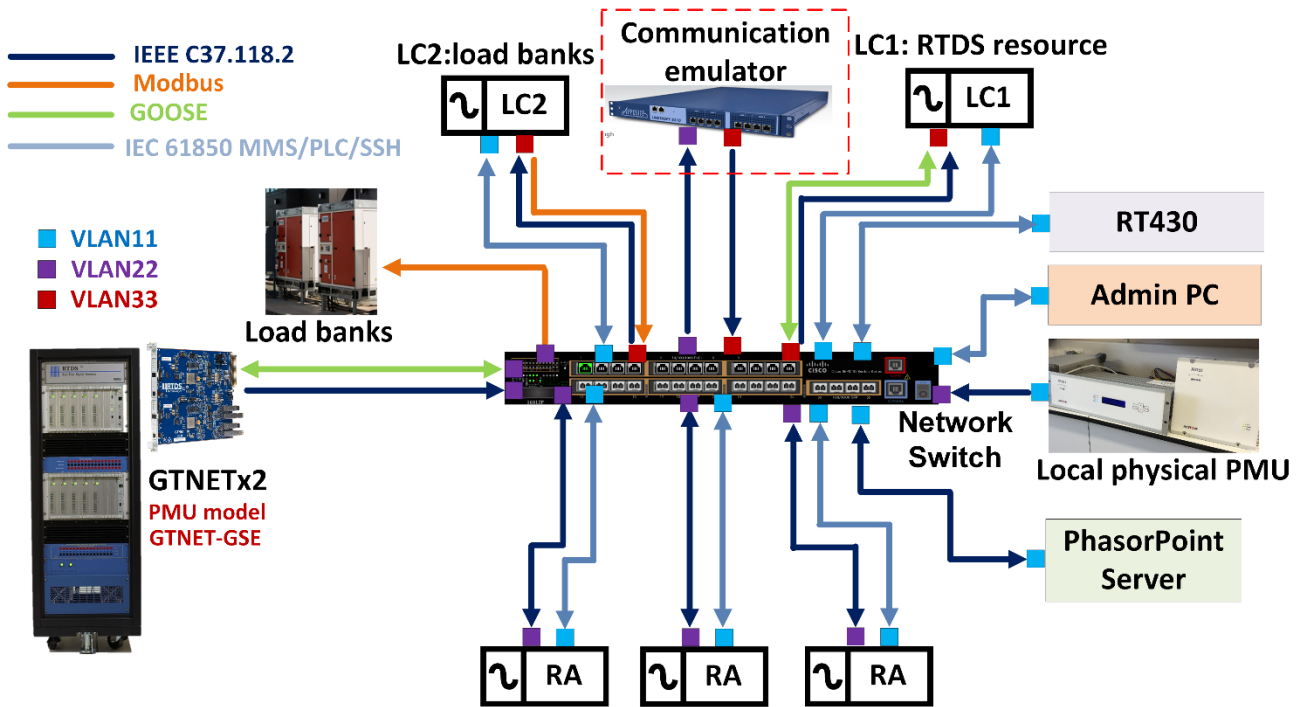


Figure 43. Network setup for testing the impact of regional network's performance

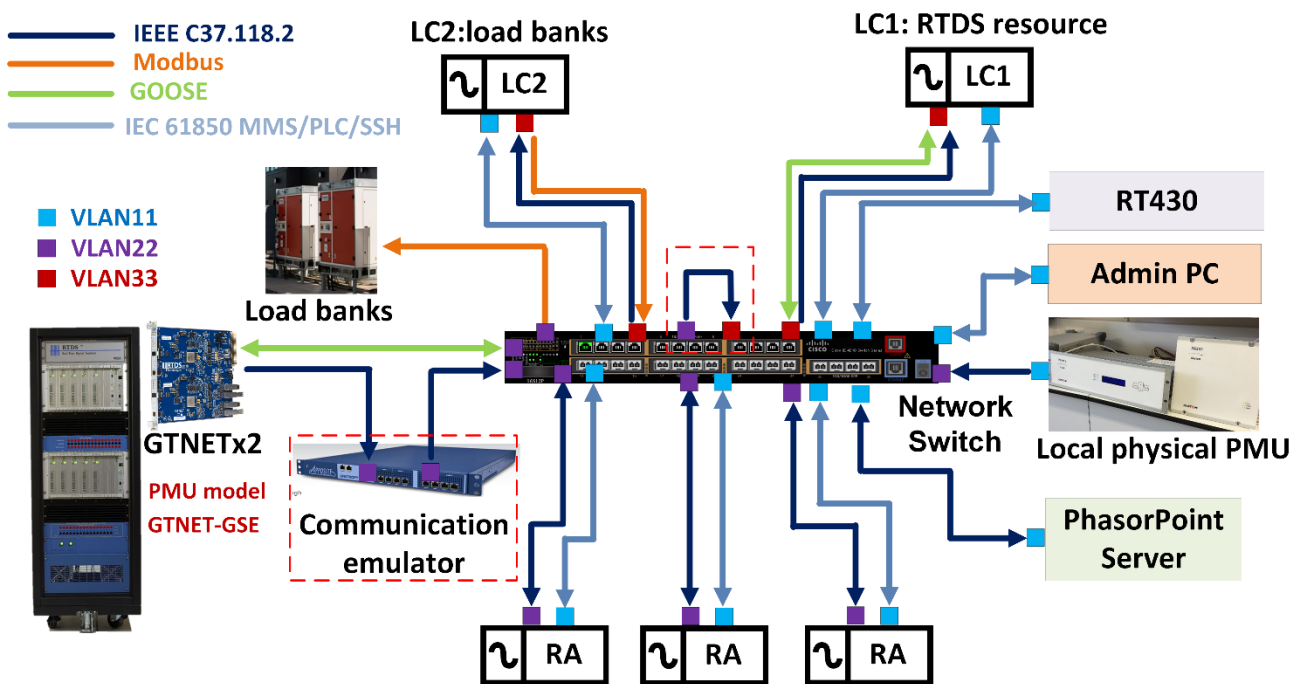


Figure 44. Network setup for testing impact of wide-area network's performance

APPENDIX B: TEST RESULTS FOR THE EMULATION OF THE WIDE-AREA COMMUNICATION NETWORK USING A BUFFERING WINDOW OF 200 MS

B1. Impact of latency

The buffering window was increased from 100 ms to 200 ms and the fixed latency test results are shown in Figure 45. The latency between RA1 and LC2 was gradually increased from 0 and the latency reached 178 ms and the confidence level dropped to 66.67% at T₁. Similar processes were repeated for the link between RA2 and LC2 and the link between RA3 and LC2. It was found that 178 ms is the latency limit for 200 ms of buffering window, i.e. if the communication delay is greater than 178 ms, the data packets will be discarded. When the confidence level dropped below 50% at T₂, the system wide visibility is lost, so the measured system RoCoF becomes zero.

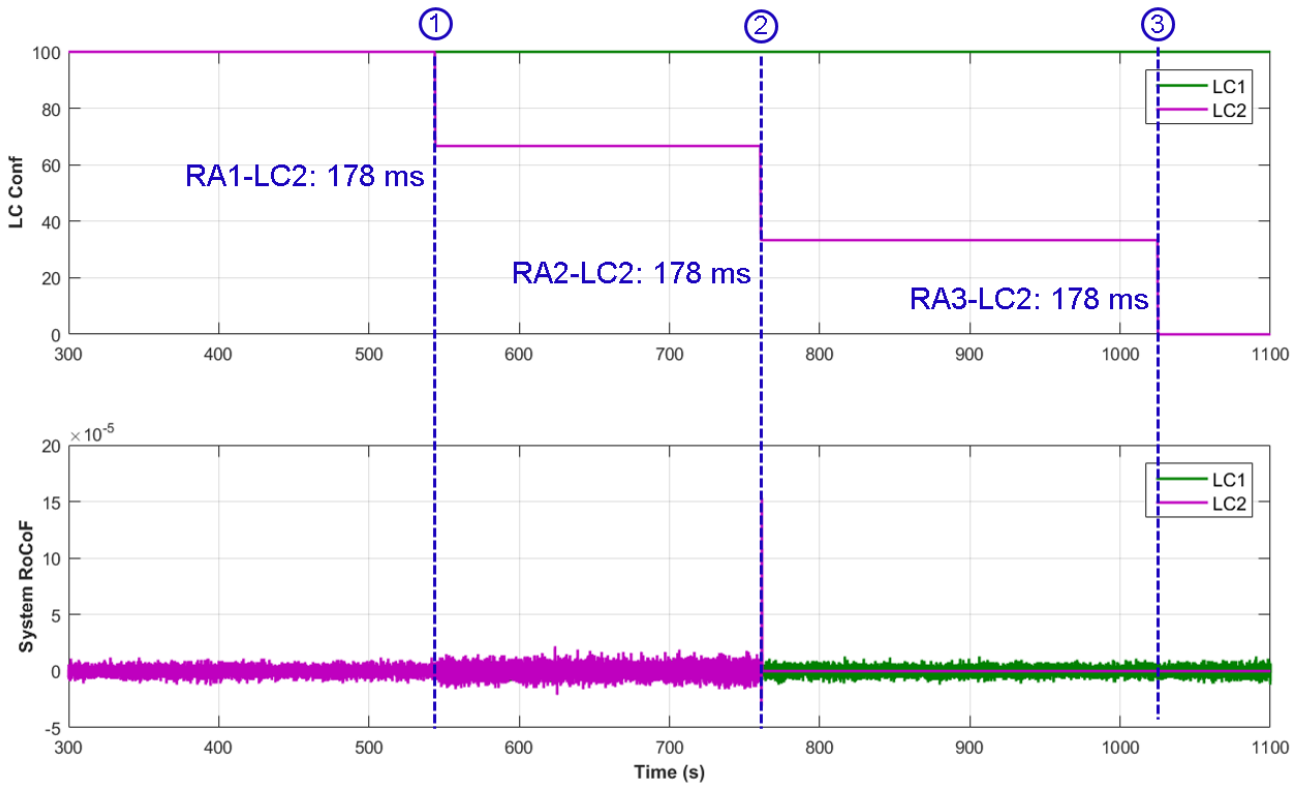


Figure 45. Latency limit test for 200 ms buffering window

B2. Impact of latency with jitter

From the fixed latency test presented in Appendix B1, it can be seen that the maximum latency limit for a buffering window of 200 ms is 178 ms. During the tests, the mean latency and jitter were gradually increased to evaluate how their changes would affect the packets being transmitted to the LCs. Similar to the 100 ms buffering window tests, the higher of the mean latency and jitter, the more likely the data will be discarded. Figure 46 and Table 6 presents an example where the mean latency was set as 170 ms with increasing jitter levels.

Figure 47 presents the probability of the packets being discarded in relation to the mean and jitter levels, where the mathematical derivation is presented in Equation (2) in Section 6.7.

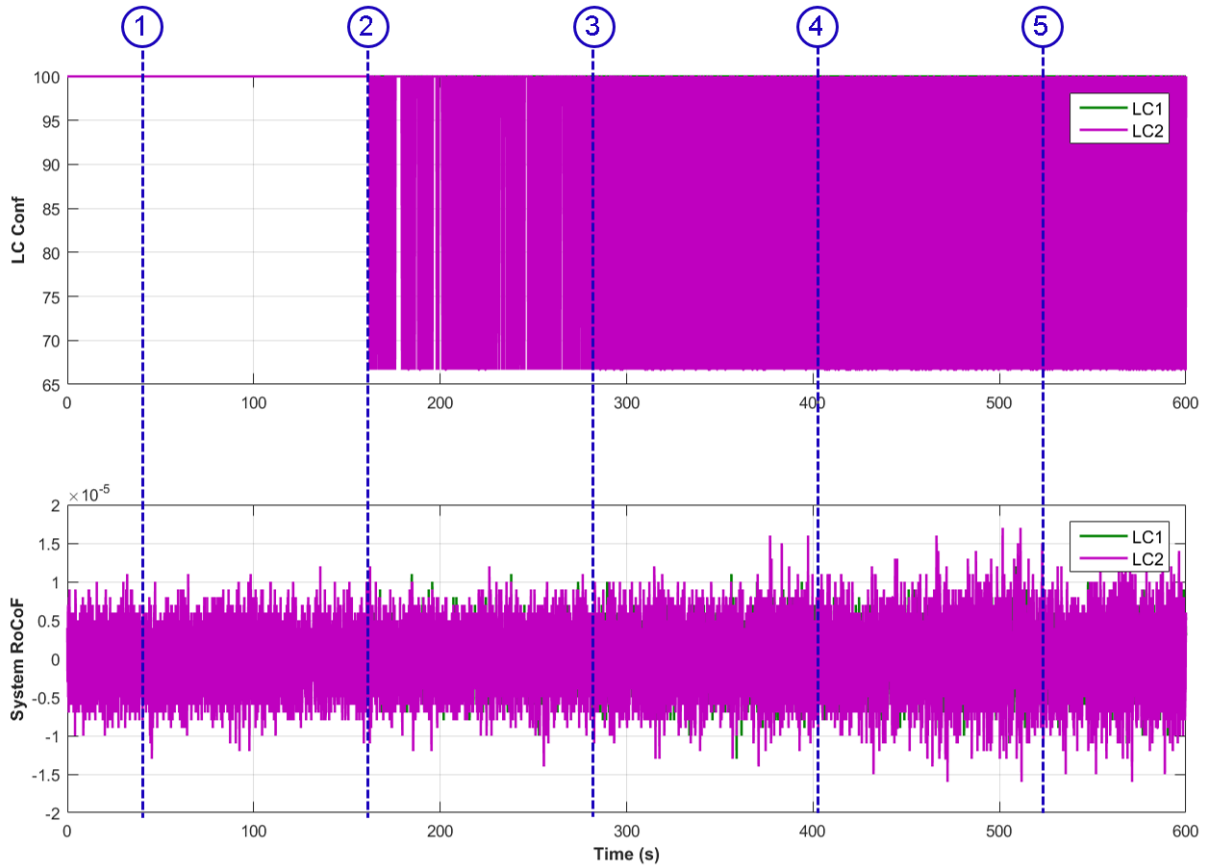


Figure 46. Test results of jitter emulation in the wide-area communication network with a mean latency of 170 ms (200 ms buffering window)

Table 6. Jitter emulation in the wide-area communication network with a mean latency of 170 ms (200 ms buffering window)

Time	Jitter (Standard Deviation)
T1 (40 s)	1 ms
T2 (160 s)	2 ms
T3 (280 s)	3 ms
T4 (400 s)	4 ms
T5 (520 s)	5 ms

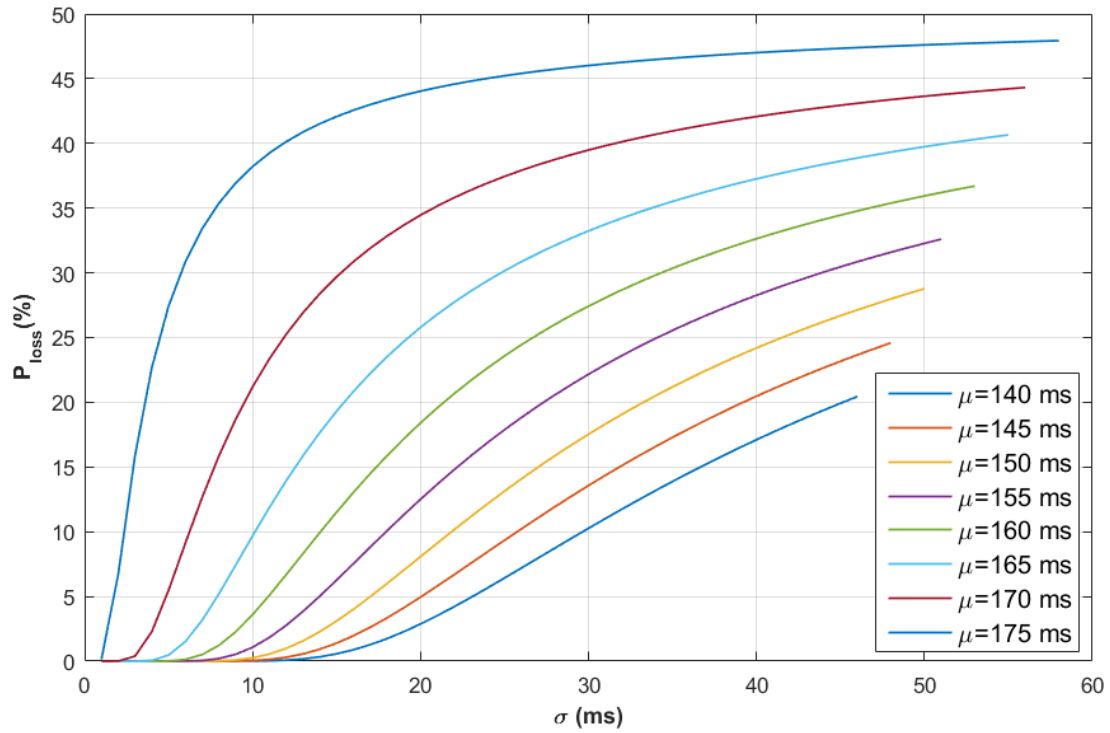


Figure 47. Probability of a packet being discarded in relation to mean latency and jitter levels

APPENDIX C: TEST RESULTS FOR THE EMULATION OF THE REGIONAL COMMUNICATION NETWORK

C1. Impact of latency

In this test, fixed latencies were introduced in the communication links between PMUs and RAs. The test results are shown in Figure 48. The emulation test parameters and the key observations are presented in Table 7.

From the test, it can be found that the latency limit between the PMUs and the RAs is around 82 ms for a 100 ms data buffering window.

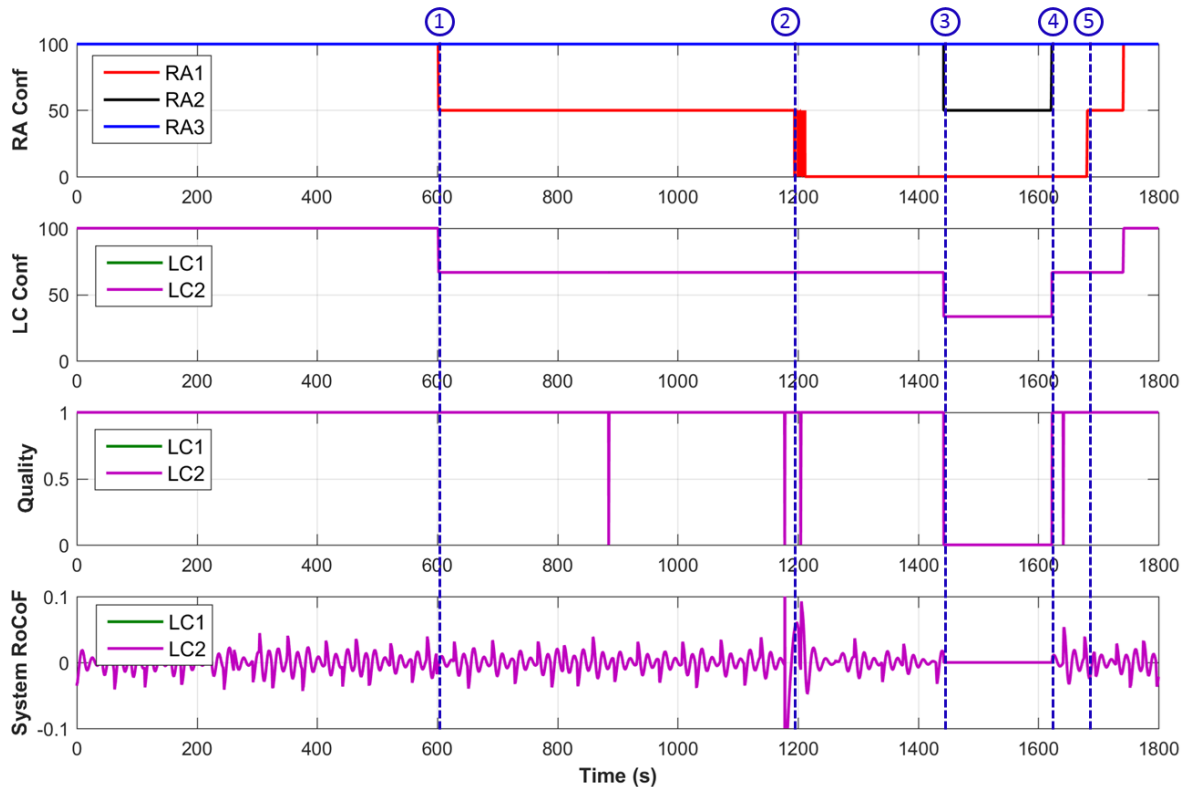


Figure 48. Impact of communication latency between PMUs and the RAs

Table 7. Latency emulation in the regional communication network

Time	Observations
T_1 (600 s)	<ul style="list-style-type: none"> Latency between R1-PMU1 and RA1 increased from 0 ms to 82 ms. RA1 confidence level dropped to 50%. LC1 and LC2 confidence level dropped to 66.67%.
T_2 (1200 s)	<ul style="list-style-type: none"> Latency between R1-PMU2 and RA1 increased from 0 ms to 82 ms. RA1 confidence level dropped to 0%. LC1 and LC2 confidence level remained at 66.67%.
T_3 (1200 s)	<ul style="list-style-type: none"> Latency between R2-PMU1 and RA2 increased from 0 ms to 81 ms. RA2 confidence level dropped to 50%.

	<ul style="list-style-type: none"> LC1 and LC2 confidence level remained at 33.33%, RoCoF quality dropped to 0, and system RoCoF also dropped to 0.
T ₄ (1620 s)	<ul style="list-style-type: none"> Latency between R2-PMU1 and RA2 removed. RA2 confidence level returns to 100%. LC1 and LC2 confidence level returned to 66.67%, RoCoF quality returned to 1, and system RoCoF measurement became available.
T ₅ (1680 s)	<ul style="list-style-type: none"> Latencies between PMUs in Region 1 and RA1 started to be removed in sequence, and eventually back to the initial ideal communication conditions, where there is no intentional latency.

B2. Impact of latency with jitter

In this test, a mean latency of 50 ms was emulated at the links between PMUs and LC2 with a range of different jitter levels.

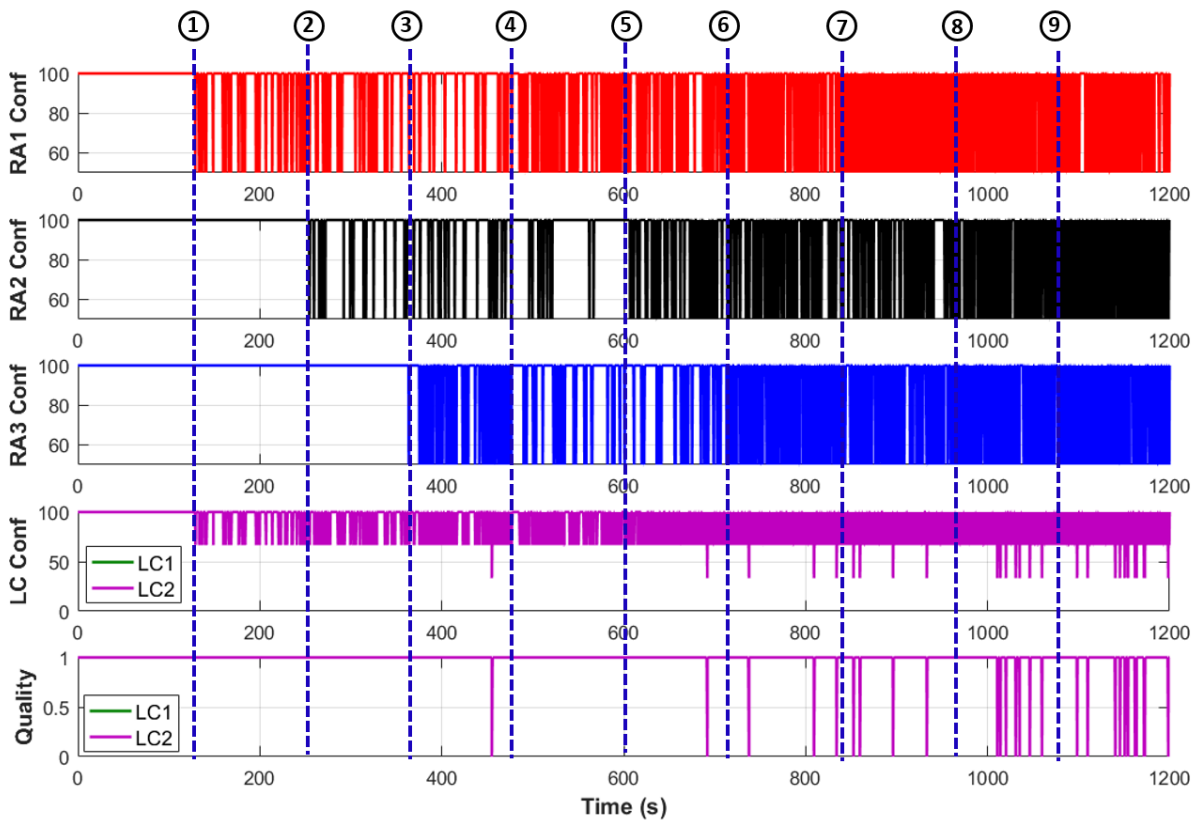


Figure 49. Impact of communication jitter between PMUs and RAs

Table 8. Jitter emulation in the regional communication network

Time	Communication link	Jitter (Standard Deviation)
0 s	All PMUs to RAs links	0 ms
T1 (120 s)	R1_PMU1 to RA1	12 ms
T2 (240 s)	R2_PMU1 to RA2	12 ms

T3 (360 s)	R3_PMU1 to RA3	12 ms
T4 (480 s)	R1_PMU1 to RA1	14 ms
T5 (600 s)	R2_PMU1 to RA2	14 ms
T6 (720 s)	R3_PMU1 to RA3	14 ms
T7 (840 s)	R1_PMU1 to RA1	16 ms
T8 (960 s)	R2_PMU1 to RA2	16 ms
T9 (1080 s)	R3_PMU1 to RA3	16 ms

B3. Impact of BER

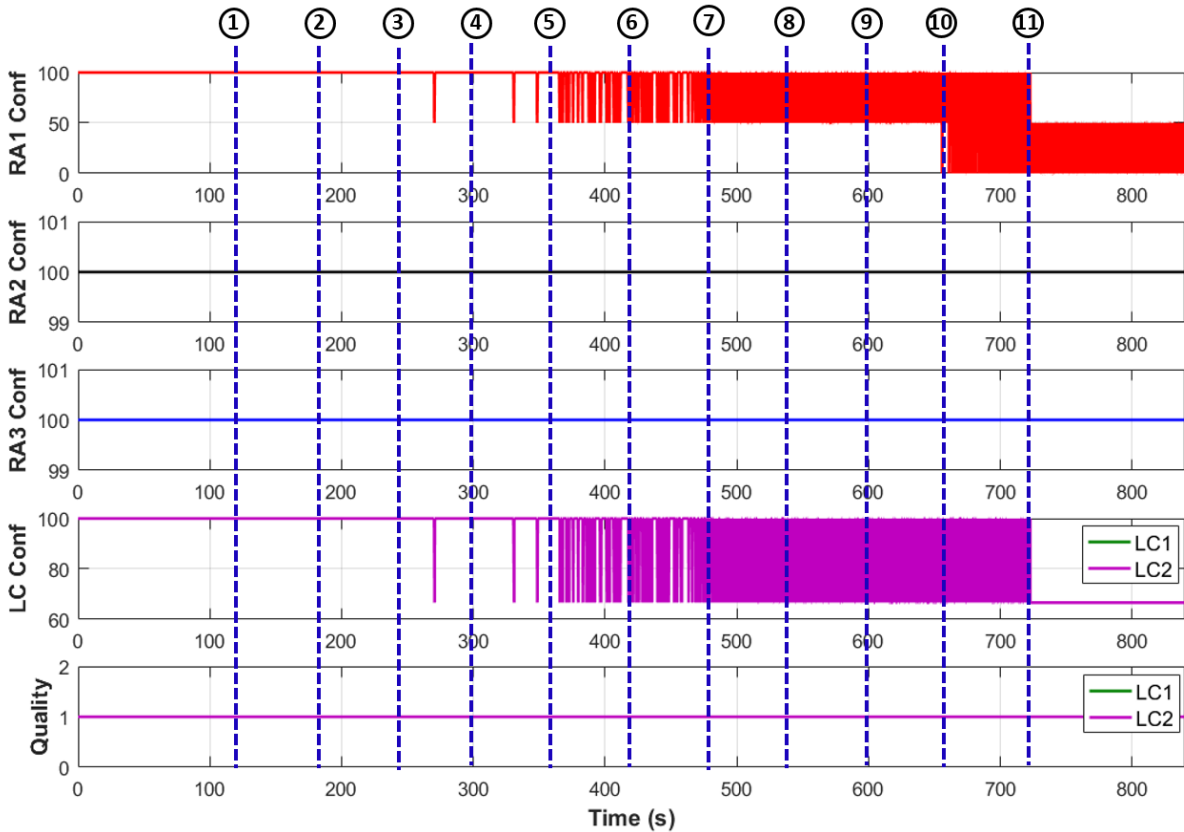


Figure 50. Impact of communication BER between PMUs and RAs

Table 9. BER emulation in the regional communication network

Time	Communication link	BER
0 s	RA1 to LC1 RA2 to LC1 RA3 to LC1	0
T ₁ (120 s)	R1_PMU1 to R1	1 × 10 ⁻⁷
T ₂ (180 s)	R1_PMU2 to R1	1 × 10 ⁻⁷

T ₃ (240 s)	R1_PMU1 to R1	1× 10 ⁻⁶
T ₄ (300 s)	R1_PMU2 to R1	1× 10 ⁻⁶
T ₅ (360 s)	R1_PMU1 to R1	1× 10 ⁻⁵
T ₆ (420 s)	R1_PMU2 to R1	1× 10 ⁻⁵
T ₇ (480 s)	R1_PMU1 to R1	1× 10 ⁻⁴
T ₈ (540 s)	R1_PMU2 to R1	1× 10 ⁻⁴
T ₉ (600 s)	R1_PMU1 to R1	1× 10 ⁻³
T ₁₀ (660 s)	R1_PMU2 to R1	1× 10 ⁻³
T ₁₁ (720 s)	R1_PMU1 to R1	1× 10 ⁻²

B4. Impact of loss of packets

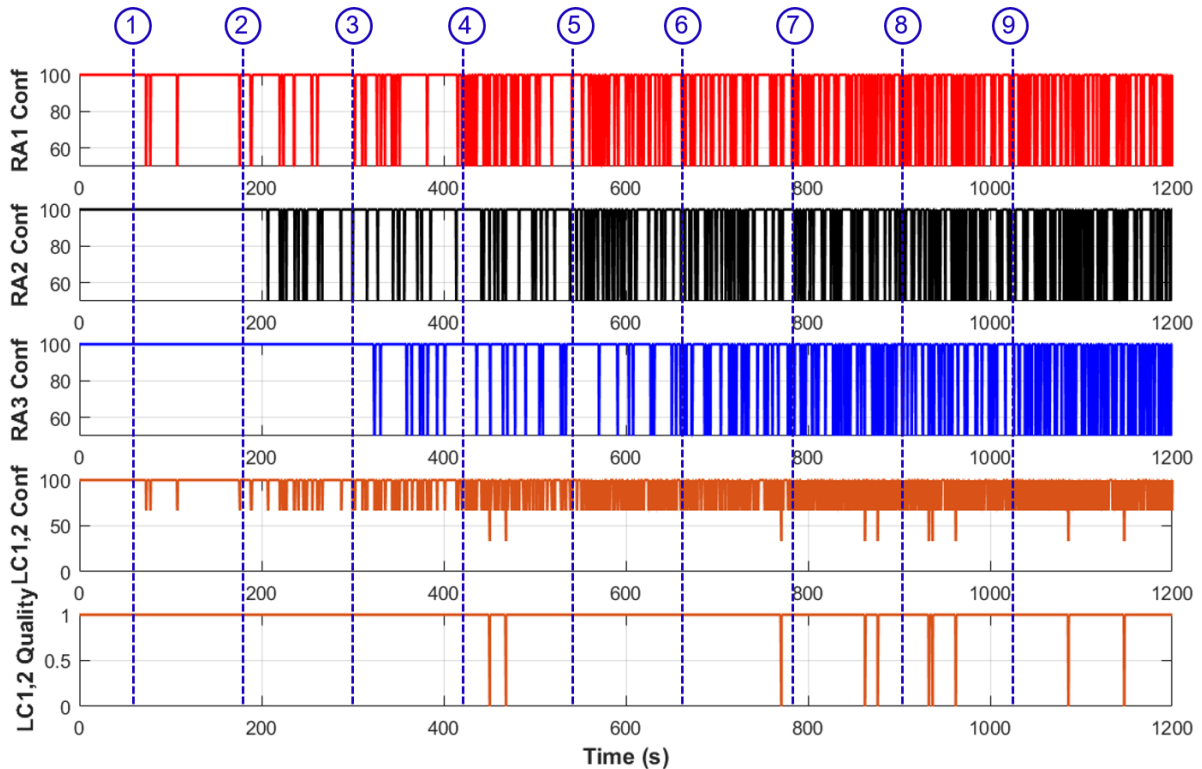


Figure 51. Impact of loss of packets at communication links between PMUs and RAs

Table 10. Loss of packets emulation in the regional communication network

Time	Communication link	Loss of Packets Rate
0 s	RA1_PMU1 to RA1 RA1_PMU1 to RA1 RA1_PMU1 to RA1	0%
T ₁ (60 s)	RA1_PMU1 to RA1	0.2%



T ₂ (180 s)	RA2_PMU1 to RA2	0.2%
T ₃ (300 s)	RA3_PMU1 to RA3	0.2%
T ₄ (420 s)	RA1_PMU1 to RA1	0.6%
T ₅ (540 s)	RA2_PMU1 to RA2	0.6%
T ₆ (660 s)	RA3_PMU1 to RA3	0.6%
T ₇ (780 s)	RA1_PMU1 to RA1	1%
T ₈ (900 s)	RA2_PMU1 to RA2	1%
T ₉ (1020 s)	RA3_PMU1 to RA3	1%



APPENDIX C: RESOURCE AVAILABILITY INFORMATION

The resource availability information for the resources controlled by LC1 and LC2 for all of the tests presented in this report is presented in Table 11.

Table 11. Resource availability information

	LC1	LC2
Resource type	1	1
Availability	true	true
Positive available power	300 MW	300 MW
Negative available power	300 MW	300 MW
Positive power response time	0.1 s	0.1 s
Negative power response time	0.1 s	0.1 s
Power ramp up rate	1000MW/s	1000MW/s
Power ramp down rate	1000 MW/s	1000 MW/s
Positive power max duration	80s	80s
Negative power max duration	80s	80s

APPENDIX D: MATHEMATICAL ANALYSIS OF THE IMPACT OF JITTER AND LOSS OF PACKETS

This section provides a mathematical analysis of the relationship between the loss of packets rate and the probability of the EFCC scheme's ability to maintain wide area visibility and perform the required control actions. The following is a list of definitions of the parameters used in the analysis. It should be noted that, as discussed in Section 5.2.3, if the latency exceeds the maximum limit due to jitter, the packet will be discarded, which is equivalent to the case where the packet is lost. Therefore, the variable P_{loss} can also represent the probability where the packet exceeds the maximum latency limit due to jitter.

- P_{loss} : the probability of loss of packets during data transmission or packets exceeding the maximum latency limit. In the case of a packet being discarded due to jitter, the relationship between P_{loss} and latency and jitter is presented in Equation (2) in Section 5.2.3.
- P_{No_WA} : at each time instance, the probability of EFCC scheme losing wide-area visibility.
- T : the period of time that is being investigated.
- ΔT : packet reporting interval, and $\Delta T = 20\text{ ms}$ for the EFCC scheme.
- K : total number of RAs (thus the number of links to a LC), e.g. in this work, there are 3 RAs, so $K = 3$.
- N : at each time instance, the number of samples required from RAs to maintain wide-area visibility, e.g. the LC needs at least 2 out of 3 samples from the 3 RAs at each time instance to remain wide area visibility, then $N = 2$.
- P_T : the probability of the EFCC scheme's ability to maintain wide-area visibility thus operate correctly over a period of T .

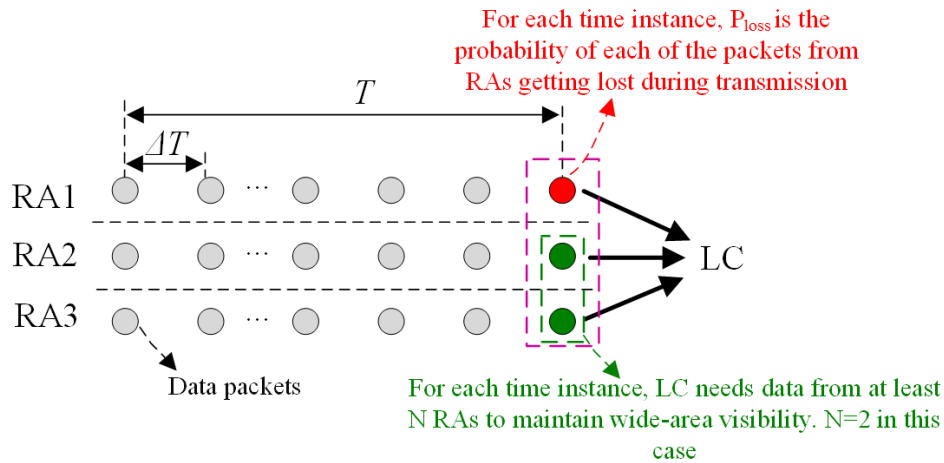


Figure 52. Packets transmitting from RAs to LCs

Figure 52 illustrates the packet transmitting from RAs to a LC. At a particular time instance, the probability of losing wide area visibility is:

$$P_{No_WA} = P_{loss}^K + {}^K C_{K-1} P_{loss}^{K-1} (1 - P_{loss}) + \dots + {}^K C_{K-N+1} P_{loss}^{K-N+1} (1 - P_{loss})^{N-1}$$

For a time period of T , the total number of samples is: $T/\Delta T$, and the probability of maintaining wide-area visibility during this period of time is:

$$P_T = (1 - P_{No_WA})^{T/\Delta T}$$

For this work, $K = 3$; $N = 2$, so

$$P_{No_WA} = P_{loss}^3 + {}^3 C_2 P_{loss}^2 (1 - P_{loss})$$

Since the EFCC scheme is required to make control decisions within 500 ms, T should not exceed 500 ms. The following presents the expressions for P_T with T ranging from 100 ms to 500 ms, and the relationship between P_{loss} and P_T is plotted in Figure 53 (this figure presents the same information as in Figure 33 and is duplicated here for convenience).

- If $T=100\text{ms}$, $P_T = (1 - P_{No_WA})^5$
- If $T=200\text{ms}$, $P_T = (1 - P_{No_WA})^{10}$
- If $T=300\text{ms}$, $P_T = (1 - P_{No_WA})^{15}$
- If $T=400\text{ms}$, $P_T = (1 - P_{No_WA})^{20}$
- If $T=500\text{ms}$, $P_T = (1 - P_{No_WA})^{25}$

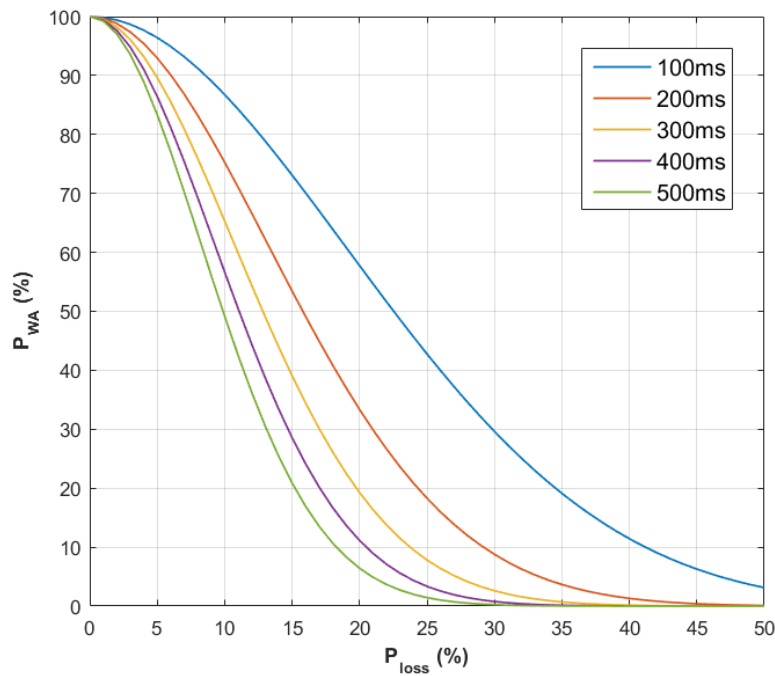


Figure 53. Relationship between P_{loss} and P_T

APPENDIX E: RAW DATA FOR THE STATISTICAL ANALYSIS OF IMPACT OF JITTER AND LOSS OF PACKETS

Table 12. Raw data for the curves presented in Figure 33

P_{Loss}	$P_T(100\text{ ms})$	$P_T(200\text{ ms})$	$P_T(300\text{ ms})$	$P_T(400\text{ ms})$	$P_T(500\text{ ms})$
0%	100.00%	100.00%	100.00%	100.00%	100.00%
1%	99.85%	99.70%	99.55%	99.41%	99.26%
2%	99.41%	98.82%	98.24%	97.66%	97.08%
3%	98.68%	97.39%	96.10%	94.84%	93.59%
4%	97.69%	95.43%	93.22%	91.06%	88.95%
5%	96.43%	92.98%	89.66%	86.46%	83.37%
6%	94.92%	90.10%	85.53%	81.18%	77.06%
7%	93.19%	86.84%	80.92%	75.41%	70.27%
8%	91.24%	83.24%	75.95%	69.29%	63.22%
9%	89.09%	79.37%	70.71%	62.99%	56.12%
10%	86.76%	75.28%	65.31%	56.67%	49.17%
11%	84.28%	71.02%	59.85%	50.44%	42.51%
12%	81.65%	66.66%	54.43%	44.44%	36.28%
13%	78.89%	62.24%	49.11%	38.74%	30.57%
14%	76.04%	57.82%	43.96%	33.43%	25.42%
15%	73.10%	53.43%	39.06%	28.55%	20.87%
16%	70.09%	49.13%	34.43%	24.14%	16.92%
17%	67.04%	44.94%	30.12%	20.19%	13.54%
18%	63.95%	40.89%	26.15%	16.72%	10.69%
19%	60.85%	37.02%	22.53%	13.71%	8.34%
20%	57.75%	33.35%	19.26%	11.12%	6.42%
21%	54.67%	29.88%	16.34%	8.93%	4.88%
22%	51.61%	26.64%	13.75%	7.10%	3.66%
23%	48.60%	23.62%	11.48%	5.58%	2.71%
24%	45.65%	20.84%	9.51%	4.34%	1.98%
25%	42.76%	18.29%	7.82%	3.34%	1.43%
26%	39.95%	15.96%	6.38%	2.55%	1.02%
27%	37.22%	13.86%	5.16%	1.92%	0.71%
28%	34.59%	11.96%	4.14%	1.43%	0.50%
29%	32.05%	10.27%	3.29%	1.06%	0.34%
30%	29.62%	8.77%	2.60%	0.77%	0.23%
31%	27.29%	7.45%	2.03%	0.55%	0.15%
32%	25.08%	6.29%	1.58%	0.40%	0.10%
33%	22.98%	5.28%	1.21%	0.28%	0.06%
34%	20.99%	4.41%	0.92%	0.19%	0.04%
35%	19.12%	3.65%	0.70%	0.13%	0.03%
36%	17.36%	3.01%	0.52%	0.09%	0.02%
37%	15.71%	2.47%	0.39%	0.06%	0.01%
38%	14.17%	2.01%	0.28%	0.04%	0.01%
39%	12.75%	1.62%	0.21%	0.03%	0.00%
40%	11.43%	1.31%	0.15%	0.02%	0.00%
41%	10.21%	1.04%	0.11%	0.01%	0.00%
42%	9.09%	0.83%	0.08%	0.01%	0.00%
43%	8.06%	0.65%	0.05%	0.00%	0.00%
44%	7.12%	0.51%	0.04%	0.00%	0.00%
45%	6.27%	0.39%	0.02%	0.00%	0.00%
46%	5.50%	0.30%	0.02%	0.00%	0.00%
47%	4.81%	0.23%	0.01%	0.00%	0.00%



48%	4.18%	0.17%	0.01%	0.00%	0.00%
49%	3.62%	0.13%	0.00%	0.00%	0.00%
50%	3.13%	0.10%	0.00%	0.00%	0.00%

Table 13. Raw data for the curves presented in Figure 35

σ	P_{Loss} at different mean latencies (μ)							
	40 ms	45 ms	50 ms	55 ms	60 ms	65 ms	70 ms	75ms
1 ms	100%	100%	100%	100%	100%	100%	100%	99.87%
2 ms	100%	100%	100%	100%	100%	100%	100%	93.32%
3 ms	100%	100%	100%	100%	100%	100%	99.62%	84.13%
4 ms	100%	100%	100%	100%	100%	99.94%	97.72%	77.34%
5 ms	100%	100%	100%	100%	99.98%	99.53%	94.52%	72.57%
6 ms	100%	100%	100%	99.99%	99.87%	98.49%	90.88%	69.15%
7 ms	100%	100%	100%	99.95%	99.49%	96.84%	87.35%	66.59%
8 ms	100%	100%	99.98%	99.80%	98.78%	94.79%	84.13%	64.62%
9 ms	100%	99.99%	99.91%	99.47%	97.72%	92.57%	81.30%	63.06%
10 ms	99.99%	99.95%	99.74%	98.93%	96.41%	90.32%	78.81%	61.79%
11 ms	99.97%	99.87%	99.45%	98.17%	94.91%	88.14%	76.65%	60.75%
12 ms	99.92%	99.70%	99.02%	97.24%	93.32%	86.07%	74.75%	59.87%
13 ms	99.83%	99.44%	98.44%	96.16%	91.69%	84.13%	73.08%	59.13%
14 ms	-	99.08%	97.72%	94.98%	90.07%	82.34%	71.61%	58.48%
15 ms	-	98.61%	96.90%	93.74%	88.49%	80.69%	70.31%	57.93%
16 ms	-	-	95.99%	92.47%	86.97%	79.17%	69.15%	57.44%
17 ms	-	-	-	91.20%	85.52%	77.78%	68.10%	57.00%
18 ms	-	-	-	89.93%	84.13%	76.49%	67.16%	56.62%
19 ms	-	-	-	-	82.83%	75.31%	66.31%	56.27%
20 ms	-	-	-	-	-	74.22%	65.54%	55.96%
21 ms	-	-	-	-	-	-	64.84%	55.68%
22 ms	-	-	-	-	-	-	64.19%	55.42%
23 ms	-	-	-	-	-	-	63.60%	55.19%
24 ms	-	-	-	-	-	-	-	54.97%
25 ms	-	-	-	-	-	-	-	54.78%